THE PRODUCTION OF ELLIPTIC INTERFERENCES IN RELATION TO INTERFEROMETRY

PART II

By CARL BARUS

Hazard Professor of Physics and Dean of the Graduate Department in Brown University

WASHINGTON, D. C.

Published by the Carnegie Institution of Washington

1912

THE PRODUCTION OF ELLIPTIC INTERFERENCES IN RELATION TO INTERFEROMETRY

PART II

By CARL BARUS

Hazard Professor of Physics and Dean of the Graduate Department in Brown University

WASHINGTON, D. C.

Published by the Carnegie Institution of Washington

1912

CARNEGIE INSTITUTION OF WASHINGTON

PUBLICATION NO. 149, PART II

PRESS OF J. B. LIPPINCOTT COMPANY
PHILADELPHIA, PA.

PREFACE.

The present report is, in the main, an extension of my work on the displacement interferometer described in the preceding investigation (Publication No. 149 of the Carnegie Institution of Washington); but beyond this, it is a contribution to the theory of coronas and their practical application for the measurement of sizes of fog-particles in cloudy condensation. In other words, if the source of light is not simple, but a doublet of two interfering beams as in chapter VI, indistinguishable from a simple source in case of white light, the coronas must show concentric dark interference rings, for the same reason that the spectra in case of the grating show elliptic loci of interference. It is therefore from rings of this general character that measurements of precision with coronas may be obtained. In its practical aspects chapter VI deals with the production of elliptic interferences with plane reflecting gratings instead of transparent glass gratings, as the former are much easier to rule. Again, the special type of linear fringes, produced by identical halves of a reflecting grating with their rulings parallel to the slit and nearly in the same plane, probably has a direct bearing on the theory of coronas, as in both cases an interference phenomenon is superimposed on the diffractions.

In chapters VII, VIII, and IX I have included certain incidental experiments on fog-particles made by aid of the coronas of cloudy condensation. The first investigation shows that the angular aperture of coronas is independent of the thickness of the layer of fog, single and triple layers, each about 6 inches thick, giving the same (continuous) corona. The next investigation adduces the curious result that when the diameter and size of the fog-chamber diminish indefinitely relative to the size of the exhaust pipe, its efficiency does not uniformly increase, but that it is rather more efficient for the (virtually) larger nuclei and less efficient for the smaller groups. Certain allied results on the rate of decay of nuclei of different sizes produced by mild X-radiation in dust-free wet air are added. These show the remarkable result that the coefficient of decay increases from less than one-tenth of the usual value for ions in dry air, to even 50 times the normal value, as the nuclei range in dimensions from very large to very small sizes. Hence if these nuclei be regarded as water-drops, they evaporate more and more rapidly to a persistent limiting small diameter, in proportion as they are larger. In the last investigation (chapter IX), I have returned to the moot subject of the regular persistent nuclei produced by strong X-rays, through earthed metallic aluminum screens and a fog-chamber of wood, with the endeavor to find the lower limit of the density of ionization which must be reached before these typical persistent nuclei (*i.e.*, those requiring little or no supersaturation to precipitate con-

densation) are formed. This chapter deals with large persistent nuclei produced by X-rays and is thus in a measure supplementary to the preceding. From both I conclude that the decay of ions as such beyond the scope of easy determination by the electrometer with the production of neutral pairs and multiples finds its counterpart in the growth of persistent nuclei, as the result of such coalescence. These nuclei now fall specially within the scope of detection by the fog-chamber. The number of persistent nuclei produced by the X-rays (*caet. par.*) will increase with the time of exposure at an accelerated rate, inasmuch as the nuclei or ions present themselves take part in the production, and these are present in continually greater number, as the lower limit of size decreases.

In chapter X the equation derived in the preceding report (No. 149, chapter V) for the displacement of the center of ellipses produced by the opaque mirror on the micrometer is tested throughout the spectrum and for all angles of incidence. This requires a knowledge of the indices of refraction of the glass of the grating for all wave-lengths. A method of total reflection suitable to the case, where only a flat spicule of glass is at hand, was therefore developed and applied.

In conclusion, a displacement interferometer is described, combining the desiderata of rigidity, lightness, and portability, and provided with long arms of invariable length and with sufficiently high mirrors to admit of the introduction of bulky apparatus, like a fog-chamber, between them. The apparatus is peculiarly adapted for the measurement of the refraction of gases at high temperatures, and conversely for the measurement of high temperatures by means of the refraction of a gas, as well as for the measurement of the adiabatic transformations of a gas, either dry or wet, and at all temperatures. It is hoped that the researches may develop fruitfully in this direction, and some promising work has already been completed.

Chapter XI, with a special view to an application of the interference method, endeavors to measure the degree of adiabatic expansion encountered in fog-chambers of such dimensions as I have used. To actually measure the ratio of specific heats much more voluminous apparatus will be necessary, and the present form of the interferometer is not adapted for air-chambers large in their vertical dimensions. An interesting result of the investigation is the marked difference of the heat ratio for wet and dry air, data from which it should be possible to compute the amount of water precipitated per cubic centimeter.

My thanks are due to Miss Ada I. Burton, who assisted me with rare efficiency both in the editorial part of the work and in the preparation of diagrams, as well as in the experimental parts and in the extended computations which a research of the present kind demands.

CARL BARUS.

BROWN UNIVERSITY, *December* 1911.

CONTENTS.

CHAPTER XI.—*The Degree of Adiabatic Expansion in Gases Rapidly Cooled, as Observed by Displacement Interferometry.*

CHAPTER VI.

ELLIPTIC INTERFERENCES WITH REFLECTING GRATINGS.

51. First method.—There are two or three typical cases in the use of reflecting gratings for the production of interferences in the spectrum, each of which shows peculiarly interesting features. The first of these is given in fig. 34 and corresponds closely to the method described for transmission gratings in a preceding paper. If L is the source of light and M a glass plate grating, it was shown that plane mirrors in the positions G_m and G_n, each reflecting a spectrum from M, produce elliptical interferences whenever the rays returned after passing M by transmission and reflection, respectively, are made to overlap in the spectrum, under suitable conditions.

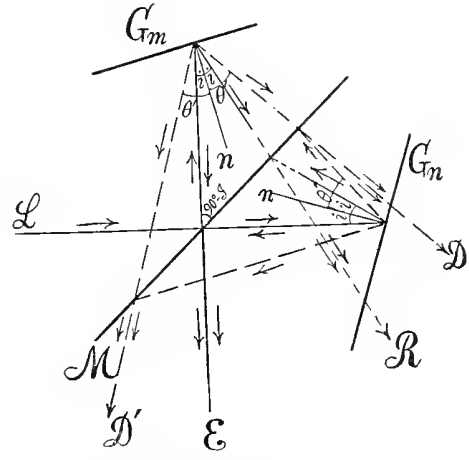

FIG. 34.—Diagram showing production of elliptic interferences from mirror M and reflecting gratings G_m and G_n.

The present method is the converse of this, since the gratings and the opaque mirrors change places. Parallel rays from L strike the plate of glass M and the component rays reach identical reflecting gratings G_m and G_n, placed symmetrically with respect to M at an angle i to the E and L directions. The undeviated rays pass off eccentrically at R and are not seen in the telescope at E. They may, however, be seen in an auxiliary telescope pointed in the line R and they then facilitate the adjustments. Rays diffracted at the angle $2i$, however, are respectively transmitted and reflected by M and interfere in the telescope in the line E. Similarly rays diffracted at an angle $\theta' > i$ interfere in the line D.

To make the adjustment it is sufficient to bring the Fraunhofer lines in the two spectra seen at E into complete coincidence, horizontally and vertically. Coincidence of slit images at R (at least vertically) aids in the same result. It is also necessary that the rulings on G_m and G_n and the slit shall be parallel, or that the images of slit and spectra shall lie between the same horizontals. One of the gratings, G_n, may now be moved parallel to itself by the micrometer screw until the elliptic interferences appear. If the plate M is not half-silvered there are three groups of these, as described in the preceding paper. Each group passes from the initial degree of extreme fineness, through maximum size, to a final degree, for a play of the screw of about 1 mm. There is the usual radial motion of the fringes, together with the drift through the spectrum as a whole. To bring out the set of solitary ellipses, the silvered surface of M should be toward the light and remote from the eye. As a rule the adjustment is difficult, as an extra condition is imposed in the parallelism of the slit and the rulings of the gratings. The ellipses are liable to be coarse, with their axes oblique, clearer in some parts of the spectrum than in others, unless means are provided for placing the rulings accurately parallel. Even when well adjusted they are rather polygonal than rounded in their contours. They are about as strong with non-silvered glass M as with half-silvered glass; but in view of the multiple spectra the adjustment is much more difficult in the former case.

It has been suggested that the white slit image must appear eccentrically in the direction R. Hence if a special telescope is directed in this line, the final adjustment is reached on coincidence of the proper slit images, provided the rulings of the gratings and the slit are parallel.

For $\theta' > i$ the second series of interference spectra occurring at D eccentrically is broader, but only on perfect adjustment does it occur simultaneously with the other set. In fact, since for the preceding case $i = \theta$, or

$$2 \sin i = \lambda/D$$

and in the present case,

$$\sin \theta' - \sin i = \lambda/D$$

therefore

$$\sin \theta' = 3 \sin i = 3 \sin \theta$$

There is also an available set in the second order to the left of E. In the gratings used above D lies in front of G_n, being nearer the E than the L direction.

52. Inversion of the method.—The occurrence of the undeviated ray R suggests another method; for if the white ray R is reversed, *i.e.*, comes from an eccentric collimator, slit images will be seen in telescopes at L and E, whereas overlapping spectra will appear in the direction D' eccentrically and in the lines R and R' One of the latter may be lost in the collimator. The former occurs for the same angle θ', so that

$$\sin \theta' = 3 \sin i$$

Moreover, if $I=45°$ is the angle of incidence of L upon M when sodium light is taken, so that $\theta'=26°\ 14'$, $i=8°\ 28'$, the R, D, D' rays make angles $2i$, $\theta'+i$, $\theta'-i$, respectively, with the E direction; or the sum of the angles at D and D' with the E line is $2\theta'$, their difference $2i$, and the rays D, R, D' intersect at a common center on G_m. Hence if we place the plane of G_m at the center of the spherometer and arrange M and G_n eccentrically, the angles may be measured as before.

53. Second method. Resolution of the slit image.—If the sharp white images of the slit in a Michelson apparatus for the case in which the incident light consists of parallel white rays from a collimator be accurately superimposed and the opaque mirrors be set at the proper distances from the semi-transparent mirror by the micrometer, the slit image may itself be viewed through a grating and will then show elliptic interferences in all the spectra. The apparatus is here eccentric, while the grating (either transmitting or reflecting) must be at the center of the spectrometer, if angles are to be measured. The same is true for any of the other superimposed white slit images in the above or the earlier experiments and may even be repeated with successive transmitting gratings. It is interesting to note that the position of the center of ellipses is at the same wavelength in all the spectra, though the form of ellipses may differ enormously. The same phenomenon may thus be seen by a number of observers at the same time, each looking through his own telescope.

It is this phenomenon which may be repeated with the fog-particles of cloudy condensation instead of with the grating and must then give rise to concentric black interference rings symmetrical with the colored field. Measurements of precision in case of the coronas are thus feasible, in view of the varying distances apart of these rings, increasing in size as they do with diminishing sizes of fog-particles.

54. Third method. Parallel gratings.—In this case the two halves of the grating are treated displaced parallel to themselves from their original coplanar position in the grating from which they are cut. Their mounting is thus something like the case of the two black plates of Fresnel's mirror apparatus, one of the plates being adapted for displacement parallel to itself.

In fig. 35, g and g' show the two halves of the grating cut along the plane S, normal to the plates and parallel to the rulings. The half g' is provided with a micrometer screw, so that it may be successively moved from the position g' in fig. 35 to the position g' in fig. 36, through all intermediate positions, while the half g remains stationary. Each of the halves g and g' is controlled by three adjustment screws (horizontal and vertical axes of rotation), to secure complete parallelism of the faces of the grating. Each, moreover, may be rotated around a horizontal axis to place the lines parallel to the slit of the collimator. The duplex grating is mounted on a

spectrometer, as is usual for reflection. Finally, each half may be raised and lowered and moved horizontally to and fro, parallel to itself, so that the half gratings when coplanar may approximately reproduce the original grating.

After each of the spectra is clear as to Fraunhofer lines, the interferences here in question are produced by bringing these lines (the D lines, for instance) into perfect coincidence, horizontally and vertically. Under these circumstances if the distance apart, e, is suitably chosen, the interference fringes will appear throughout the spectrum. These consist of an approximately equidistant series of lines parallel to the slit, *i.e.*, vertical lines, which are finer, *cæt. par.*, as the breadth of the crack at S between the gratings is larger. They may be increased from the extreme fineness as they enter the range of visibility, to a maximum coarseness (in the above

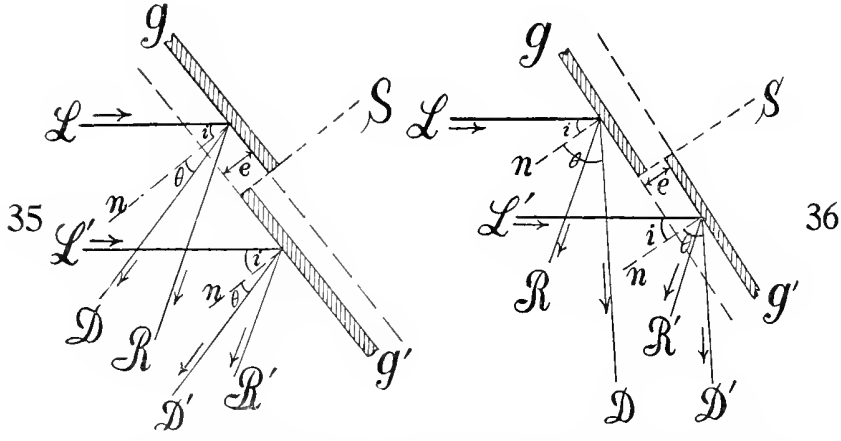

FIGS. 35 AND 36.—Diagram showing production of interferences from identical gratings, nearly in same plane, with their rulings parallel to the slit.

experiments) of about 3 to 5 minutes per fringe, after which they vanish. They can not, in practice, be passed through infinite size; neither can they be produced symmetrically on the two sides of the adjustment for infinite size. They can not, in other words, be changed from the positive to the negative condition of appearance.

The occurrences are in fact as follows: If as in fig. 35, $i>\theta$ (parallel white rays coming from L and L', R and R' being reflected, D and D' diffracted rays for the normal n), the grating g' must be in advance or forward of g. If now the air-space e is reduced micrometrically, g' retreating, the lines travel in a given direction (from left to right) through the spectrum, while at the same time they grow continually larger until for a minimum value of e still positive they vanish as a whole. The period of indistinctness before evanescence is not marked.

On the other hand, if $\theta'>i$, as in fig. 36, the grating g' must be to the rear of g and the air-space e is throughout negative. If this is now decreased

numerically the lines travel through the spectrum in the opposite direction to the preceding case, while at the same time they coarsen until they vanish as a whole as before. The grating g' is still behind g when this occurs.

Finally, if for any suitable value of e the grating g' is moved in its own plane without rotation away from g, so as to widen the crack at S between them, the fringes grow continually finer until they pass beyond visibility, and *vice versa; i.e.*, as the crack at S is made smaller the lines continually coarsen.

55. Nature of the evanescence.—The fact that the lines vanish as a whole and almost suddenly after reaching their maximum distance apart is very peculiar, as is also the fact that they can not be passed through infinite size or made to appear symmetrically on both sides of this adjustment. To investigate this case I provided both the collimator and the telescope with slits, so that the parts of the grating g and g' from which the interfering pencils come might be investigated.

If a single vertical slit about 1 mm. wide is passed from right to left toward the objective of the telescope, a black line passes across the field of the spectrum, which line is merely the image of the crack at S. In the diagram (fig. 37) the G rays, for instance, come from the edge of both gratings g and g', whereas the R rays and the V rays come from but a single grating. Now, when the space e is diminished, the black band at G gradually vanishes and in its place appear the coarsest fringes producible. When the slit F is removed these coarse fringes disappear. The fringes visible through the slit have, however, both an inferior and superior limit of angular size. When e is diminished to zero they vanish and when e is sufficiently increased they again vanish, though they now appear when the slit is either removed or widened. From this it follows that the coarsest fringes come from the edges of the crack S of the gratings, and that the remainder of the grating will not produce coarse fringes. By moving the slit the fringes may be made to appear in any other part of the spectrum.

The same fact may be proved by putting the vertical slit F over the lens of the collimator and allowing the white light L to fall on the edges of the grating at S. Coarse fringes limited as to range and size are then seen throughout the spectrum at g.

Whenever the slit or vertical stop is used, the fringes are exceptionally sharp and easily controlled for micrometry. It is not even necessary to adjust the two spectra horizontally with the same care as when no slit is used, but the vertical coincidence of spectrum lines must be sharp. Naturally the use of the slit has one drawback, as the resolving power of the grating is decreased and the spectrum lines are only just visible. The adjustment, however, may be made before the slit is added. A few examples may be given. For a slit 1 mm. wide over the telescope or collimator, only the immediate edges at the crack S, about 0.5 mm. each in

breadth, are active. A narrow range of large fringes is seen in the field, easily controlled by the micrometer screw. With a slit 3 mm. in width the lower limit is much increased, the upper diminished, to a size of about 3 inches per fringe. In the absence of the slit the field is free from fringes. With a slit 6 mm. wide, the upper limit is again decreased, the lower much increased; nevertheless the finest fringes appear only after the slit is removed. Using double slits over the collimator, each 1 mm. wide and 3 mm. apart, fringes of medium size limited at both ends appear; 3 mm. slits 6 mm. apart show only the very fine fringes, but both sizes are still limited. Finally, when all but about 0.5 mm. of the edge of the crack of the grating g' is screened off, whereas the whole grating g (about one-half inch square) is without a screen, all the fringes from the maximum size to

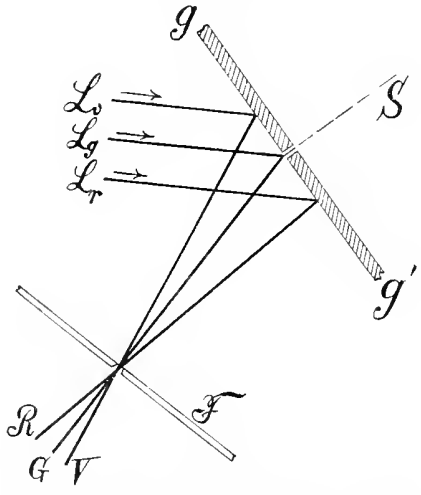

FIG. 37.—Diagram showing effect of a slit in front of telescope.

complete evanescence beyond the range of visibility are producible. Naturally if the edge of g' is quite dark everything vanishes.

It follows, therefore, that pairs of corresponding rays are always in question. These corresponding rays are at a definite ND apart, where D is the grating space and N the number of lines per centimeter of the grating in question. This distance ND is greater as the fringes are smaller and may be of the order of a centimeter when the fringes pass beyond the range of visibility. Again ND is equal to the width of the crack when the largest fringes vanish. Finally, when ND is zero, as is the original unbroken grating, the size of the fringes is infinite.

It has been stated that the use of the slit or a laterally limited objective is advantageous because all the lines are much sharper. Inert or harmful illumination is cut off. If the slit is over the objective of the telescope only a small part of the field of view shows the lines; if placed over the

objective of the collimator, the fringes are of extreme clearness throughout the spectrum. It may be ultimately of advantage to use the edge near the crack g' only, together with the whole of g; for if a small strip of g' at the crack S is used with the whole of g, the smaller fringes are weakened or wiped out. Thus the inner edge of the nearer grating with successive parts of the further grating is chiefly effective in the production of these interferences.

To bring the two edges quite together was not possible in my work, as they were rough and the apparatus improvised.

56. Data.—Some measurements were attempted with the view only of checking the equations presently to be deduced. The adjustment on an ordinary spectrometer is not firm enough and the fringes being very fine (a few minutes of arc) are difficult to follow unless quite stationary.

Table 18, however, gives both the values of de/dn, displacement per fringe, for different angles of incidence i and of diffraction θ, and $d\theta/dn$, the angular deviation per fringe at the D line. In measuring the latter it was necessary to count the fringes between the C and D lines and divide their angular distance apart by these numbers. As e can not be measured, its successive increments Δe from the first position are given. These are presently to be associated with the corresponding increments of $dn/d\theta$.

TABLE 18.—Values of $d\theta/dn$, etc. $i = 53° 15'$. $D = 200 \times 10^{-8}$ cm.

Observed.						Computed.			
No. of fringes	θ and θ'	$d\theta/dn$	$dn/d\theta$	$\Delta dn/d\theta$	Δe	At θ $\Delta dn/d\theta$	At θ' $\Delta dn/d\theta$	Mean $\Delta dn/d\theta$	Region.
120	30° 27′	1′ 17″	3080	1130	0.025	1260	1028	1140	Between C and D lines.
75	28 14	1 46	1950						
	Diff. 2° 13′								
90	29° 09′								
71	28 14	46	4438	1000	.025	1116	1027	1072	Near C line
55	Diff.	1 0	3438	1188	.050	....	....	....	
36	55′	1 32	2250		.075	....	....	....	
24	30° 27′	1 50	1875	1328	.025	1259	1196	1228	Near D line
41	29 43	1 4	3203						
	Diff. 44′								

57. Equations.—In fig. 38, L and L' represent a pair of corresponding white rays, reflected into R and R' and diffracted into D and D' at angles i and θ, respectively. The half gratings g and g' are separated along the crack S, and g' is movable parallel to itself by a micrometer screw normal to g'. Let the normal distance apart of the gratings be e. The incident rays L, L' strike the originally coplanar grating at points N rulings apart,

or ND cm. apart, if D is the grating space. In the separated grating let these points be at a distance c apart. Let d (the broken line ia) be the incident wave-front and h the corresponding diffracted wave-front and call the angle between c and d, γ.

When there is reinforcement the path difference of the rays L and L' from the incident (d) to the diffracted (h) wave-front, may be

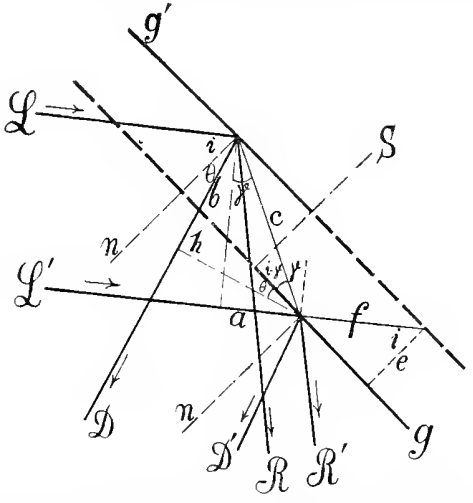

FIG. 38.—Diagram showing production of interferences from two identical nearly coplanar gratings, with rulings parallel to slit. Details.

written $n\lambda = b - a$, where b and a are the distances of h and d from the points of incidence of L and L' on the grating g and g' respectively. If, finally, f is the length of the prolongation of L' between the gratings we may write in succession

(1) $$d = ND \cos i$$

(2) $$f = e \sec i$$

(3) $$a = ND \sin i - e \sec i$$

(4) $$\tan \gamma = a/d$$

(5) $$C = ND \cos i \sec \gamma$$

(6) $$b = c \sin (i + \theta - \gamma)$$

To these should be added

(7) $$dN/de = \tan i/D$$

Hence after removing γ and arranging

$$n\lambda = ND \left\{ \cos i \sin (i+\theta) - \sin i \cos (i+\theta) - \sin i \right\} + e \sec i \,(1 + \cos (i+\theta))$$

which reduces to

$$n\lambda = ND(\sin\theta - \sin i) + e\sec i\,(1+\cos(i+\theta)),$$

or since

$$\sin i - \sin\theta = \lambda/D$$

finally

$$(8)\qquad (n+N)\lambda = e\frac{1+\cos(i+\theta)}{\cos i} = \frac{2e\cos^2(i+\theta)/2}{\cos i}$$

This must therefore be regarded as the fundamental equation of the phenomenon. Equation (7), however, leads on integration to

$$(9)\qquad N = e\tan i/D + N_0,$$

where N_0D is the width of the crack.

If the value of N from (9) be put into (8), together with the equivalent of λ/D, it appears after reduction that

$$(n+N_0)\,\lambda = e(\cos i+\cos\theta) = 2e\cos\frac{i+\theta}{2}\cos\frac{i-\theta}{2}$$

The case of $N=0$, $e>0$ would correspond to the equation

$$(10)\qquad n\lambda = e\,(1+\cos(i+\theta))/\cos i = 2e\cos^2\frac{i+\theta}{2}/\cos i$$

which is only a part of the complete equation (8). For $i>\theta$, one active half, kh, is necessarily partly behind the other half, $k'h'$, and therefore not adapted to bring out the phenomenon as explained, unless $e=0$.

58. Differential equations. Displacement per fringe, de/dn.—To test equation (8) or (10) increments must be compared. The latter gives at once, since N is constant relative to e like i, θ, and λ,

$$(11)\qquad \frac{de}{dn} = \frac{\lambda}{\cos i+\cos\theta} = \frac{\lambda}{2\cos\frac{i+\theta}{2}\cos\frac{i-\theta}{2}}$$

which is the interferometer equation when the fringes pass a given spectrum line, like either D line, which is sharp and stationary in the field. Equations (7) and (11), moreover, give after reduction

$$(12)\qquad dN/dn = \tan i\tan\frac{i-\theta}{2}$$

Table 18 contains values of de/dn computed from (11), made under widely different conditions ($i>\theta$, $i<\theta$, first and second order). The agreement is as good as the small fringes and the difficulty of getting the grating normal to the micrometer screw in my improvised apparatus admit. If this adjustment is not perfect N_0 changes with e. From equation (12), moreover,

$$(12')\qquad \frac{dN}{dn} = \frac{dN}{d\theta}\frac{d\theta}{dn} = \frac{dN_0}{d\theta}\frac{d\theta}{dn} = \frac{dN_0}{dn}$$

since N_0 is constant only relative to e when θ varies.

59. Deviation per fringe, etc., $d\theta/dn$, $d\theta/de$.—These measurements are still more difficult in the absence of special apparatus, since e is not determinable and the counting of fine flickering fringes is unsatisfactory; but the order of results may be corroborated by observing the number of fringes between two Fraunhofer lines, like the C, D, and other lines used. Differentiating equations (8) and (10) for variable n, λ, θ, and N (since $dN/d\theta$ is equal to $dN_0/d\theta$, equation (12')) and inserting $-D\cos\theta$ $d\theta/dn = d\lambda/dn$, it follows after arranging that

$$\frac{d\theta}{dn} = \frac{\lambda^2}{eD}\frac{1+dN/dn}{1+\cos(i+\theta)} = \frac{\lambda^2}{eD}\frac{1}{\cos i\,(\cos i+\cos\theta)} \tag{13}$$

or

$$\frac{d\theta}{dn} = \frac{\lambda}{e\cos i}\tan\frac{i-\theta}{2}$$

Combining this with (11)

$$\frac{d\theta}{dn} = \frac{\lambda}{eD\cos i} = \frac{\sin i-\sin\theta}{e\cos i} \tag{14}$$

Since, in equation (13), e is not determinable, it is necessary to compare increments $\Delta dn/d\theta$ in terms of the corresponding increments Δe, whence

$$\Delta(dn/d\theta) = \left(\cos i/\lambda\tan\frac{i-\theta}{2}\right)\Delta e \tag{15}$$

Table 18 also contains data of this kind computed separately for the Fraunhofer lines, D, C, etc., employed and their mean values. To find the mean width of fringes between these lines, their angular deviations were divided by the number of fringes counted between them at different values of e. The results agree as closely as the difficulty of the observations warrants. One may note that without removing N, the corresponding coefficients would be $\Delta d(n+N)/d\theta$, and these are much more in error, here and in the preceding cases. If from $d\theta/dn$, e is eliminated in terms of $(n+N)$ the equation is

$$\frac{d\theta}{dn} = \frac{\lambda}{D}\frac{1}{(n+N_0)\cos i} \tag{16}$$

so that for a given value of i, θ, N_0, they decrease in size with n. If $n=0$, they reach the limiting size

$$\frac{d\theta}{dn} = \frac{\lambda}{DN_0\cos i}$$

If the crack N_0D should be made infinitely small, they would be infinitely large. To pass through infinity, N_0 must be negative, which has no meaning for $i>\theta$, or would place one effective edge of the crack S behind the other. These inferences agree with the observations as above detailed. If, however, $i<\theta$, a negative value of N_0 restores equation (16) for $n=0$ to equation (17), as was actually observed (figs. 35 and 36).

Finally, equation (14) might be used for observation in the incremented form

$$\Delta(de/d\theta) = \frac{D \cos i}{\lambda} \Delta e \tag{17}$$

but I did not succeed with it. One loses track of the run of a fringe with de.

60. Colored slit images and disk colors of coronas.—In the above experiment the fringes were but a few minutes apart. It is obvious, however, that if N_0 is sufficiently small the fringes will grow with decreasing n, in angular magnitude, until there are but a few black bands in the spectrum. Under these circumstances, the undeviated image of the superimposed slits must appear colored, particularly so if an effect equivalent to N_0 is present throughout the grating. This phenomenon of colored slits is apparently of interest in its bearing on the theory of coronas, where there is also an interference phenomenon superimposed upon a diffraction phenomenon, as is evidenced by the brilliant disk colors. For instance, suppose a corona were produced by a sufficient number of fog-particles distributed throughout a plane normal to the undeviated rays. Now let the alternate particles be moved *in the same way* slightly to the rear of their original position and let the distance between the two planes be small relatively to the wave-length of light. In such a case there should be two identical coronas, superimposed in all their parts, and they should therefore interfere. Inasmuch, however, as even small fog-particles are of the order of size of 0.0001 cm. and their mean distance apart 50 times larger, *i.e.*, 0.005 cm., it remains to be proved whether such an effect can be looked to as an explanation of the disk colors of coronas.

CHAPTER VII.

INDEPENDENCE OF CORONAS OF THICKNESS OF THE FOG-LAYER.

61. Introductory.—As an adequate theory of coronas is yet to be given, experiments with a definite bearing on the various features of the phenomenon are desirable. In earlier work* I endeavored to elucidate the character of the interference phenomenon superimposed on the diffraction phenomenon, whereby the disks of coronas with white light eventually show a rhythmic succession of colors. A theory was suggested corresponding to that given by Verdet for the lamellar grating. Inferences so deduced were quantitatively in accord with facts. I showed that the reappearance of the same type of corona corresponds to a succession of diameters of fog-particles in the order of the natural numbers $n = 1, 2, 3, 4$, etc. Further, in a survey of coronas obtained with monochromatic light (mercury), it appeared that the disk and the first ring are alternately luminous in a way corresponding to the interference phenomenon in question. Finally, that in case of even the largest true coronas fog-particles of an order of size greater than 10^{-4} cm. were in question, beyond which the corona degenerates into a mere fog.

In a preceding paper† I touched upon the question of the interference of coronas due separately to two successive layers of fog-particles normal to the line of sight, with each other, but the quantitative relations did not seem to be as promising as interferences inferred from the mere thickness of fog-particles, already alluded to in comparison with the lamellar grating.

62. Effect of thickness. Apparatus.—From the point of view of the elementary theory the effect of the thickness of the fog-layer should be negligible; but it does not by any means follow that this is actually the case. In very many experiments with coronas the thickness of the fog-layer is not at the observer's disposal or cases of different thicknesses have to be compared. Hence the following experiment was devised with the object of definitely testing the question:

In fig. 39 FF' is a cross-section of the fog-chamber, a long rectangular trough of wood, cloth-lined and provided with two glass plates g and g' on the broad sides of the trough. The pool of water is seen at w. Two mirrors M and M', of plate glass, horizontally hinged at h and h' and capable of being displaced parallel to their own plane by virtue of the screw-extension

* See Publication No. 96, Carnegie Institution of Washington, Part I, 1908; Part II, 1910. American Journal of Science, XXIV, pp. 309–312, 1907 (cycles of coronas); *ibid.*, XXV, p. 224, 1908 (axial colors); *ibid.*, XXVII, pp. 73–81, 1909 (mercury light).

† *Cf.* Proc. Am. Phil. Soc., April, 1911.

adjustment s and s', are attached parallel to each other. The lower margin of M is somewhat above the upper margin of M'. Hence the observer on the left of the apparatus (in front) sees the direct rays $A\ A'$ from the source as well as the reflected rays $B\ M\ M'\ B'$. By properly adjusting the angle α, the small round distant source of white light and its image in the mirrors (A' and B' respectively) may be made to coincide at the upper edge of M'. In such a case the corona due to the direct rays produced by a single thickness, $d = 15.5$ cm., of fog-layer, should exactly coincide with, *i.e.*, be the complement of, the coronas due to the reflected rays and produced by a triple thickness, $d' = 46.5$ cm., of fog-layer, if the variation of thickness in question is without effect. Otherwise the coronas should be dislocated at the margin of the mirrors.

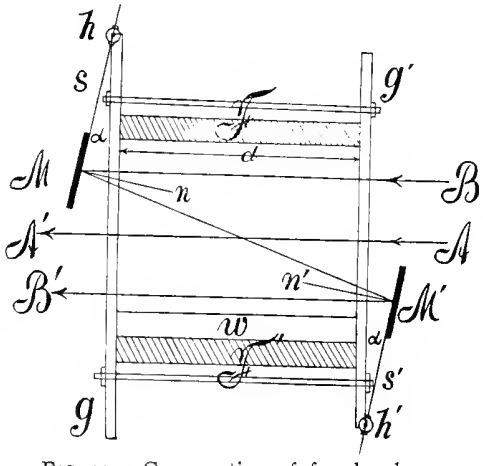

FIG. 39.—Cross-section of fog-chamber, showing path of direct and reflected rays.

63. Results and summary.—These experiments were carried through in regular series, for the dust nuclei of ordinary air as well as for an artificial nucleation due to phosphorus. The exhaustions were made systematically every 2 minutes. The coronas due both to the A rays (direct) and the B rays (reflected) were read off as quickly as possible, after which filtered air was introduced to dispel the coronas by evaporating the fog-particles. In this way about 20 coronas were successively compared, from the largest easily observable, having an aperture of about 34°, to the small ones of vanishing size, the nucleation ranging from about 10^6 to zero (particles per cubic centimeter) and the fog-particles from a diameter of about 2×10^{-4} cm. to 10^{-3} cm.

In no case was there any dislocation of coronas, or of color, detected, though naturally the coronas in case of reflection from the mirrors were somewhat more yellowish in color (due to the reflecting surfaces) and less vivid (due to the reflections and greater thickness of fog-layer; for it is hardly probable that the fog-particles are quite of a size). The continuity of corresponding colored rings, however, was exact within the limits of observation. Hence thicknesses of 15 cm. and over 46 cm. produce identical coronas identical in aperture; or the thickness of the cloud-layer is without influence on the coronas.

CHAPTER VIII.

EXPERIMENTS WITH A VERY SMALL FOG-CHAMBER, TOGETHER WITH DATA ON THE DECAY OF LARGE AND SMALL NUCLEI.

64. Small fog-chamber.—Tables 19 and 20 contain results with exceptionally small fog-chambers in relation to the size of the vacuum-chamber and the diameter of the connecting tube. They are compared with the data of the smallest of the fog-chambers recently* observed. The dimensions of the cylindrical chambers of glass were, respectively, length 20 cm., diameter 6.5 cm. for the pint chamber and length 16 cm., diameter 11 cm. for the quart chamber, both attached to a 2-inch brass exhaustion pipe 15 cm. long.

TABLE 19.—Small (quart) fog-chamber. $l = 16$ cm.; $r = 5.5$ cm.; cleaned with 8 exhaustions; vapor nuclei and x-ray effect; barometer 76.40 cm. at 24.5°; n in the exhausted F. C.

	$\frac{\delta p}{p}$	cor. s	$n \times 10^{-3}$		$\frac{\delta p}{p}$	cor. s	$n \times 10^{-3}$
Vapor nuclei	0.203	0.0	0.0	Vapor nuclei	0.383	*y o* 15	773
	0.220	0.0	0.0		0.357	6.1	50
	0.249	0.0	0.0		0.343	4.3	18.3
	0.275	0.0	0.0		0.327	2.9	5.0
	0.291	2.0	1.4		0.304	2.4	2.9
	0.307	2.5	2.9		0.290	2.0	1.5
	0.327	3.5	8.5	Ions (x-rays)	0.210	0.0	0.0
	0.333	4.0	14.2		0.250	1.0	0.2
	0.345	4.4	19.7		0.275	*y o* 13.0	425
	0.356	5.8	41.2		0.301	*g* 17	825
	0.367	8.5	136		0.321	*v* 19	1310
	0.380	12.2	417		0.334	*r* 20	1620
	0.393	*g* 16.7	1087		0.304	*v* 19	1260
	0.393	*g* 17.5	1290		0.268	*r* 10.2	186
	0.410	*v* 18.5	1570		0.253	2.3	2.1
	0.415	*v* 18	2180		0.244	1.0	0.2
	0.435	*r*	2740				
	0.487	*r o* 21	3760				

The results computed in the usual way are given above, $s/30$ denoting the approximate angular diameter of the coronas, δp the drop of pressure, n the number of nuclei per cubic centimeter in the exhausted fog-chamber. The goniometer in this case was a special contrivance shown in fig. 40, in which the eye was at the near wall of the fog-chamber and the needles for measuring angles beyond the far wall. This makes it possible to use small fog-chambers and yet measure large apertures.

* *Cf.* Publication No. 96, Carnegie Institution of Washington, Part II, §27 *et seq.*, 1910.

The results contained in these tables show curiously enough that for smaller exhaustions the small fog-chamber is more efficient than the larger fog-chamber (fig. 41), but at larger exhaustions (δp) the reverse is the case (figs. 42 and 43). Similarly, or compatibly with this result, ions are more easily caught by the small fog-chamber than by the large chamber, whereas the finer vapor nuclei are more easily caught by the larger chamber. In both cases the number caught increases with the exhaustion (δp), continually. The upper coronas of the pint chamber, however, are not brilliant in color and they are diffuse in character. The goniometer measurement nevertheless shows very definite increase of aperture for increased exhaustion, even throughout the same color or type of corona. It follows, then, that increased exhaustion must continually bring down more water, even at the highest exhaustion used. The number of nuclei eventually caught approaches 5 million per cubic centimeter.

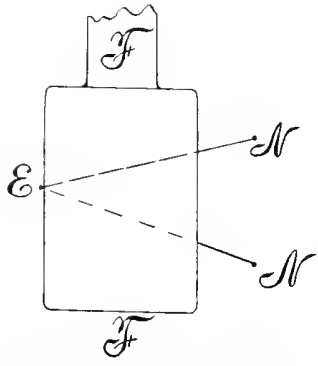

FIG. 40.—Diagram of fog-chamber and straddling goniometer.

The above results are difficult to discuss. It is, however, probable that

TABLE 20.—Pint bottle fog-chamber; length 20 cm. (glass*) and 15 cm. brass, radius 6.5 cm.; cleaned with 17 exhaustions. Vapor nuclei found in ascending and descending exhaustions; barometer, 75.87 cm. at 27.5°; new (straddling) goniometer, n in exhausted F. C.

	$\frac{\delta p}{p}$	cor. s	$n \times 10^{-3}$		$\frac{\delta p}{p}$	cor s	$n \times 10^{-3}$
Vapor nuclei	0.257	?	0.0	Ions (x-rays)	0.230	0.0	
	0.278	?	0.0		0.248	0.0	0.0
	0.299	1.5	.5		0.270	*c* 12	325
	0.328	3.0	5.4		0.290	*c* 18	1100
	0.353	*g* 7.0	76.8		0.311	*r* 20	155
	0.360	*vb* 10.0	217		0.373	*r* 24	3210
	0.369	*g* 14	600		0.443	*y'* 26	450
	0.385	*g'* 16	980		0.305	*r* 20	1520
	0.401	*c* 18	1310		0.276	*g*	708
	0.414	*c* 18.5	1570		0.261	*r* 9	123
	0.432	*r'* 19	1771		0.250	4.0	11.4
	0.457	*r'* 20	2140		0.244	.0	
	0.490	*r'* 22	2910	Vapor nuclei	0.263	faint 1.0	.2
	0.540	*r'* 24†	3990		0.296	2.0	1.5
	0.418	*c* 17	1335		0.346	5.0	27.1
	0.390	*g*	876		0.361	10.0	214
	0.373	*o* 14	603				
	0.343	*r* 6.2	51				
	0.325	3.5	9.0				
	0.303	3.0	5.2				
	0.282	.0	.0				

*Brass pipe not included.
†Aperture of *r'* continually increasing, coronas diffuse.

as the fog-chamber becomes smaller, the rapidity of radiation from without inward increases conformably with the smaller bulk of air adiabatically

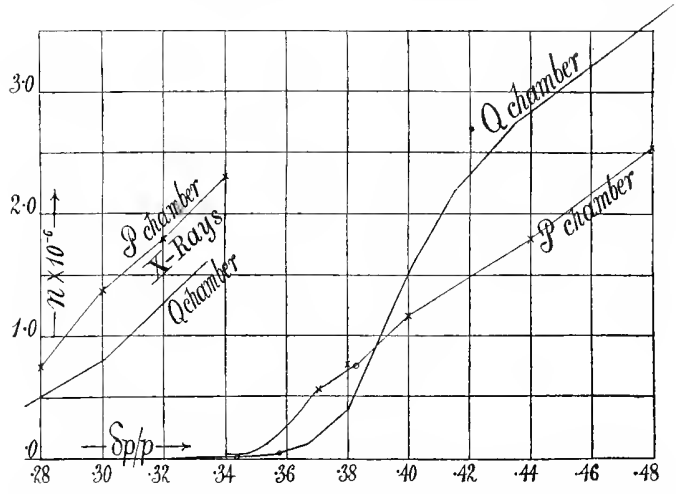

FIG. 41.—Number, n, of nuclei per cubic centimeter, caught at different exhaustions, in case of pint and quart fog-chambers.

cooled by sudden exhaustion; or, other things being equal, that conditions favorable to the attainment of a high degree of adiabatic cooling are more

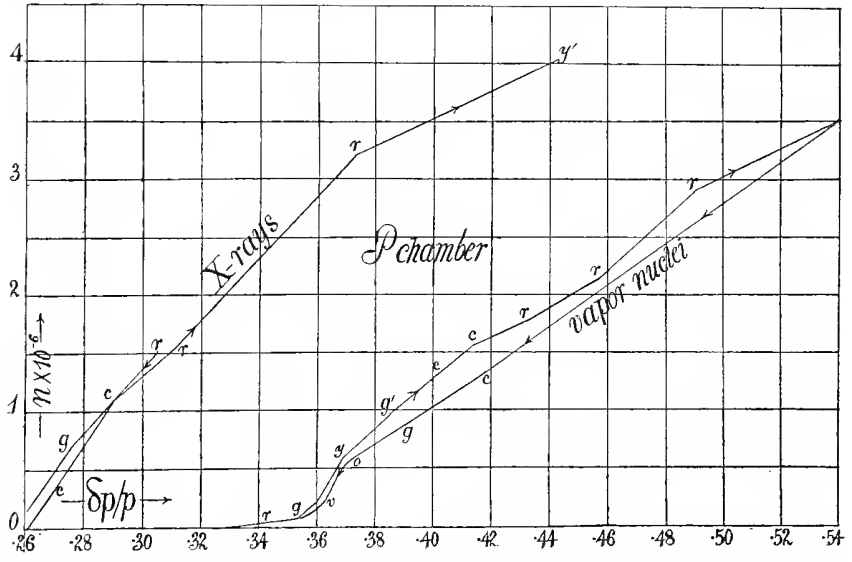

FIG. 42.—Number, n, of nuclei per cubic centimeter, caught at different exhaustions, in cases of pint and quart fog-chambers.

easily met, in proportion as a larger bulk of air is cooled. On the other hand, however, the increased bulk is more difficult to exhaust with ade-

quate rapidity. In case of the quart fog-chamber in comparison with the pint fog-chamber, each with an identical 2-inch exhaustion pipe, these transitional relations seem to be manifest in the experiments made.

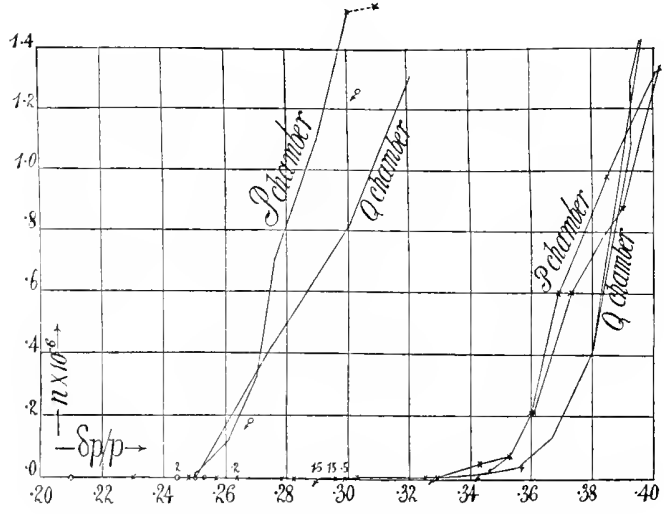

FIG. 43.—Sudden drop of pressure δp from total pressure p.

65. Decay of different sizes of ions.—A second series of experiments into which I entered at some length and which, though from the nature of the experiment they can not lay claim to a high order of precision,

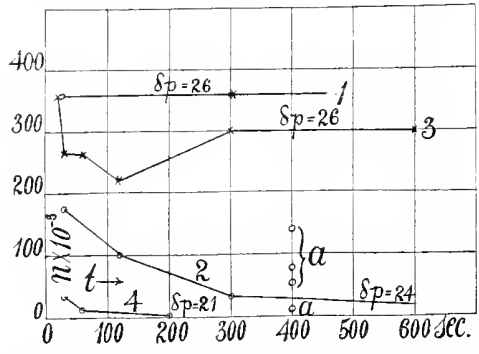

FIG. 44.—Number of nuclei per cubic centimeter in the lapse of time, after cut-off of X-radiation, for different drops of pressure δp; a, vapor nuclei belonging to series 1 and 3.

nevertheless lead to very definite results, is contained in tables 21, 22, and 23. These ions were produced by X-rays (of moderate intensity) in an aluminum-covered fog-chamber with short exposures to an X-ray bulb and a glass fog-chamber. The data show that no persistent nuclei of the

usual large type are appreciably produced, since if present they require almost no supersaturation of moist air for condensation. Moreover, the vapor nuclei of dust-free wet air are not caught in the presence of ions, or else their number is specially determined and smaller in comparison

TABLE 21.—Rate of decay for different sizes of ions. Aluminum-covered fog-chamber.

$\delta p/p$	t Lapse sec.	$n \times 10^{-3}$	$b \times 10^{6}$	$r \times 10^{7}$
0.35	D. f. air	77		0.43
	30	360		
	300	360		
	D. f. air	140		
0.32	D. f. air	9.5	0.10	0.48
	30	175		
	120	100		
	300	31		
0.35	30	360		0.43
	D. f. air	54		
	30	265		
	60	265		
	120	220		
	300	300		
	600	300		
	D. f. air	140		
0.28	30	33	2.0	0.60
	60	12		
	60	12		
	200	2.3		

TABLE 22.—Decay of different sizes of ions.

$\delta p/p$	t Lapse sec.	$n \times 10^{-3}$	$b \times 10^{6}$	$r \times 10^{7}$
0.26	0	73.8	43	0.66
	30	0.9		
	15	1.3		
0.28	0	484	2	0.61
	30	15.7		
0.30	15	32.8	3	0.54
	60	6.4		
0.33	15	36.8	0.4	0.48
	60	29.7		
	30	29.7		
	120	21.8		
	240	6.2		
	D. f. air	4.4		
0.35	15	55.0	0.1	0.43
	30	113.5		
	60	86.7		
	120	55.0		
	240	38.8		
	D. f. air	31.3		

with the ions obtained by the X-rays. This premised, the tables give the relative drop of pressure $\delta p/p$ from p, and the lapse of time t between the instant the X-radiation is cut off and the instant of the exhaustion made to catch ions, together with the number of nuclei, n per cubic centimeter, caught. The column r is an estimate of the size of nuclei obtained from the drop of pressure δp and b is the rate of decay.

In table 21, reproduced in fig. 44, the nucleation discovered in dust-free wet air at any $\delta p/p$ in the absence of X-radiation is always relatively small, even at the highest exhaustions made (see points a in figure).

TABLE 23.—Decay of different sizes of ions.

$\delta p/p$	t Lapse sec.	$n \times 10^{-3}$	$b \times 10^{6}$	$r \times 10^{7}$
0.26	0	39.6	30	0.66
	30	1.1		
0.28	0	378	3	0.61
	30	12.4		
0.30	30	16.8	4	0.54
	60	6.4		
	120	2.4		
	0	630		
0.33	30	24.8	0.5	0.48
	60	57.6		
	120	26.1		
	240	9.1		
	30	24.8		
	D. f. air	5.5		
	60	47.0		
	*30	34.8		
0.35	30	109.2	0.1	0.44
	60	79.7		
	120	51.7		
	240	46.1		
	D. f. air	34.7		

* Aluminum screen on.

Nevertheless, in the first and third series the persistence of ions surviving as much as 10 minutes after exposure is remarkably large, as if all nuclei (vapor nuclei and ions) were eventually caught together. Series 3 passes erratically through a minimum, but nevertheless points to an almost indefinite persistence throughout. On the other hand, at the lower exhaustion, series 2 and 4, the number of nuclei soon vanishes. The rates of decay determined by the usual equation

$$\Delta \frac{1}{n} = b\Delta t \text{ or } dn/dt = -bn^2$$

in series 2, however, are usually less than $b = 10^{-7}$. In series 4 the rate would be about $b = 2 \times 10^{-6}$, but too few nuclei are present for certainty of measurement. The chief interest lies in series 1 and 3, showing that at

a sufficiently high drop in pressure, $\delta p/p = 0.35$, the ions produced in dust-free moist air by the X-rays decay at phenomenally small rates, or are almost indefinitely persistent, whereas larger nuclei decay faster in proportion to their size.

Similar facts are brought out by tables 22 and 23, constructed on the same plan and showing the drop of pressure δp from the total pressure p, from which the radius r of the drop is estimated. The nucleation n is given after the lapse of seconds t since the X-radiation ceased. From this the coefficient of decay b is computed. Both tables show that as $\delta p/p$ decreases or r increases, b increases at a rapidly accelerated rate, from very small values $b = 10^{-7}$, to enormous values. The small coefficient b is less than one-tenth the normal value obtained for ions with the electrometer (of the order of 10^{-6}), while the large values are nearly 50 times the normal value.

The interpretation of these results is made difficult by the variability of the X-ray bulb. It is safe to assert, however, that the large ions or nuclei produced by the X-rays in dust-free wet air vanish with relatively enormous rapidity, whereas the very small nuclei are almost indefinitely persistent, and that there is a definite relation between the rate of decay and the size of nucleus. If, therefore, we regard these nuclei as water droplets of different sizes, evaporation is rapid until a limiting diameter depending on the intensity of radiation is reached, after which evaporation nearly ceases. It is also probable, and will be further brought out in the next chapter, that the limiting diameter increases with the intensity of radiation. If, therefore, as has been supposed, the X-rays produce any chemical body which may go into solution, the greater or less abundance of this body, supplied by greater or less intensity of X-radiation, would account for larger or smaller persistent nuclei. The next chapter is a further contribution to this question.

CHAPTER IX.

ON THE PERSISTENT NUCLEI PRODUCED BY THE X-RAYS.

66. Introductory.—Throughout many of my experiments on condensation* and particularly during the earlier work,† I made use of a fog-chamber impregnated, when hot, with a mixture of wax and Burgundy pitch. These chambers were usually of an elongated rectangular form, with plates of glass on the opposed broad sides, cemented on, while hot, with an intervening layer of flat cotton wick saturated with the same molten mixture, and allowed to cool under pressure. Wooden clamps on the outside are a safeguard against any yielding due to the viscosity of the cement. Such fog-chambers may be made rigorously tight and they last for years, even when charged with water. The coronas are strong (the fog-layers being thick), visible without distortion and measurable throughout their extent, even when approaching 50° of aperture with a 6-inch stratum of fog-particles, or more.

These fog-chambers have the additional advantage of being exceedingly pervious to soft X-rays, and hence throughout my work I encountered the phenomenon of persistent nucleation, produced in dust-free wet air by the X-rays, when acting continuously for a period of minutes. I can not but think that the occurrence of persistent nuclei, as an accompaniment of an adequately strong and adequately prolonged X-radiation, are an important property of these rays. It would ally them in quality with ultra-violet light, with which C. T. R. Wilson‡ and others obtained similar results. The present observations would, therefore, have some bearing on the probability of the pulse theory, which has recently been put seriously on the defensive by Prof. H. Bragg.§

Again, if it is true that beyond a certain density of ionization (a sufficient number of ions per cubic centimeter) the ions invariably react on each other, or on the wet dust-free medium, to produce permanent nuclei of enormous size by any method whatsoever, this fact is itself a result of importance.

Nevertheless, these effects of X-light have not always been taken seriously. Thus, for instance. Mr. C. T. R. Wilson‖ states: " . . . . results, obtained with a chamber of wood impregnated with resinous cement and not rigorously shielded from all possible direct electrical effects from an

* Publication No. 62, Carnegie Institution of Washington, pp. 18–21, 1907.
† Am. Journ. of Sci., XIX, pp. 175–184, 1905; Publication No. 40, Carnegie Institution of Washington, pp. 1–16, 1906.
‡ C. T. R. Wilson, Phil. Trans., A, vol. 192, pp. 412 *et seq.*
§ Nature, vol. 85, p. 491, 1911.
‖ C. T. R. Wilson, Nature, vol. 74, p. 620, 1906.

X-ray bulb placed a few centimeters from it, are not free from ambiguity." Criticism of this kind, it seems to me, is quite gratuitous; for it is the first thing anybody under such circumstances would try for himself, viz, to see whether discrepancies due to electro-static or other induction or to resonance are really absent. To do this it is merely necessary to place a tin plate before the bulb, whereupon no persistent nuclei are obtained at all comparable with the yield of nuclei through an identical aluminum plate. Naturally I repeatedly shielded the whole apparatus; but apart from this Wilson knows, for he made this experiment, as I also did, that a fog-chamber damp within shields itself. I doubt whether it need even be cloth-lined, as mine always were. Here I would also like to add a word in defence of the above type of fog-chamber. If there were within any source of nuclei whatsoever, that fact could not escape detection; for the chamber must be rigorously and permanently dust-free before any experiments can be tried with it.

Again, in a controversy with G. C. Simpson,* Wilson† remarks:

> It is quite true that spark discharges in air, as well as other ionizing processes which are accompanied by chemical effects, do produce large persistent nuclei in addition to the ordinary ions; a lightning-flash would, therefore, almost certainly produce such nuclei.

As to spark discharge Wilson says (Phil. Trans., *l.c.*, p. 439): "No condensation nuclei were produced except when the point of wire was luminous when viewed in the dark." Wilson's evidence is, therefore, in turn ambiguous as to large nuclei produced from ions, for to draw such an inference he should first sift out the metallic particles transferred. Furthermore, the action of ultra-violet light, which produces persistent nucleation similar in character to that in question, is not a normal ionizing process, even if slow-moving ions are produced. So far as I can see, the only unambiguous ionizing process productive of persistent nuclei is given by my experiments with X-rays which Wilson has not only not acknowledged, but done his best to discredit. It is true that in the meantime E. Barkow,‡ in Professor Richarz's laboratory, succeeded in corroborating the fact that persistent nuclei are produced by X-light, but as he worked with an aluminum screened glass fog-chamber, he was obliged to use X-radiation pushed to the limit of intensity.

In view of this unsatisfactory state of the case, I have on two occasions incidentally resumed the experiments for persistent nuclei, once about a year ago, and again quite recently. I used an ordinary 4-inch spark coil energized by 6 or 7 storage cells and a Foucault interrupter. The common X-ray bulbs 4 inches in diameter, or even the smaller bulb 3 inches in diameter, functioned equally well. They were placed above or at the end of the long rectangular fog-chamber, the conventional earthed screen of tin plate, with a hole in it 4 inches in diameter, covered with aluminum foil,

* G. C. Simpson, Phil. Mag., XVII, p. 619, 1909.
† C. T. R. Wilson, Phil. Mag., XVII, pp. 634–641, 1909; *cf.* 640.
‡ E. Barkow, Inaugural Dissertation, Marburg, 1906.

being interposed for safety. To close this hole with a tin plate, or even a glass plate in the case of the coil specified, is to cut off all effects so far as the production of persistent nuclei is concerned. Ions, of course, are still produced in abundance. The time of exposure was usually about 2 minutes and the lapse of time prior to exhaustion thereafter usually 1 minute. As a rule, the exhaustion was such as would not catch ions, so that exhaustion could be made if necessary even during exposure.

67. Older series of experiments.—A brief digest may be given of the work of last year. The endeavor to further identify the persistent nuclei was begun with the normal cylindrical glass fog-chamber and the old X-ray bulbs Nos. 0 to 4 heretofore described (*l.c.*). The chamber may be cleaned with a rubber probang and the cap is to be earthed. Aluminum jackets were provided for the body. No effect was obtainable for exposures of 2 minutes and longer. The chamber was then tested with the walls dry, with an absence of earth connection, with aluminum tubes and brass tubes within, with long exposures up to 5 minutes, all to no effect. Persistent nuclei were not producible. Only once, in a first experiment, with the vibrator not quite normal in action, I obtained about 25,000 nuclei per cubic centimeter through glass. The experiment could not be repeated. Cold bulbs were as inefficient as warm bulbs. The X-ray bulbs were then softened till the anodal light appeared and then successively sparked to hardness. No effect was observable. Meanwhile all the bulbs showed good shadows on a fluorescent screen.

The small glass fog-chamber was now installed, but no further success was obtainable. The failure to obtain persistent nuclei through glass contrasts strangely with the marked results obtained on an earlier occasion.* The difference may be due either to a more efficient bulb, or to a thinner fog-chamber used in the latter case. But a full explanation is yet to be found.

Persistent nuclei were not again detected until the wood fog-chamber described (45 by 15 by 15 cubic centimeters) was installed, with the X-ray bulb at a distance of about $D = 10$ cm. above it. Here bulb No. 4, for a two-minute exposure and a thirty-second lapse, gave at once 89,000 nuclei per cubic centimeter, repeatedly and strong. The wood fog-chamber was now encased in aluminum above and with tin plates on the sides and end, with an apparently even greater advantage in the production of persistent nuclei. Thus, for instance, 165,000 nuclei per cubic centimeter were obtained, after a lapse of 1 minute succeeding an exposure of 2 minutes; while a tin plate on top (completing the tin case) absolutely removed all action. The persistent nuclei are thus due to X-radiation and not to induced or Herzian effects. The coronas are characteristic, being heavy with much rain, and the second exhaustion, for cleaning, frequently shows larger

* Publication No. 62, Carnegie Institution of Washington, p. 18, 1907.

coronas than the first. Spontaneous generation of nuclei during long exposure could not be detected. A trial of the available bulbs under like circumstances, for efficiency, showed (n nuclei per cubic centimeter)

No. 0, $n=0$ No. 1, $n=26{,}000$ No. 2, —— No. 3, $n=1{,}600$ No. 4, $n=90{,}000$–$165{,}000$

so that only bulbs No. 1 and No. 4 were good producers of persistent nuclei, at a distance of 10 cm. from the fog-chamber.

Next day, however, the effect of No. 4, for the same distance, $D=10$ cm., had materially weakened, as if the dampness had penetrated the wood until it became all but impervious. The results, for an exposure of 3 minutes, were, for instance,

No. 0, $n=0$ No. 1, $n=20{,}000$ No. 2, $n=14{,}000$ No. 3, $n=0$ No. 4, $n=6{,}000$

No. 1 with longer exposures, 5 minutes, gave 35,000 nuclei for all lapses of time. The further trial to soften No. 3 was ineffectual, and continued so after sparking to hardness. In the pursuit of this group of experiments, bulbs Nos. 1, 3, and 4 gradually became inefficient. Cooling with water, variations at the interrupter, etc., did not improve the results. The fog-chamber seemed to gradually shut off radiation coming from a distance of 10 cm., and the bulbs deteriorated.

The top of the fog-chamber was now covered with thin aluminum 0.05 cm. thick and the X-ray bulbs were placed close to it, so that the distance, D, was now reduced to zero. The production of persistent nuclei was again strong, No. 4 after an exposure of 2 minutes, for instance, showing 46,000 nuclei, in many successive experiments. Secondary radiation from lead, etc., produced no result.

Summarizing the above experiments, it appears that all bulbs lose the power of producing persistent nuclei after continued use. They soon cease to penetrate glass or even wood from a distance. Close up to the wood walls, however, the effect (through an aluminum screen for safety) is always marked. A wood fog-chamber aging in damp air seems to grow continually less pervious, or dry wood is superior to damp wood. The test showing that an aluminum-covered chamber is pervious, whereas a tin-covered chamber is not so, is sufficient to guarantee the radiation effect, as compared with possible discrepancies due to induction and resonance. So also is the difference in the efficiency of bulbs. Secondary radiation is powerless to produce persistent nuclei. Spontaneous generation could not be detected in these experiments.

68. Recent experiments.—The two fog-chambers used were of wood. No. 1 had just been charged with water; the wood fiber, therefore, was dry within, whereas No. 2 had held a charge of water for about a year and the fiber was probably wet. As a result, No. 1 was found to be much more pervious than No. 2.

Table 24 gives an exhibit of the results, showing the fog-chamber and bulb used, the time of exposure, the time of observation (lapse) after exposure, the distance, D, between the outside of the bulb and the fog-chamber, the apertures of coronas, s, in the first and second exhaustions, and n, the corresponding nucleation. The corona of the first exhaustion was usually distorted and not measurable. The fog was allowed to subside completely, which it did almost at once, after which filtered air was introduced and a second identical exhaustion made. These second coronas are uniform, and in systematic work the first nucleation may, in a measure, be inferred from them. The column marked ions shows the number present under a sufficiently high exhaustion to catch them all. In this case the exhaustion is made during exposure, because of the rapid decay. The remarks refer to the presence or absence of the tin screen placed over the aluminum cover between bulb and fog-chamber to cut off radiation, to the character of the bulb used, etc. Some comparative experiments are made with radium, the available strength of which did not produce persistent nuclei. In the following paragraphs I shall give a brief description of the features of the phenomenon.

TABLE 24.—Results of experiments with persistent nuclei. Wood fog-chambers. $\delta p = 17$ cm. Fog-chamber within metal screen with Al below bulb. Coil with 6–7 storage cells.

I. BULBS (4″) OVER FOG-CHAMBER.*

Bulb No.	Exposure.	Lapse.	$n_1 \times 10^{-3}$	$n_2 \times 10^{-3}$	$n \times 10^{-3}$ (ions)	D	Remarks.
	min.	*min.*					
N	1	1	Fog.	17	....	0	
N	1.5	..	Fog. 64	37	....	0	
N	1.5	1	0	..	....	0	Tin shield on.
N	1.5	1	Fog.	59	....	0	Off.
N	1.5	2	Fog.	35	....	0	
7″ spark							
u	1	1	0	..	....	0	Very hard.
0	1.5	1	Fog.	12	....	0	
N	2	1	Fog.	10	....	0	
3	2	1	Fog.	37	....	0	
N	2	1	Fog.	17	....	0	
No evidence of soaking. Difference due to bulb and sparker. Fog-chamber changed. Soaked a year and more impervious. Quite tight.							
N	2	1	0.5	....	....	0	
U	4	1	2.6	....	.. .	0	Softened.
	4	1	9.5	....	....	0	
	10	1	39	....	....	0	
	10	1	39	....	....	0	
All the preceding facts brought out on smaller scale. Time of exposure important.							

*Fog-chamber not quite tight. Short exposure has no effect; acceleration on increase of time. All bulbs active unless too hard for energizing. First fog a whirlwind. Disk or strip of tin as large as bulb cuts off all effect.

TABLE 24—Continued.

II. BULB (4″) AT END OF FOG-CHAMBER.

First fog decreases to nothing from bulb to free end of chamber.

Bulb No.	Exposure.	Lapse.	$n_1 \times 10^{-3}$	$n_2 \times 10^{-3}$	$n \times 10^{-3}$ (ions)	D	Remarks.
	min.	*min.*					
N	2	1	Fog. 12	4	....	1	
N	2	1	Fog.	9	....	1	Tin jacket on.
N	2–3	1	Fog elliptic	10	....	1	
N	5	1	Fog. end to end	35	....	1	
N	5	1	0	....	....	1	Tin screen before bulb.
N	5	1	Fog. end to end	29	....	1	
N	5	1	Fog.	7	....	1	1½″ hole in screen
N	5	1	3	.6	....	1	¾″ hole in screen
N	5	1	0	....	....	1	½″ hole in screen
Tests made for persistent nuclei and ions at different distances, successively. Also with radium.							
N	5	1	10.8	16	670	1	
	5	1	20	1.6	530	4	X-rays
	5	1	1.2	....	400	10	X-rays
	5	1	.4	....	330	24	
I–V	....	....	....	....	130	..	Radium on side.
I–V	3 hours	....	....	....	270	..	Radium within.
Time effect (exposures).							
N	5	1	59	....	....	1	
	2	1	23	....	....	1	
	1	1	.3	....	....	1	
	5	1	0	....	....	1	Tin screen.
Time lapse after exposure.							
N	5	1	7	2.0 1.6	....	1	
	5	2	11	....	....	1	
	5	4	14	....	....	1	
	5	1	7	....	....	1	

III. SMALL BULB (3″) No. 2, AT END OF FOG-CHAMBER.

N	5	1	21	3	....	1	
2	5	1	Fog. 130	25	....	1	
2	5	1	0	....	....	1	Glass screen 15 cm. thick.
N	5	1	0	....	....	1	Do.

69. Initial fogs.—These are as a rule distorted as heretofore described,* and in a long fog-chamber with the bulb near one end they decrease in size from this to the other end, which is liable to be free from nuclei. Frequently, therefore, the nucleation must be estimated from the second corona, the cloud being precipitated on the nuclei not caught in the first exhaustion. The first nucleation may be three or more times larger.

But it is the whirlwind character of this first fog to which I wish chiefly to refer. It is quite dissipated in a relatively short time, precisely as if it were under the influence of a point discharge. True, the X-ray tube, if in action, is liable to make the surrounding atmosphere strongly negative; but that any electrification should exist on the fog-chamber, 2 or 4 minutes after exposure, is out of the question. In my apparatus the whole is kept permanently earthed through the metallic vacuum-chamber. Nevertheless, I most carefully jacketed the fog-chamber with tin during exposure, though the effect was obviously *nil*. I also supposed that the fog-particles precipitated on persistent nuclei might carry charge; but no evidence of this could be obtained. The whirlwind is, therefore, probably due to gravitational readjustment of very heavy fog-particles, precipitated on large persistent nuclei.

Another characteristic feature observed in the production of persistent nuclei is this, that the number per cubic centimeter increases at an accelerated rate with the time of exposure, for a fixed ionization. In other words, the number produced per second by exposure to X-rays increases with the number present. The condition is thus an inversion of the case of the decay of ions, and it is probable that a similar quadratic law, but with positive coefficients, will be applicable. Again, the accelerated production specified is sufficient evidence of generation of nuclei within the medium and not at the walls of the vessel.

Compatibly with this result, the number of the persistent nuclei caught increases, within certain limits, with the time elapsed after the given X-radiation ceases. Thus more are liable to be caught 2 minutes after exposure than 1 minute after exposure; and more 4 minutes than 2 minutes after. Observations of this kind were extremely difficult to make in a way quite trustworthy, because of the variability of the X-ray bulb, and I adduce the mean results of a large number of trials.

70. Amount of ionization needed to produce persistent nuclei.—The ionization, n per cubic centimeter, may be varied by placing the X-ray bulb at different distances, D, from the outside of the fog-chamber, and estimated at a sufficiently high exhaustion to catch them all, by aid of the coronas. The persistent nuclei (n per cubic centimeter) produced in a given time (5 minutes) under the same conditions are determined, in turn, by a correspondingly low exhaustion, after the lapse of 1 minute after exposure to the rays.

* Am. Journ., XIX, pp. 185–194, 1905.

The ionization thus must exceed at least 300,000 per cubic centimeter if a crop of persistent nuclei requiring scarcely any supersaturation to condense water-vapor is to be observable, within a few minutes of exposure. The number of these nuclei found, in view of the distorted coronas, etc., is, of course, an estimate; but it is none the less clear that here again the rate of production of large persistent nuclei increases at an accelerated rate with the ionization.

One may note that in no case was it possible to obtain persistent nuclei on exposure through a glass plate 0.15 cm. thick. This glass plate, in case of the coil used, cuts off all influence almost as effectually as tin plate. I am at a loss to account for this result, as on an earlier occasion persistent nuclei were obtained in abundance through glass. The frequency of similar results might in fact lead one to suggest the possibility of a special kind of X-radiation as the cause of persistent nuclei.

The radium used was sealed in aluminum tubes, so that chiefly the γ rays are in question. The available amount of radium in my possession, compatibly with the ionization produced, is insufficient to generate persistent nuclei in any time. It is none the less important to actually demonstrate that if the ionization produced by radium is sufficient in amount, it will really produce persistent nuclei. Wilson,* indeed, assents to this, referring again to the point discharge.

Radiation.	D	Ions $n\times10^{-3}$	Persistent nuclei, first exhaustion $n\times10^{-3}$	Persistent nuclei, second exhaustion $n\times10^{-3}$
	cm.			
X-rays	1	700	108	16.0
	4	500	20	1.6
	10	400	1.2	....
	24	330	.4	....
Radium, just outside	....	130	.0	....
within, exposure 3 min	....	270	.0	....

Since there is no evidence that persistent nuclei of the present type are associated with some specific kind of mild radiation, the conclusion of the last chapter, *viz*, that these nuclei are ultimately solutional nuclei and that the solute is produced spontaneously in dust-free wet air by the X-rays, is plausible. It is merely necessary to admit that the difference in size of the nuclei of the preceding and the present cases is due to the greater penetration of X-radiation in the latter; *i.e.*, to the greater abundance of the soluble body in question for the case of larger nuclei.

* ". . . that such nuclei should, under appropriate conditions (the occurrence of chemical action giving rise to soluble products) grow into larger bodies is what might be expected; such a growth has for example been observed in the case of the ions arising from a point discharge." (Nature, vol. 74, p. 620, 1906.)

This explanation fails to account, however, for one essential point: it does not easily suggest why the number of persistent nuclei produced per cubic centimeter increases at an *accelerated rate* with the time of exposure to X-radiation, *caet. par.*, a fact long since conclusively brought out in my earlier reports.* The rate at which persistent nuclei are produced increases with the number present, which means that the nuclei or the ions present *must take part* in the production. If, however, it is granted (as I have also shown at length) that the number of nuclei or ions increases in marked degree as the lower limit of size diminishes, and (for simplicity) that the growth of any nucleus increases directly with the time of exposure to the X-rays, then an accelerated increase of persistent nuclei in the same time may be predicted. For nuclei in continually increasing number must fall within the scope of the low exhaustion with which the persistent nuclei in question are to be caught. The coarseness and whirlwind character of the first corona are evidently pointed in the same direction.

* *Cf.* Presidential address, Phys. Review, XXII, pp. 82–110, 1906.

CHAPTER X.

THE RECTIFICATION OF THE SPECTRUM BY THE AID OF TOTAL REFLECTION, TOGETHER WITH A COMPUTATION OF THE SHIFT OF ELLIPSES IN ELLIPTIC INTERFEROMETRY.

71. Introductory.—In my work of last year,* the quantity $\mu - \lambda \frac{d\mu}{d\lambda}$ (μ index of refraction of glass, λ wave-length) occurred in the reductions and in the absence of direct data I temporarily made use of the corresponding quantity computed from standard data for a somewhat similar glass. In this way the amount of displacement of the centers of ellipses per centimeter of displacement of the micrometer was determined. It must, however, frequently be necessary to find $d\mu/d\lambda$ from a small piece of glass, and I have therefore tested the following method in which a Kohlrausch total reflectometer slides along the graduated rail of Rowland's adjustment for the grating, as modified for the plate grating by M. Barus and myself.†

The method is then further modified, in a way that is applicable when a glass grating is given for investigation, as in the immediate problem, but not otherwise. It admits of some interesting applications, as, for instance, to the refraction of the material of film gratings.

In all cases of solids, the refraction of the more strongly refracting liquid in which the solid is submerged must of course be known for all wave-lengths; but this is true for carbon disulphide. If the liquid indices are not known throughout, in terms of wave-length, they may be determined by aid of an air-plate, using virtually the same apparatus and method. I shall give examples of all these measurements below.

72. Apparatus.—In figure 45, AA and BB are the two fixed rails of Rowland's adjustment at right angles to each other. R, joining the vertical axes at a and p, is the cross-rail, stretching from the slide D, which carries the grating g, to the slide C which carries the total reflectometer T. Slides C and D move at right angles to each other and the position x of C is measured along the brass millimeter scale ss by aid of the vernier v.

The rail BB is further provided with a slide F for the plane mirror m, by which white light is thrown upon the slit c on the slide S, through the condensing lens L'. L'' is the achromatic collimating objective and the rod k (which may be grasped in front at h when necessary) is adapted for clamping S and L'' together at the principal focal distance of the latter. The collimator SL'' does not move with D. The grating g, fixed to a hori-

* Publication No. 149, Carnegie Institution of Washington, Part I, 1911. The Production of Elliptic Interferences in Relation to Interferometry.

† American Journal of Science, XXXI, 1911, pp. 85–95.

zontal disk with a spring and three leveling screws, is securely fastened to the table t, which here preferably rotates with the end a of the rod R. The grating, in other words, is kept normal to R, so that the angle of diffraction is zero, while the angle of incidence alone varies when C passes from end to end of AA. If x_1 and x_2 measured on s be the positions of C for identical lines of the spectrum,

$$\lambda/D = (x_2 - x_1)/2R$$

where D is the grating space and R the length ap.

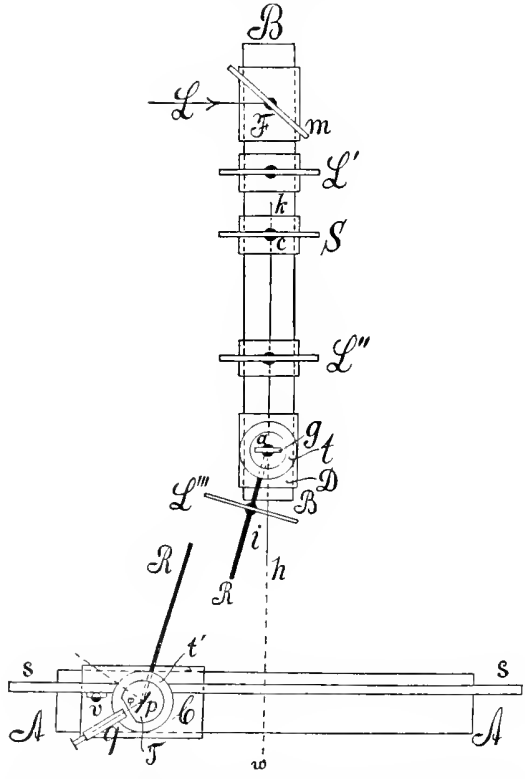

FIG. 45.—Plan of Rowland mounting, adapted for a plate film grating and used for rectification of the spectrum of glass, by total reflection.

The lens L''' on R is the objective of a telescope which focusses the colored image of the slit at the slide C, so that it may there be viewed by an ocular preliminarily. The latter is held in a standard placed on the table t' revolving on a common axis p with this end of R. When the ocular is replaced by the total reflectometer T, of which p is the plate of glass (properly centered) to be examined and q the telescope, the weak lens L''' is superfluous; but as a rule it need not be removed and is rather advantageous in condensing light when sunlight is not used.

When sunlight is used, the lens L''' may be moved a trifle backward so as to put the colored images of the slit slightly in front of the cylindrical glass vessel T of the total reflectometer. If the adjustment is properly made the lines are adequately visible in the telescope q and the index may be found for a given Fraunhofer line without reference to the scale ss. Without sunlight the scale ss is essential. Naturally the images seen in the telescope are not sharp, inasmuch as the cylindrical mantle of the bottle acts as one of the lenses; but they are clear enough for the purpose. It is usually more satisfactory, however, to ignore the lines and to determine the index of refraction for successive positions x of the carriage C on the rail AA, given by the scale ss.

With the total reflectometer revolvable, as a whole, on its axis, the two symmetrical positions of q relative to R give the double angle of total reflection, or 2φ, for the given liquid (usually carbon disulphide) in which the glass plate p is submerged. The graduated circle of the instrument with which the telescope q is rigidly connected is available for the measurement of angles.

73. Methods.—When the air-plate is used for the measurements of the indices of refraction of the liquid, the telescope q is directed along the rail R and $2\varphi_t$ found by rotating the plate p until the two limits or ends of the visible part of the spectrum successively coincide with the cross-hairs. The spectrum is usually nearly homogeneous in color; but the ends are liable to show interference fringes. Simultaneously the position x of the slide C and the temperature t of the liquid are read off. Thus if

$$N_t = 1/\sin \varphi_t$$

be the index * of the liquid at t,

$$N_{20} = N_t(1+\alpha(t-20)) = (1+\alpha(t-20))/\sin \varphi_t$$

is the index at 20°. For carbon disulphide, at mean temperatures, $\alpha = .0008$, nearly.

Again, if the glass-plate is now introduced and similar measurements $\varphi_{t'}$, t' be made at x, the index of the plate will be

$$n = N_{t'} \sin \varphi_{t'} = N_{20} \sin \varphi_{t'}/(1+\alpha(t'-20))$$

or

$$n = \sin \varphi_{t'}(1+\alpha(t-t'))/\sin \varphi_t$$

Two symmetrical sets of values are thus obtained, one for each of the two first orders of spectra at x_1 and x_2 on opposed sides of the undeviated white ray w. This method does not usually succeed very well, for it presupposes that in case of the air-plate and glass-plate, which are successively inserted, the total reflection occurs at identical parts of the spectrum for identical positions x along the scale s. But supposing the adjustment trustworthy,

* In conformity with Kohlrausch's notation, N and n are here used as symbols for index of refraction. They are replaced by μ, below.

the wave-length corresponding to any given n is found from the two positions x_1 and x_2 at which the same n occurs, from the equation

$$\lambda = D(x_2 - x_1)/2R$$

In general it is preferable to use the air-plate first to find the indices of refraction of the liquid, if these are not known throughout the spectrum. There will thus be given two symmetrical curves for the two first orders of spectra, separately. Their distance apart $x_2 - x_1$ for the given values of N determines the wave-length λ sought; *i.e.*, if N is plotted in terms of x, the horizontal distance apart of the two curves is the $x_2 - x_1$ which determines the wave-length for the index N selected. Hence N is given in terms of λ and should be reduced to 20°. In case of many liquids, in particular carbon disulphide, N is well known in terms of wave-length at the outset, so that the air-plate is superfluous.

The observations with the glass-plate are made in the same way. The symmetrical curves for $\sin \varphi_{t'}$ at t', reduced to $\sin \varphi'$ at 20°, as found from the two first orders of spectra, are first plotted in terms of x. Hence their distance apart for two equal values of $\sin \varphi'$ is $x_2 - x_1$, from which the wave-length λ is computed. This datum in turn gives the appropriate (known) value N of the index of the liquid, all at 20°, so that finally

$$n = N \sin \varphi'$$

74. Examples. Liquids.—The circle of the Kohlrausch total reflectometer is only a little over 3 inches in diameter and the reading is just within 0.1 degree of arc. The index of carbon disulphide, moreover, varies, relatively speaking, in marked degree with temperature; *i.e.*, 0.0008 per degree centigrade. Unless unusual precautions are taken, therefore, one can not expect the units of the third place to be quite trustworthy, as it corresponds to about 0.07′ of arc. The apparatus in my possession was an old instrument, and a high order of precision was of secondary interest and not attempted.

TABLE 25.—Air-plate between thin plates of glass in CS_2. Temp. $t = 22.2°$. $N_{20} = (1 + .00176)/\sin \varphi_t$.

x	Mean φ_t	N_{20}	N_{20}	x_2	x_1	$\lambda \times 10^6$
cm.						
66.15	38.14°	1.6220	1.6230	193.30	67.20	62.82
70	37.98	1.6278	1.6290	189.00	70.40	59.08
75	37.69	1.6385	1.6340	185.60	73.10	56.04
80	37.24	1.6553	1.6390	183.10	75.30	53.70
85	36.69	1.6766	1.6450	181.00	77.20	51.71
175	36.99	1.6649	1.6500	179.10	78.80	49.96
180	37.46	1.6471	1.6560	177.40	80.10	48.47
185	37.79	1.6347	1.6610	176.00	81.30	47.17
190	37.99	1.6275	1.6670	174.50	82.60	45.78
195	38.16	1.6215	1.6720	173.40	83.90	44.58
			1.6780	172.50	85.30	43.44

I will first take the case of an air-plate with carbon disulphide. A film of air was inclosed between two small plates of microscope cover-glass by cementing them at their edges with glue. In another case, plates of glass 0.3 centimeter thick were similarly prepared. Examples of the results

TABLE 26.—Air-plate between thick plates of glass in CS_2. Temp., $t = 18.3°$

x	Mean φ_t	N_{20}	N_{20}	x_2	x_1	$\lambda \times 10^6$
cm.						
66.15	38.00°	1.6220	1.6180	193.10	64.30	64.16
70	37.73	1.6318	1.6230	189.70	66.80	61.22
75	37.40	1.6441	1.6290	186.70	69.00	58.63
80	36.93	1.6620	1.6340	184.00	71.20	56.19
85	36.15	1.6928	1.6390	181.50	73.30	53.90
172	36.66	1.6726	1.6450	179.50	75.10	52.01
175	36.98	1.6601	1.6500	177.80	76.90	50.26
180	37.43	1.6430	1.6560	176.30	78.50	49.71
185	37.73	1.6318	1.6610	174.80	79.80	47.32
190	37.94	1.6241	1.6670	173.40	81.20	45.93
195	38.18	1.6155	1.6720	172.10	82.30	44.73
			1.6780	170.90	83.20	43.69
			1.6840	170.00	84.00	42.84
			1.6890	169.30	84.60	42.19

are given in tables 25 and 26. In each table the position x of the total reflectometer on the rail AA is given, together with the corresponding angle of total reflection φ_t, of the air-plate and the value of N_{20} reduced to 20°.

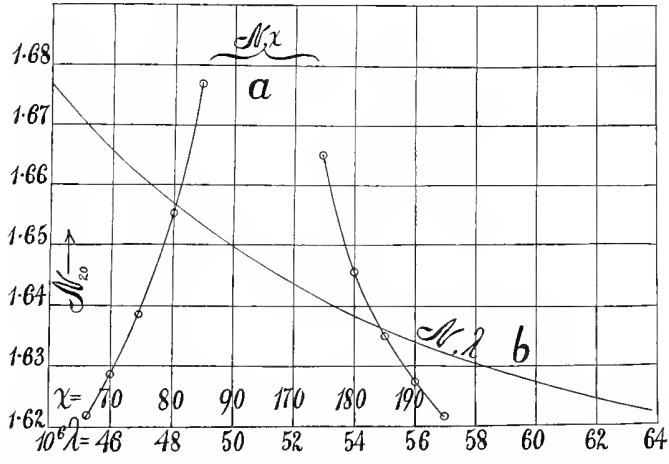

FIG. 46.—Graphs showing index of refraction of CS_2 for (*a*) different positions, x, of air-plate on graduated rail, and (*b*) different wave-lengths.

The curves, figs. 46(*a*) and 47(*a*), show the value of N_{20} in terms of x. These curves should be quite symmetrical to the vertical, so that for any height N_{20}, $(x_1+x_2)/2$ is constant.

Similarly a given horizontal N_{20} determines the values $x_2 - x_1$ for the computation of the wave-length λ. The film of the grating had nominally 15,050 lines to the inch and the oblique rail R was 169.4 cm. long. Hence

$$\lambda = \frac{x_2 - x_1}{15{,}050 \times .3937 \times 2 \times 169.4} = 4.98 \times 10^{-7} (x_2 - x_1)$$

These values x_2, x_1, λ, and N_{20} are also given in tables 25 and 26, for the successive values of N_{20} used, and figs. 46(b) and 47(b) show the corresponding dispersion curves for carbon disulphide at 20°, resulting.

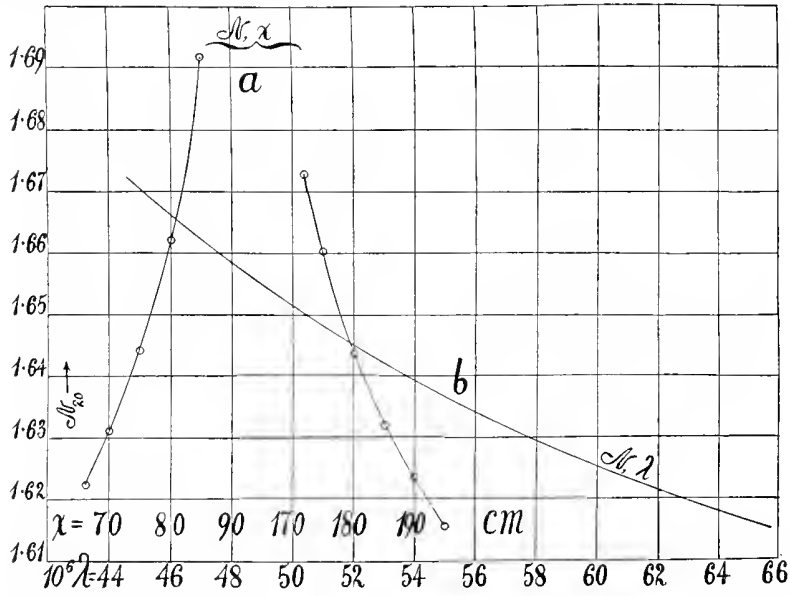

FIG. 47.—Graphs showing index of refraction of CS_2 for (a) different positions, x, of air-plate on graduated rail, and (b) different wave-lengths.

The curves for N_{20} in terms of λ, both for thick and for thin glass-plates holding the air-plate between them, are systematically above the standard values given by Kohlrausch.* The difference is 2 to 3 units in the third place, which would be equivalent to 2.5° in temperature, or about 0.06° of angle at the vernier, or else to some systematic error or to an actual difference in composition of the liquid. I did not consider it worth while to seek for the cause of this constant systematic difference of absolute results, seeing that the differential coefficients of the curves figs. 46(b) and 47(b) would be correctly given, and these are chiefly in question.

75. Examples. Solids.—The treatment of a solid medium is similar, except that the total reflections are observed by reflected light. If the data for carbon disulphide be taken at 20°

$$n = N_{20} (1 - a(t - 20)) \sin \varphi$$

* Kohlrausch, Lehrbuch der Praktischen Physik, p. 712, 1910.

Tables 27 and 28 contain the data for x, φ, and $(1-a(t-20))\sin\varphi$, which refers the case to 20°. Figures 48(a) and 49(a) show the values of the corrected $\sin\varphi$ in terms of x. The curves, as they should be, are nearly symmetrical to the vertical or $(x_1+x_2)/2$ is nearly constant for the same sine.

TABLE 27.—Refraction of the glass of the grating. Temp., 21.8°.
$n = N_{20} \sin\varphi\ (1-.00144)$.

x	Mean φ	Sin φ	Sin φ	x_2	x_1	$\lambda\times10^6$	N_{20}	n
cm.								
66.15	70.00°	0.93834	0.9360	191.70	69.90	60.67	1.6245	1.5206
70	69.60	.93592	.9340	187.80	72.70	57.34	1.6292	1.5217
75	68.96	.93199	.9320	185.50	75.00	55.04	1.6335	1.5224
80	68.16	.92688	.9300	183.40	77.30	52.85	1.6391	1.5244
85	67.03	.91937	.9280	181.40	79.10	50.96	1.6441	1.5258
172	65.70	.91008	.9260	179.70	80.60	49.37	1.6489	1.5269
175	66.80	.91781	.9240	178.40	82.20	47.92	1.6538	1.5281
180	68.08	.92637	.9220	177.20	83.50	46.68	1.6588	1.5294
185	68.89	.93153	.9200	176.10	84.60	45.58	1.6634	1.5303
190	69.54	.93556	.9180	175.00	85.60	44.53	1.6682	1.5314
195	70.03	.93850	.9160	174.10	86.50	43.64	1.6728	1.5323

TABLE 28.—Refraction of the glass of the grating. Temp., 19.2°.
$n = N_{20} \sin\varphi\ (1+.00064)$.

x	Mean φ	Sin φ	Sin φ	x_2	x_1	$\lambda\times10^6$	N_{20}	n
cm.								
66.15	69.56°	0.93760	0.9360	189.20	69.20	59.78	1.6254	1.5214
70	69.19	.93534	.9340	186.10	71.80	56.94	1.6298	1.5223
75	68.54	.93124	.9320	183.50	74.20	54.45	1.6350	1.5239
80	67.55	.92476	.9300	181.30	76.20	52.35	1.6404	1.5255
85	66.28	.91608	.9280	179.60	77.80	50.71	1.6447	1.5263
172	66.29	.91615	.9260	177.60	79.40	49.08	1.6499	1.5278
175	67.11	.92182	.9240	176.40	80.50	47.77	1.6540	1.5283
180	68.11	.92847	.9220	175.10	81.50	46.63	1.6588	1.5294
185	68.84	.93316	.9200	173.80	82.70	45.38	1.6641	1.5310
190	69.38	.93650	.9180	172.80	83.80	44.33	1.6691	1.5323
195	69.81	.93913	.9160	171.90	85.00	43.29	1.6747	1.5340

If now the distance apart of equal values of the reduced $\sin\varphi$ be taken, *i.e.*, if x_2-x_1 be found for nearly equal increments of $\sin\varphi$, the former values determine λ, from which the corresponding N_{20} for carbon disulphide is found in turn.

In this way the data for the values of n to be computed are found, and n may now be expressed in terms of the λ used. Tables 27 and 28 also contain x_2-x_1, λ, N_{20}, for carbon disulphide, taken from Kohlrausch's tables, and n for the glass. Figs. 48(b) and 49(b) show the final dispersion curves, index of refraction n varying with wave-length λ for the glass of the grating. The constants of these curves will be computed below and their character will then appear.

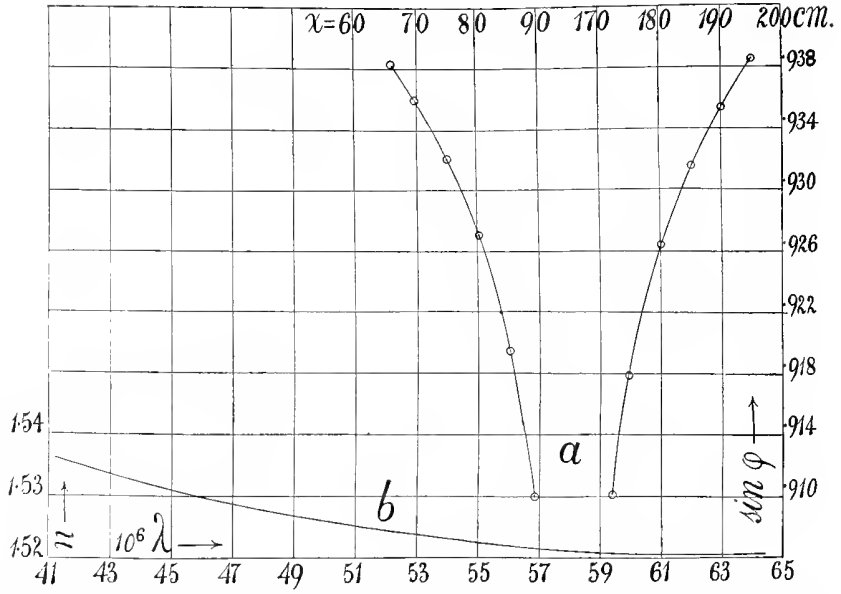

FIG. 48.—*a*, graphs showing refraction of glass submerged in CS_2 for different positions of totally reflecting plate on graduated rail; *b*, dispersion curves for glass plate of grating.

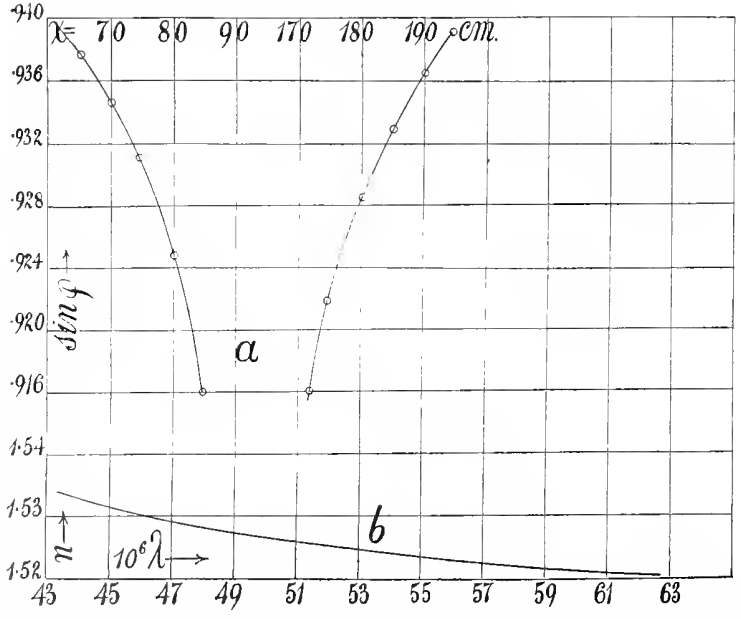

FIG. 49.—*a*, graphs showing refraction of glass submerged in CS_2 for different positions of totally reflecting plate on graduated rail; *b*, dispersion curves for glass plate of grating.

76. Independent measurements.—As an example of coördinated work, in which the index of the liquid and of the solid are simultaneously found, the following experiment may be cited. The air-plate was inclosed between two thin plates of microscope cover-glass. In such a case the limits of total reflection are determinable both for the reflected rays and for the transmitted rays. The angle φ in the former case gives the index of refraction n of the glass, in relation to the liquid (carbon disulphide), since

$$n = N \sin \varphi$$

whereas the angle φ_0 in the latter case gives the index of the liquid alone, or

$$N = 1/\sin \varphi_0$$

Hence

$$n = \sin \varphi / \sin \varphi_0$$

needing no correction for temperature.

In an experiment made at 18.3° with the plate of microscope glass in question inclosing the air-film, $\varphi = 68.90°$ and $\varphi_0 = 38.02°$, whence $n = 1.5198$. Using $\varphi = 68.90°$ as found and the tabulated data for carbon disulphide from Kohlrausch, $N = 1.6291$, $n = 1.5199$, which happens to agree accurately with the preceding n.

77. Prism (liquid CS_2) and submerged grating.—The present method for the above purpose makes use of the grating directly. This is inclosed in a suitable closed trough, preferably triangular in form, with windows of plate-glass and filled with carbon disulphide. If the grating is mounted with its ruled face coinciding with the axis of rotation, as in Kohlrausch's total reflectometer, the angle of total reflection may be measured in all parts of the spectrum. The Fraunhofer lines which are simultaneously in focus are used for reference in succession. Parallel rays of sunlight from a collimator are thrown into one face of the liquid prism, normally to its plane. They emerge at the other face. The undeviated rays are ignored, while the telescope is directed toward the first order of diffraction spectra, this emergence also being not far from normal. Like the first order of spectra, the second and third orders may often be used with advantage, the limit of total reflection being identical in all spectra on the same side of the undeviated ray. Fig. 50 shows the details of the apparatus. *ABC* is an equilateral hollow prism of wood, closed above and below, but provided with the plate-glass windows *a*, *b*, *c*. The whole interior, except the plate, is thoroughly coated with a thin layer of glue, which renders it impervious to carbon disulphide. The windows also are glued into place, while the top is merely screwed down and therefore removable. This is, moreover, centrally perforated, to receive a brass tube 1.25 inches in diameter, which carries the graduated circle *ee*, the alidade, and the axial clutches of the total reflectometer. The telescope *T* is fixed to *ee* by an arm (not shown), so that *T*, *ee*, *ABC* make a rigid

system. To introduce large objects like the grating, the whole top is removed. Small objects may be introduced through the tube, as in Kohlrausch's instrument.

Figure 50 shows an adjustment made under conditions of total reflection. L is a beam of white sunlight, entering nearly normally to a, totally reflected at d from the plate-glass grating p, ruled on the front face, and emerging obliquely at R. This is the undeviated beam. The first order of spectrum emerges at D, also nearly normal to the plate c, and is seen in the telescope T The second and third orders of spectra appear to the

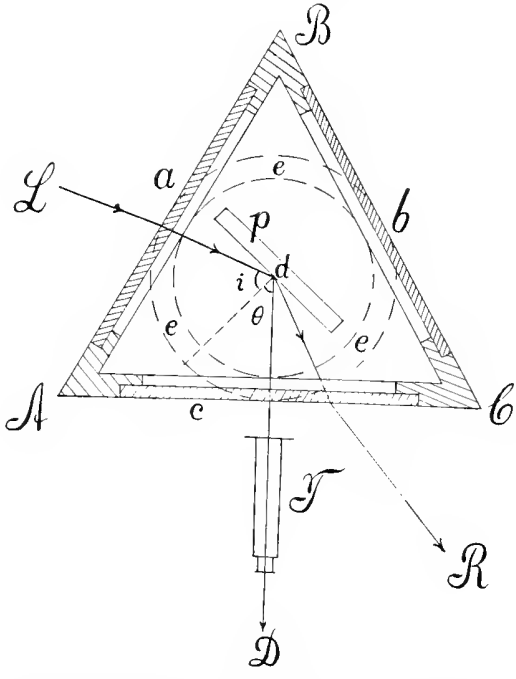

FIG. 50.—Hollow prism of wood with glass sides, containing CS_2, in which plate of grating is submerged for total reflection.

left of D, in succession. The spectra on the other side of R are not usually available. Moreover, the reading of these would be different than the reading for the case where the angle of diffraction θ is smaller than the angle of incidence i.

The limit of total reflection moves through the spectrum both with the rotation of the prism as a whole (which must therefore be on an axle) and with the independent rotation of the plate p, actuated by the alidade rotating within ee. In the definite adjustment this limit must coincide both with the spectrum line λ for which n is to be found, and with the cross-hairs of the telescope T. Three lines, in other words, are to be brought

into coincidence; but after a little practice this succeeds fairly well, unless the limit of total reflection is too faint. As a rule, since T rotates with the prism, if the limit of total reflection is put on the cross-hairs in any part of the spectrum, it will remain there on rotating the alidade till the spectrum line selected is brought to the same coincidence by turning the alidade. The adjustment is then repeated in succession for greater precision.

After taking the reading for the position in figure, the light is introduced through b and the symmetrical position of p found. The difference in angular reading is the double angle of total reflection, 2φ. The adjustment in the first spectrum holds equally for the second and third orders, and it is in the latter that the phenomenon is liable to be particularly clear and the adjustment correspondingly precise. The beam of white light should illuminate the whole grating whose ruled face is very nearly on the axis of rotation d of the alidade. Sunlight is essential for these measurements, since the spectrum lines are to be used. This was not of course necessary in the preceding paragraph.

The following example of results obtained in this way may be given:

TABLE 29.

Line.	2φ	t	n	n from figs. 48(b) and 49(b)
D	138.28°	19.0°	1.5210	{ 1.5215 1.5206
E	136.53°	18.7°	1.5244	{ 1.5240 1.5250

which is practical coincidence within the errors of observation and thus verifies the above work as a whole.

78. The dispersion constants of the glass of the grating.—To reduce these data for practical purposes it will be sufficient within the range and relatively to the precision of observations to assume the simplified form of Cauchy's equation,

$$n = A + B/\lambda^2$$

if n_E is the index for the E line and λ_E its wave-length

$$n - n_E = B\left(\frac{1}{\lambda^2} - \frac{1}{\lambda^2_E}\right)$$

from which B may be computed for each pair of values of n and λ. The results are given in table 30. B was found separately from each of the curves (figs. 48(b) and 49(b)). The values of $n - n_E$ and λ are chosen as near the observations as possible.

The results for $n-n_E$ agree as well with the observed data as the small instrument used can warrant. The two groups show a displacement with reference to each other which is probably due to temperature. A few outstanding larger differences are errors, since they occur irregularly.

TABLE 30.—Index of refraction of glass n in terms of wave-length, λ. $n-n_E=B(1/\lambda^2-1/\lambda^2_E)$. Mean $B=48\times10^{-12}$.

Observed $n-n_E$	$\lambda\times10^6$	Mean $B\times10^{12}$	Computed $n-n_E$	Observed $n-n_E$	$\lambda\times10^6$	Mean $B\times10^{12}$	Computed $n-n_E$
−.0035	58.880	48.9	−.0035	−.0046	60.076	47.5	−.0040
+.0032	48.319	....	+.0033	+.0014	50.013	....	+.0019
.0090	43.338	....	.0084	.0113	41.296	....	.0107
.0011	51.109	....	.0011	.0019	49.614	....	.0022
−.0041	60.573	....	−.0043	−.0043	59.528	....	−.0037

From table 30 the value of the differential coefficient

$$\frac{d\mu}{d\lambda}=-\frac{2B}{\lambda^3}$$

may also be obtained for any wave-length λ. This and the corresponding value* of

$$\mu-\lambda\frac{d\mu}{d\lambda}=\mu+\frac{2B}{\lambda^2}$$

needed in the reduction of the observations of the earlier paper† will be computed by accepting the mean value $B\times10^{10}=0.48$.

79. Computation of the shift of centers in elliptic interferometry.—In the preceding report,‡ I showed that the path difference, y, corresponding to the centers of ellipses throughout the spectrum is

$$y=\frac{e}{\cos R}\left(\mu-\lambda\frac{d\mu}{d\lambda}\right) \qquad (1)$$

where e is the thickness of the glass and μ its index of refraction, for any given color of wave-length λ. R is the corresponding angle of refraction for light incidence at an angle I, or $\sin I=\mu\sin R$. In the former experiment $I=45°$. In view of the oblique position of the grating, however, the micrometer motion N of the opaque mirror introduces an additional displacement. Let N be the coördinate for this mirror. Then

$$N=y-e\,\mu\sin R\tan R. \qquad (2)$$

Hence the readings of the micrometer are determined by (subscripts c referring to centers of ellipses)

$$N_c=\frac{e}{\cos R}\left(\mu\cos^2R-\lambda\frac{d\mu}{d\lambda}\right) \qquad (3)$$

* The symbol μ for index of refraction is resumed throughout the following paragraphs.
† Publication No. 149, Carnegie Institution of Washington, 1911, p. 69.
‡ Publication No. 149, Carnegie Institution of Washington, §44, p. 66 *et seq.*, 1911.

For the present purpose it is sufficient to assume

$$\mu = A + B/\lambda^2$$

and to take the E line as a standard of reference, whence

$$\mu - \mu_E = B\left(\frac{1}{\lambda^2} - \frac{1}{\lambda^2_E}\right)$$

Table 31, then, gives an exhibition of the quantities here in question, computed both for light crown glass, $10^{10}B = 0.456$, in accordance with the data for μ and λ given in Kohlrausch's tables, and for the glass of the grating actually used, $10^{10}B = 0.48$, as measured in the above paragraphs. Δy_c and ΔN_c refer to distances from the value corresponding to the E line. N_c, y_c, and λ are in centimeters and the angle of incidence is 45°.

TABLE 31.—Light crown glass. $10^6\lambda_E = 52.70$. $10^{10}B = 0.456$. Computed values of y and N.

Lines.	B	C	D	E	b	F	G
$10^6 \times \lambda$ . . .	68.70	65.63	58.93	52.70	51.80	48.61	43 08
μ.	1.5118	1.5128	1.5152	1.5186	1.5192	1.5214	1.5267
R.	27° 53′	27° 52′	27° 49′	27° 45′	27° 44′	27° 42′	27° 35′
$d\mu/d\lambda$. . . .	281.26	322.62	445.62	623.10	656.14	793.96	1140.64
y_c	1.1779	1.1799	1.1853	1.1920	1.1941	1.1981	1.2091
Δy_c	−.0141	−.0121	−.0067	.0	+.0021	+.0061	+.0171
N_c	.9235	.9257	.9315	.9390	.9412	.9456	.9578
ΔN_c	−.0155	−.0133	−.0075	.0	+.0022	+.0066	+.0188
Plate glass of the grating. $10^6\lambda_E = 52.70$. $10^{10}B = 0.48$.							
$10^6 \times \lambda$ . . .	68.70	65.63	58.93	52.70	51.80	48.61	43.08
μ.	1.5179	1.5179	1.5205	1.5240	1.5252	1.5270	1.5326
R.	27° 46′	27° 46′	27° 41.7′	27° 37.5′	27° 37′	27° 34′	27° 27.3′
$d\mu/d\lambda$. . . .	296.07	339 60	469.08	655 90	690.68	835.76	1200.70
y_c	1.1820	1.1841	1.1890	1.1962	1.1980	1.2025	1.2140
Δy_c	−.0142	−.0121	−.0072	.0	+.0018	+.0063	+.0178
N_c	.9288	.9309	.9367	.9447	.9464	.9516	.9643
ΔN_c	−.0159	−.0138	−.0080	.0	+.0017	+.0069	+.0196

Measurements of N_c were now made with the aid of a Fraunhofer micrometer reading to a few ten thousandths of a centimeter. The opaque mirror was adjustably mounted on a slide and moved normally to itself, in order to put the centers of ellipses successively in coincidence with the B, C, D, etc., lines of the spectrum. At each coincidence a reading was made, care being taken to proceed in one direction only. As there are four spectra more or less in coincidence, it is easily possible to select the wrong line. By temporarily screening off the reflection from one mirror, however, and then marking the line desired of the remaining pair by the cross-hairs of the telescope, mistakes are usually avoidable. In the extreme blue and red it is often difficult to see the lines clearly in the superimposed spectra, so that the data for the B and G lines are not quite so trustworthy.

In fact, the ellipses come out sharpest when but a narrow strip of the grating is used; whereas the resolving power of the grating or general sharpness of lines increases with the breadth of the grating. If the whole grating is used (an intense spot of sunlight focussed on the slit) the adjustment must be very perfect and the surfaces quite true to bring out the ellipses; this is not the case if parallel rays fall on the slit and the whole divergence in the collimator is due to the diffraction of the slit. With optical plate-glass none of these difficulties would appear.

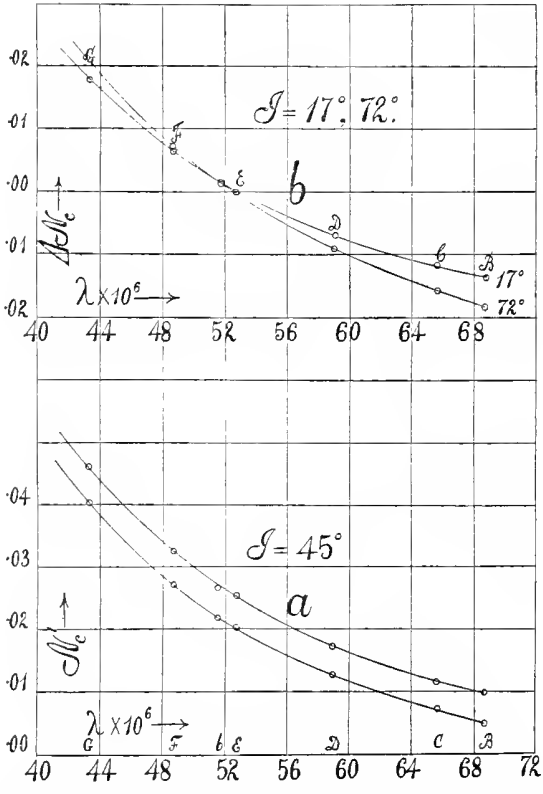

FIG. 51.—Graphs showing displacement of opaque mirror (micrometer motion) to place center of ellipses in different parts of spectrum, for case of different angles of incidence, I.

Apart from drawbacks of this nature, which require patience for their removal, the measurements are quite satisfactory as a whole, as may be seen in fig. 51(*a*).

In table 32 I have given the observed results, N'_c being the arbitrary drum-reading of the micrometer and its equivalent in centimeters, from which $\Delta N_c = N'_c - (N'_c)_E$ is deduced, relatively to the position $(N'_c)_E$ corresponding to the E line. Different values of $(N'_c)_E$ in the two series of fig.

51(*a*) are due to the backlash in the micrometer, as the mirror traveled in opposed directions in these cases.

In the last two columns of table 32 the observed mean data are compared with the computed data for ΔN_c in table 31. The results are practically

TABLE 32.—Observed values of the shift of ellipses compared with the computed values of table 31 ($B \times 10^{10} = 0.48$).

Line.	$10^6\lambda$	N'_c Drum	N'_c cm.	ΔN_c	N'_c Drum	N'_c cm.	ΔN_c	Mean ΔN_c obs.	Mean ΔN_c comp.
B....	68.70	18.6	0.0093	−0.0162	9.6	0.0048	−0.0157	−0.0160	−0.0159
C....	65.63	23.0	.0115	− .0140	14.4	.0072	− .0133	− .0137	− .0138
D....	58.93	34.6	.0173	− .0082	25.5	.0127	− .0078	− .0080	− .0080
E....	52.70	....	.0255	.0	....	.0205	.0	.0	.0
b....	51.80	53.3	.0267	+ .0012	43.6	.0218	+ .0013	+ .0012	+ .0017
F....	48.61	65.0	.0325	+ .0070	54.4	.0272	+ .0067	+ .0069	+ .0069
G....	43.08	92.4	.0462	+ .0207	80.7	.0404	+ .0199	+ .0203	+ .0196

coincident, except at the *G* line, where the ellipses were too dark to be seen distinctly. Hence equation (3) for N_c may be accepted as correct. If we write it

$$N_c = \frac{e}{1\ \overline{\mu^2 - \sin^2 I}} \left((\mu^2 - \sin^2 I) - \mu\lambda \frac{d\mu}{d\lambda} \right) \tag{4}$$

and put $m^2 = \mu^2 - \sin^2 I$, $x = \log \mu$, the equation becomes

$$N_c = e\left(m - \frac{dm}{dx} \right) \tag{5}$$

On integration and reduction this may be written

$$e\mu \cos R = \lambda\ (C - \int N_c d\lambda/\lambda^2) \tag{6}$$

where C is a constant of integration. Unfortunately equation (6) is too complicated for the computation of μ when N_c is observed in terms of λ throughout the spectrum; for the reference to the standard E line gives (sin I = constant)

$$1\ \overline{\mu^2 - \sin^2 I}/\lambda - 1\ \overline{\mu_E^2 - \sin^2 I}/\lambda_E = -\frac{1}{e} \int_E \Delta N_c \frac{d\lambda}{\lambda} \tag{7}$$

If, however, I is very small, or $R = 0$,

$$\frac{\mu}{\lambda} - \frac{\mu_E}{\lambda_E} = -\frac{1}{e} \int \Delta N_c \frac{d\lambda}{\lambda} \tag{8}$$

Let $\mu = B(1/\lambda^2 - 1/\lambda_E^2)$ as above. Then either equation (3) or equation (8) for $I = 0$, leads to

$$(\Delta N_c)_0 = (N_c - N_E)_0 = 3eB\ (1/\lambda^2 - 1/\lambda_E^2) \tag{9}$$

This equation is to be tested in the following paragraph.

In conclusion, the effect of a change of the angle of incidence I on N_c may be added. Since

$$N_c = e\mu \cos R + 2e\, B/\lambda^2 \cos R$$

$$dN_c/dI = (dN_c/dR)\ (dR/dI) = N_c \sin 2I/2\ (\mu^2 - \sin^2 I)$$

whence

$$dN_c/dI$$

is zero when $I = 0°$ and $I = 90°$ while at $45°$

$$(dN_c/dI)_{45} = N_c/(2\mu^2 - 1)$$

or the intermediate values are significant. The effect of R is thus marked for intermediate angles between $0°$ and $90°$.

80. Continued. Case of I = 0°.—The limiting values of I in equation (7) are interesting. They correspond to the form of interferometer approached in figure 52, where gg is the face of the grating, I the incident ray, M and N the two opaque mirrors symmetrically inclined relatively to the grating. Rays R are refracted and rays D are diffracted. In figure 52 the spectra on the left of R are also available; but they are often complicated with the orders of spectra of the undeviated ray before it has

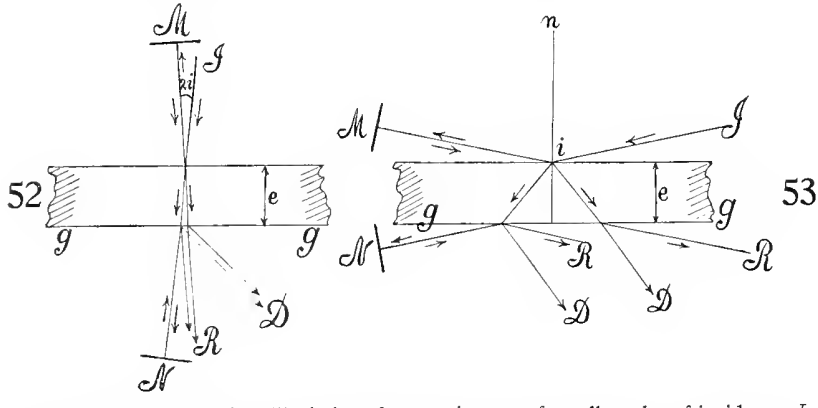

FIG. 52.—Adjustment for elliptic interference, in case of small angles of incidence, I.
FIG. 53.—Adjustment for elliptic interference, in case of large angles of incidence, I.

been reflected. To avoid these, one should observe between the spectra of the non-reflected ray, or else in the region of non-reflected spectra of the third or higher orders, as these are too faint to interfere with the reflected spectra. They often advantageously supply fixed lines in the spectrum when arc light is used.

To realize the condition of small angle, a collimator I and the mirror N (micrometer movable parallel to itself) were fixed on the edge of the spectrometer plate, diametrically opposite to each other. The mirror M, the grating gg, and the telescope at R or D were revolvable around the axis

of the spectrometer. Grating and mirrors could be clamped. With such an adjustment all values of I, in fact, may be tested between about 10° and 80°, smaller and larger angles being excluded, because of the lateral dimensions of the apparatus and mounting.

The present method of interference is often exceedingly convenient, inasmuch as the telescope at R is almost in contact with the micrometer at N, which may therefore be manipulated with ease by the observer. A typical form of instrument will be described below in § 83.

The endeavor may now be made to compute B from the shift of ellipses as suggested in the preceding equation (9) or

$$\Delta N_c = 3eB\ (1/\lambda^2 - 1/\lambda^2_E)$$

If we compute β in

$$\Delta N_c = \beta\ (1/\lambda^2 - 1/\lambda^2_E)$$

from the observed value of ΔN_c, the mean value for the B, C, D, F, G lines is found to be $\beta = 0.975 \times 10^{-10}$. Since $e = 0.68$ cm. and $B = 0.48 \times 10^{-10}$ in table 30, $3eB = 10^{-10} \times 0.979$, which agrees very nicely with the computed value of β just stated, particularly in view of the fact that I is not yet quite zero.

Table 33 contains data computed for y_c and N_c, etc., in case of $I = 17°$ and the glass of the grating ($B \times 10^{10} = 0.48$)

TABLE 33.—Computed values of y_c and N_c when $I = 17°$. $B \times 10^{10} = 0.48$.

Lines.	B	C	D	E	b	F	G
$\lambda \times 10^6$...	68.70	65.63	58.93	52.70	51.80	48.61	43.08
μ.....	1.5179	1.5179	1.5205	1.5240	1.5252	1.5270	1.5326
R.....	11° 6′	11° 6′	11° 5′	11° 4′	11° 3′	11° 2′	11°
$d\mu/d\lambda$....	296.07	339.60	469.08	655.90	690.68	835.76	1200.70
y_c.....	1.0660	1.0677	1.0728	1.0799	1.0815	1.0860	1.0975
Δy_c.....	−.0139	−.0122	−.0071	.0	+.0016	+.0061	+.0176
N_c.....	1.0269	1.0287	1.0338	1.0410	1.0427	1.0472	1.0589
ΔN_c.....	−.0141	−.0123	−.0072	.0	+.0017	+.0062	+.0179

TABLE 34.—Observed values of ΔN_c. $I = 17°$.

Lines.	B	C	D	E	b	F	G
$\lambda \times 10^6$...	68.70	65.63	58.93	52.70	51.80	48.61	43.08
N'_c drum.	41.9	46.3	6.2	....	22.3	31.9	5.0
N'_c cm...	.0210	.0232	.0281	.0348	.0362	.0410	.0525
ΔN_c.....	−.0138	−.0116	−.0067	.0	+.0014	+.0062	+.0177
N'_c drum.	33.6	39.4	49.2	....	15.8	25.1	48.0
N'_c cm...	.0168	.0197	.0246	.0315	.0329	.0376	.0490
ΔN_c.....	−.0147	−.0118	−.0069	.0	+.0014	+.0061	+.0175
N'_c drum.	39.3	44.3	4.3	....	20.2	30.0	1.8
N'_c cm...	.0197	.0222	.0272	.0337	.0351	.0400	.0509
ΔN_c.....	−.0140	−.0115	−.0065	.0	+.0014	+.0063	+.0172
Mean:							
ΔN_c obs..	−.0142	−.0116	−.0067	.0	+.0014	+.0062	+.0175
ΔN_c comp.	−.0142	−.0123	−.0073	.0	+.0016	+.0063	+.0178

Table 34 shows the observed results. Fig. 51(*b*) (upper curve, marked 17°) distributes the observations on the computed curve for ΔN_c, when ΔN_c for the E line is zero. Table 34 also contains the mean of the observed results, compared with the computed results for the same $I = 17°$, in table 33. The agreement is not quite as good as in table 32, the impression being that some of the lines (C, D) have been mistaken in the observed work or located in the wrong spectrum. But the general order of values for the small value of R is well brought out.

81. Case of I = 90° nearly.—The further case of interest corresponds to fig. 53, where the angle $I = 72°$ and as large as it could be made in the given spectrometer. The observations for N'_c are given in table 35, N'_c being taken from an arbitrary zero on the drum of the micrometer and (owing to backlash as before) the zero changes by a fixed amount with the direction of the rotation. The spectra were very fine and sharp, but too dark at the violet end and red end.

TABLE 35.—Observed values of ΔN_c. $I = 72°$.

Lines.	B	C	D	E	b	F	G
$10^6\lambda$.....	68.70	65.63	58.93	52.70	51.80	48.61	43.08
N'_c drum.	82.2	75.6	62.4	44.4	41.5	30.4	1.4
N'_c cm...	.0411	.0378	.0312	.0222	.0208	.0152	.0007
ΔN_c.....	−.0189	−.0156	−.0090	.0	+.0014	+.0070	+.0215
N'_c drum.	89.2	83.8	70.4	52.5	49.5	36.2	5.4
N'_c cm...	.0446	.0419	.0352	.0263	.0248	.0181	.0027
ΔN_c.....	−.0183	−.0156	−.0089	.0	+.0015	+.0082	+.0236
Mean:							
ΔN_c obs..	−.0186	−.0156	−.0090	.0	+.0015	+.0076	+.0225
ΔN_c comp.	−.0177	−.0161	−.0091	.0	+.0020	+.0077	+.0222

TABLE 36.—Computed values of y_c and N_c, when $I = 72°$. $B \times 10^{10} = 0.48$.

Lines.	B	C	D	E	b	F	G
$\lambda \times 10^6$...	68.70	65.63	58.93	52.70	51.80	48.61	43.08
μ.....	1.5179	1.5179	1.5203	1.5240	1.5252	1.5270	1.5326
R.....	38° 48′	38° 48′	38° 43′	38° 37′	38° 34′	38° 31′	38° 21′
$d\mu/d\lambda$....	296.07	339.60	469.08	655.90	690.68	835.76	1200.70
y_c.....	1.3421	1.3444	1.3493	1.3562	1.3578	1.3625	1.3738
Δy_c.....	−.0141	−.0118	−.0069	.0	+.0016	+.0063	+.0176
N_c.....	.8222	.8238	.8308	.8399	.8419	.8476	.8621
ΔN_c.....	−.0177	−.0161	−.0091	.0	+.0020	+.0077	+.0222

The computed values of y_c and N_c are given in full in table 36 and ΔN_c computed is also inserted in the last line of table 35. The agreement of observed and computed is satisfactory so far as the observations as a whole are concerned. Certain lines are more discrepant than others, but the errors are irregular.

The computed graph with the observations located with reference to it is given in fig. 51(*b*) on the curve marked 72°. The two curves together

indicate the change of sensitiveness on passing from a very small to a very large angle, the slope of the curve, fig. 53, where $I=45°$ being intermediate. The method of interference given in figure 53 is very useful when observations are made with polarized light (as in the examination of doubly refracting media) and the observer finds it convenient to be near the polarizer at the slit.

82. Summary.—I conclude, therefore, that the observations made at angles of incidence $I=45°$, 17°, 72°, have verified the equation

$$N_c=e\cos R\left(\mu-\frac{\lambda}{\cos^2 R}\frac{d\mu}{d\lambda}\right)=e\cos R\left(\mu+\frac{2B}{\lambda^2\cos^2 R}\right)$$

for the shift of the centers of the ellipses satisfactorily. To restore the ellipses from one spectrum line to another is equivalent to a motion of the micrometer over $N_c-N'_c=\Delta N_c$. This constitutes a second method of interferometry of relatively low sensitiveness, *i.e.*, a coarse adjustment on the number of fringes which pass a given spectrum line. Per fringe or per vanishing ring, obviously, the displacement of the mirror on the micrometer will be a half wave-length of the part of the spectrum in question.

83. Apparatus.—Interferometry by displacement has an advantage, inasmuch as the observer never loses the ellipses, even when the displacement is sudden. Their center may always be brought back again to a given spectrum line by the micrometer. Moreover, since

$$N_c=e\mu\cos R-\frac{e\lambda}{\cos R}\frac{d\mu}{d\lambda}=e\cos R\,(\mu+2B/\cos^2 R)$$

where N_c is the reduced micrometer reading, e the thickness, μ the index of refraction of the glass-plate of the grating for the wave-length λ, R the angle of refraction, and where $\mu=A+B/\lambda^2$, the sensitiveness may be regulated by decreasing the thickness of the grating, e, by aid of a compensator of thickness e'. For the virtual thickness is now $e-e'$. Hence, since for radial motion the sensitiveness per fringe across any given Fraunhofer line is

$$dN/dn=\lambda/2$$

this may be combined with the shift of ellipses controlled by N_c, in any ratio. The limit of this procedure is conditioned by the size of the ellipses or the available size of the field of the telescope, since when $e-e'$ approaches zero the ellipses become enormous.

Furthermore, it has been shown in the report cited* that the quantity $d\mu/d\lambda$ occurring in the value of N_c may be computed preliminarily from observations of $\Delta N_c=N_c-N'_c$, between definite Fraunhofer lines, particularly when the angles of incidence I and of refraction R are small. In such a case the constant $3eB=\beta$ nearly, where $(I=0)$

$$\Delta\mu=B(1/\lambda^2-1/\lambda^2_E),\ \Delta N_c=\beta(1/\lambda^2-1/\lambda^2_E)$$

* Publication No. 149, Carnegie Institution of Washington, §44, 1911.

Finally, if ΔN is the motion of the micrometer to bring the center of ellipses back to a given line

$$\Delta N = (\mu - 1)e'$$

where e' is the thickness of the compensator. If e' is large one may expect to distinguish between the indices of refraction of a birefringent crystal, when the source of light is polarized. Again, when the arms or the interfering beams of light are long, the index of refraction of a gas and its relation to pressure and temperature are accurately determinable.

In view of these advantages among others I have constructed a definite form of apparatus for elliptic interferometry, specially adapted for general observations, such for instance as I have in view with fog-particles. The

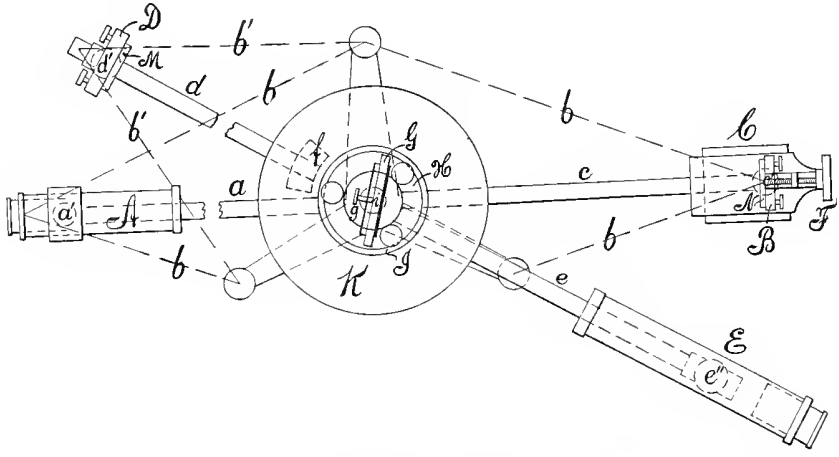

FIG. 54.—Plan of displacement interferometer; A, collimator; M, N, opaque mirrors; G, grating; E, telescope.

apparatus is to be light, portable, rigid, with relatively long distance between the opaque orthogonal mirrors M and N and the oblique mirror or grating, as well as height of mirrors above the arms, and with an easy adjustment for different angles of incidence I, large and small. As shown in figs. 54, 55, and 56, the distance between the center and either remote mirror is about 35 cm. It may easily be enlarged many times beyond this. The angles of incidence $I = 15°$, $45°$, and $75°$, are available at once for the given braces, though of course other angles may be used.

The long arms and feet of the apparatus, which in general form is naturally much like a spectrometer, are made of ¼-inch gas-pipe, and the braces are heavy strips of tin-plate, bent so as to be U-shaped in cross-section, much like umbrella steel, with the ends bolted down. In the drawing (of which fig. 54 is the plan and fig. 55 the elevation) the axles are cylindric or slightly conical. In my own apparatus sufficient rotation, 180°, of the parts was secured by ordinary well-cut gas-pipe screws.

The tripod (figs. 54 and 55) carries a standard Q of ⅜-inch gas-pipe, which is secured snugly by the cross-coupling R. From this the horizontal rigid arms a and c lead respectively to the collimator A and to the slide micrometer C and they are screwed into R parallel to the plane of fig. 55. The arm e which carries the telescope E must be revolvable around Q, a wide axle PP' and braces b'' *diverging* as they approach Q sufficing for the purpose. The telescope is used for reading only and need not be clamped. It must, however, be quite firm so as not to shake the instrument.

The long arms of gas-pipe (a, c, d, e) are not only convenient for the attachment, by ordinary clamps, of objects to be examined, but they admit of a circulation of cold water (constant temperature), entering or leaving at the feet, so that the lengths of arms are invariable, whatever be the temperature of the environment of air.

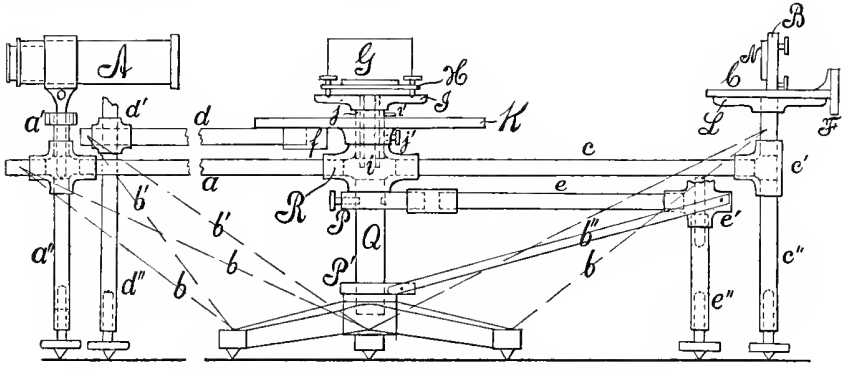

FIG. 55.—Elevation of displacement interferometer.

The standard Q is prolonged above the cross-coupling R as shown at j and the graduated plate at K (for measuring the angle of incidence I) rotates around Q prolonged. The plate may be clamped by the set-screw j'. Radially to K, the lateral arm d is bolted below the plate at f. D carries the opaque mirror N, which thus rotates around Q with K.

The adjustment chosen is such that the parts M, N, the grating G, the telescope E, and the collimator A may be displaced upward several inches, in the clear. It is thus possible, for instance, to place the fog-chamber between MG or NG.

The inside of j or Q prolonged is ground and receives the hollow cylindrical plug i of the table I and this may be clamped by the set-screws i'.

Upon I stands the grating G secured by the screw g to the ring-shaped support H which reposes in an annular gutter in I on three leveling screws. Moreover, a spiral spring (not shown) in the inside of the hollow conical tube i pulls down the ring H firmly upon I, so that nothing is liable to fall on transportation. The ruled surface of the grating G is toward the light or collimator A and in the axis of rotation. The adjustment need not be very accurate. The rulings are parallel to the slit.

Certain details of the parts of the apparatus may now be pointed out. The collimator A may be raised or lowered on its vertical stem or clamped in any position by aid of the wing-nut, a', on a longitudinally split tube. It may also be slightly inclined to the horizontal, either by the hinge indicated in the figure or by the special device shown in fig. 56, where the telescope or collimator reposes on Y's made of strips of elastic brass aa. These are so adjusted that the end of T at a' is naturally higher than at a. The ring b and the thumbscrew c then lower this end against the upward pressure of all the springs. Reading telescopes so mounted are firm and the device is very convenient if a slight inclination is to be imparted. They are removed by loosening c.

The tube a ends on the left in the cross-coupling, which also admits the adjustable standard a'' and affords an attachment for the braces bb (U-shaped in section), the other ends of which are bolted down to the nearer feet of the tripod. Thus A is held sufficiently rigid by the braced system aa'' bb. An inch or a ¾-inch objective and a 6-inch focus is sufficient and by reason of its lightness perhaps preferable to a larger and heavier tube. The slit may usually be opened about 0.5 mm.

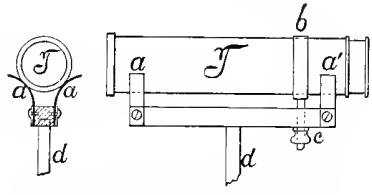

FIG. 56.—Details showing mounting of collimator and telescope.

In a similar way steadiness, elevation, and inclination of the telescope E are secured, the tubes e and e'' (adjustable foot) and the braces b'' terminating in the cross-coupling e' as has been suggested. An inch objective and a 6-inch focus is adequate. Cross-hairs are convenient but not necessary, as the spectrum lines are available when sunlight is used. If the arc light is used, strong sodium lines are usually in the field with the spectrum.

The opaque mirror M is controlled by three leveling screws (horizontal and vertical axes) and a suitable spring in the capsule D. It is adjusted vertically like the telescope and kept firm by the tubes d and d'' (adjustable foot) and braces $b'b'$, all parts meeting at the cross-coupling d'. The braces $b'b'$ are of equal length. Hence they may be bolted down to two of the feet of the tripod in succession, while the tube d together with the plate K take the three positions at 30°, 90°, and 150° to the rod a. The grating G does not turn with K, but must be specially adjusted to corresponding angles of 15°, 45°, and 75°, as easily determined by the reflected rays.

Finally, the slide micrometer is sustained by the tubes c and c'' (adjustable foot) and the braces bb, all parts meeting in the cross-coupling c'.

The latter carries the table L, to which the slide micrometer C with its drum at F is bolted down. N is the opaque mirror adjusted by three leveling screws and a spring (horizontal and vertical axes) within the capsule B. The slide should have from 1 inch to 2 inches of clear play and its displacements should be determinable to about 0.0001 cm. The opaque mirrors M and N may both be silvered on the back. They thus last indefinitely.

Since the telescope E rotates both around its own axis e'' and around the standard Q, elaborate centering of the grating G is not usually necessary. The latter is mounted between strips of cardboard or wood and secured by the screw g, the brass clutches being about twice as far apart as the thickness of the grating. In other words, the grating may be slightly moved in a direction normal to itself.

To adjust the parts, sunlight (preferably) is passed into the widened slit of the collimator, in a dark room, so that the spots falling on the mirrors M and N (the grating being suitably turned) and on the objective of the telescope E are seen and the different reflected images brought nearly into coincidence. A further adjustment is then made through the telescope E, two of the usual four images of the slit (now narrowed) being placed in coincidence horizontally and vertically by manipulating the leveling screws on B. Specks of dust, or nicks in the slit, greatly facilitate this adjustment. The telescope is then turned to the diffraction spectrum, preferably of the first order, and the drum actuated till the interferences appear. Naturally the distances GN and GM are to be approximately equal to begin with. The solitary ellipses are best for general purposes, and they usually correspond to undeviated yellowish and bluish single-slit images. The multiple-slit image is to be avoided. If the rings are not quite centered in the spectrum, they may be made so by cautiously adjusting the screws at B, which tip the mirror about a horizontal axis. The telescope should be moved with its foot sliding on a plane. The three possible positions of the mirror N (positive uncompensated, self-compensated, negatively uncompensated) are about 1 cm. apart on the micrometer, for a plate of glass 0.68 cm. thick. When the arc lamp is used the accentuated sodium lines in the spectrum may be used in place of the white undeviated images of the slit, both for adjustment of the two spectra for coincidence and as a fiducial mark, in place of the cross-hairs in the telescope. For a small angle of incidence the sodium lines of higher orders of spectra are also liable to be available.

To measure the angle of incidence I the table I is turned in its socket until the reflected image of the slit coincides with the slit itself. A hole is cut in the top or side of the collimator tube near the slit (not shown) for this purpose. Thereupon the table I is turned back again until the images coincide in the telescope. The angle read off on the graduated plate K is I, the reflected ray traveling over $2I$. The table I is provided with an index and vernier (also omitted in the diagram).

The apparatus described, being made virtually of hollow parts, is light enough to be carried about with convenience. In the case of the figure where the angle of incidence I is small, the distance from M to N is about 70 centimeters. It may easily be increased to several times this, by inserting longer gas-pipes at c and d with appropriate braces. The fringes are very stable even when the instrument stands on a table fastened to a wall-bracket. They naturally quiver when the observer is manipulating the micrometer screw, but they return at once to quiescence when the hands are removed. To obviate the quiver, *i.e.*, to follow the motion of individual rings, the usual tangent screw method may be employed.

I may add in conclusion that in order to make the rings sharply black and color, a slit about a millimeter wide, placed vertically in front of the objective of the telescope E, may be employed. This may be supported by an ordinary clamp on the arm e, the clamp giving opportunity for the lateral motion needed in adjustment.

84. Other interferences.—The same apparatus may be adapted for observing the linear diffraction-reflection interferences described by Mr. M. Barus and myself.* The equations here available are

$$\delta e = \lambda/2 \cos i \qquad \delta e' = \lambda/2 \cos \theta \qquad \delta e'' = \lambda/2(\cos \theta - \cos i)$$

where δe, $\delta e'$, and $\delta e''$ are the respective increments of the air-spaces between the face (rulings) of the grating and the parallel opaque mirror in front of it, per fringe passing the cross-hairs of the telescope or a given spectrum line, λ the wave-length of light, and i and θ the angles of incidence and diffraction in air. For the measurement of δe, λ, i, θ should be known or determinable.

For these observations let the micrometer C be removed from its plate and now bolted down on the graduated plate K (fig. 57), the tube I and appurtenances being discarded. This must be so done that the face of the opaque mirror N and the rulings of the grating g are in the axis of rotation with the lines of the grating parallel to it and the slit. Hence the mirror must be adjustable by aid of a capsule B with set-screws (horizontal and vertical axes of rotation) and springs. The grating g has its independent mounting with three similar set-screws and springs. In the figure the mirror N is stationary, *i.e.*, fixed to the rigid part C of the micrometer, while the grating is movable to and fro, *i.e.*, fixed to the slide D and actuated by the micrometer screw s and graduated head F. Usually N will be attached to some apparatus whose linear excursions are to be found, and for this purpose of attachment the cross-coupling R in fig. 55 is abundantly supplied with screw sockets (front and rear, not shown), so that such parts may be here attached. In fig. 57 the counterpoise H, for instance, has been added.

* The grating interferometer, Science, XXXI, 394, 1910; Phil. Mag. (6), XX, p. 45, 1910; Publication No. 149, Carnegie Institution of Washington, chap. 2, 1911.

To prepare for observation the plate K and the telescope E are turned until a suitable angle of incidence $i=ANs$ and of diffraction $\theta=sNE$ are obtained. The fringes are seen when g and N are sufficiently near together (the distance apart may be as much as 1 centimeter), on condition that the direct images of the slit from the front face of N and the rear face of g are in coincidence horizontally and vertically. E may be revolved for this preliminary adjustment. To find i, the angle of incidence, the graduated plate K is turned from the given position of coincidence until the image of the slit falls upon the slit itself at the end of the collimator A, a hole (not shown) being left in the collimator tube near the slit for this purpose, as explained above. If the fringes are not sharp, they may be made so by

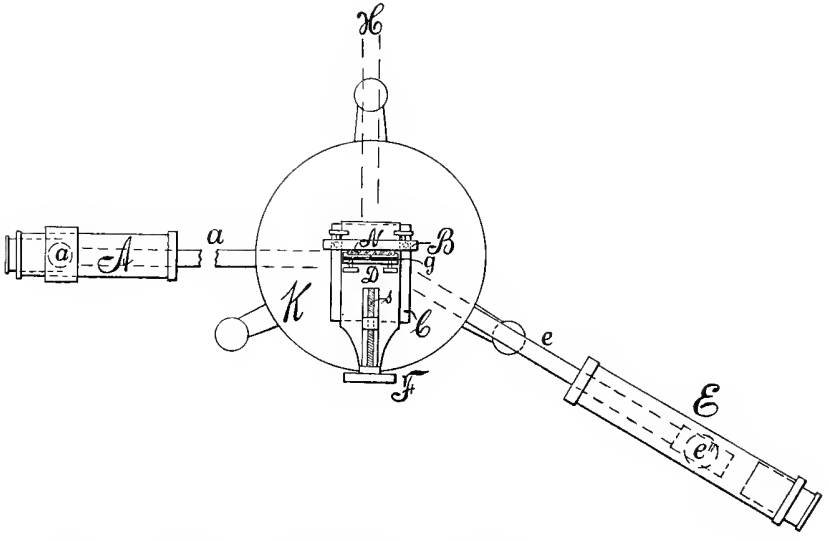

FIG. 57.—Modification of apparatus for diffraction-reflection interferometer.

further adjusting the set screws of N or g by trial. This usually succeeds easily, remembering that the fringes move about a horizontal axis normal to the mirror when the mirror moves about a horizontal axis parallel to its face. For other details the earlier paper should be consulted.

85. Other measurements: high temperature, adiabatic transformations, etc.—The displacement interferometer constructed with its arms made of gas-pipe is adapted for high-temperature investigation. For if a current of cold water at constant temperature be passed through the arms in question they will be kept at invariable length, however much the atmosphere about them may change in temperature. Furthermore, since the distance between the central grating and the opaque mirror may easily be increased to a meter or more, tubes of considerable length may be inserted in the

interfering beams of light. The displacement interferometer should be used with the angle of incidence nearly zero, in which case this angle is without effect on the micrometer reading and the observing telescope lies in a particularly convenient position side by side with the opaque mirror on the micrometer. This is thus immediately at hand.

It seemed to me, therefore, that a particularly interesting subject for investigation would be the relation of temperature and pressure of the index of refraction μ of air. According to Lorentz* the $\mu-1$ for air follows the equation

$$p=C\,(\mu-1)\,\vartheta$$

(p pressure, C constant, ϑ absolute temperature), coinciding in form to the intrinsic equation of a gas, since the temperature coefficient of $\mu-1$ for air is very nearly equal to its coefficient of expansion. Mascart finds this not quite true. Pressures are to be corrected by $(1+\beta p)$ where β is equal to 0.0000072 relative to centimeters of mercury and the temperature coefficient is $\alpha=0.00382$.

At all events, the temperature coefficient α is so large that a method of high-temperature measurement is not out of the question on the one hand, while on the other the variation of α throughout long ranges of temperature is of considerable interest. I have, therefore, made a few tentative measurements at low temperatures to test the apparatus and have found it trustworthy throughout. In table 37 the apparatus is adjusted with an angle of incidence of $I=15°$. The index of refraction is determined from the displacement of ellipses when the air contained in a longitudinal sealed tube in one of the component beams of light which interfere is alternately filled with air at pressure p and exhausted at a given temperature t. This tube was 23.8 centimeters long and of brass surrounded with a close-fitting tubular temperature bath.

The first column of table 37 shows the barometric height and degree of exhaustion (residual pressure). The second the micrometer displacement of the opaque mirror which brings the centers of ellipses back to their original position with reference to a given spectrum line. This reading is taken on the drum of the micrometer, the scale parts being 0.0005 centimeters. When electric arc light is used the accentuated sodium line is always in presence in the spectrum and makes an excellent fiducial line for the centers of the ellipses. A single exhaustion is sufficient for two readings, as the displacement occurs on exhaustion (from red to green, for instance) and is measured by the turn of the micrometer to bring the ellipses back; while on readmitting air the displacement is in the opposed direction and is again measured by restoring the center of ellipses to the position of the sodium line. If this displacement of the opaque mirror on the micrometer is ΔN centimeters the index required is

$$\mu=1+\Delta N/e$$

* See the admirable summary in Landolt and Boernstein's Tables.

if e is the length of the tube. ΔN must be given in centimeters, as shown in the third column of the table, and from this the μ of the fourth is found at the temperature t in the last column. They refer to the wave-length of the D line, as this was taken as the fiducial mark. The absolute values of μ are good, but here of relatively little interest, as no attempt was made to standardize the screw, etc., of the measuring apparatus, and the water circulation had not yet been installed. The temperature coefficient may be found without this. If, therefore, $(\mu-1)$ is expressed in terms of t the result is $\alpha=0.0036$, or of the order expected.

TABLE 37.—Index of refraction of air from shifts ΔN of ellipses. $e=23.8$ cm. Angle of incidence, $I=15°$.

Barometer. vacuum.	Shift* drum.	Mean shift ΔN	$\mu=\frac{\Delta N}{e}+1$	t
		cm.		
76.95 : 19°	13.3	0.00663	1.000279	30°(?)
	13.3			
0.5 cm.	13.3			
	13.2			
	13.5			
	13.0			
	13.6			
76.98 : 24°	13.4	.00674	1.000283	23°
	13.6			
0.4 cm.	13.3			
	13.7 ccl			
77.15 : 21°	13.4 cl	.00677	1.000284	21°
	13.8			
0.4 cm.	13.3			
	14.5 cl			
77.15 : 21°	14.5 ccl	.00727	1.000306	2°
	14.1			
0.4 cm.	15.0			
	14.4			
	14.9			
	14.1			
	14.8			

* These fluctuations are due to the absence of water circulation.

From this datum the working conditions of the apparatus may be specified. For a tube 23.8 centimeters long the micrometer displacement per degree centigrade is 0.051 scale parts or 0.0005 centimeter each; *i.e.*, the micrometer displacement is about 0.000025 centimeter per degree centigrade, or about 10^{-6} centimeter per degree centigrade per centimeter of length of tube. Thus a minimum of about 2° C. is directly appreciable in the given case, or for a tube about half a meter long a minimum of 1° C. should be appreciable at all temperatures. This, moreover, would correspond to the evanescence of two rings in succession, whereas in the above

apparatus a little less than one ring vanishes per degree centigrade, at all temperatures. The displacement of ellipses for an atmosphere of pressure is roughly from the D nearly to the E line.

In this method the arms need not be of invariable length except during the short period of exhaustion, as the data are obtained by differences.

To turn to the second method for obtaining the same results: the displacement of ellipses is accompanied by the radial motion of rings to and from the center, and the number vanishing may be counted. If λ is the mean wave-length between the initial and final positions of the rings and n is the number of rings vanishing, then the equivalent micrometer displacement would be

$$\Delta N = n\lambda/2$$

so that the micrometer reading ΔN need not be taken. Hence

$$\mu = 1 + n\lambda/2e$$

To make use of the method, a fine screw stop-cock is to be inserted through which dry air may be admitted at any rate into the exhausted tube. In this way the motion of the rings toward the center may be controlled perfectly and their evanescence counted. The experiment is very interesting. Clearly the arms must be kept at invariable length while the rings are being counted, *i.e.*, until they cease to move, when the pressure is again normal. Fig. 58 contains an example of many results of this kind. Here the abscissas denote the number of rings which have vanished and the ordinates the corresponding pressure, the latter increasing from a few millimeters to an atmosphere. The line of observations happens to be nearly continuous. An interruption of the count is, however, of no serious consequence, as the slope of the line is alone in question when the initial pressure and final pressure are known. It is surprising to note how closely these observations lie on a straight line. They do so quite within the errors of observation.

The slope of the line is

$$\frac{70.0 - 2.8}{210} = .320$$

i.e., 0.32 centimeter of mercury at 0° C. per ring vanishing, or a little over three rings (3.125) per centimeter of mercury. The mean wave-length in question (between the D and E lines) is about $\lambda = 55.8 \times 10^{-6}$. Hence, as the effective barometer was $76.95 - .500 = 76.45$ centimeters and the tube length 23.8 centimeters,

$$\mu = 1 + \frac{76.45 \times 27.9 \times 10^{-6}}{.32 \times 23.8} = 1.0002806$$

The datum obtained from the displacement of ellipses at the same temperature (unfortunately not taken) was 1.000279. Inasmuch as the water circulation was omitted during the ring measurements and the exact

value of λ was not specially found, the agreement is as close as may be expected.

The two data selected from many similar results show how easily both methods may be used for mutual corroboration. Clearly the ring method, since it involves the evanescence of about 236 rings, is more sensitive, but also less expeditious. It is not, however, necessary to observe all the rings; the disappearance of a reasonable number, say 25 or 50, establishes the rate of evanescence per centimeter of mercury, or more conveniently the number of centimeters of mercury per vanishing ring. If this is determined at the beginning and end of exhaustion the mean result is adequate.

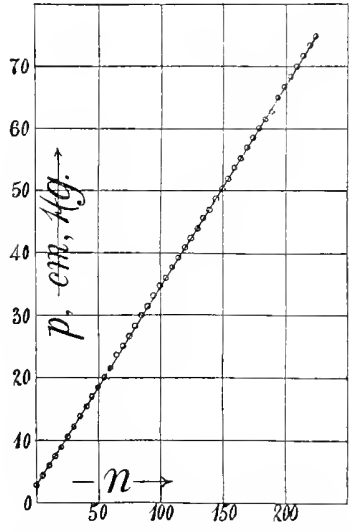

FIG. 58.—Graphs showing number of interference rings, vanishing in case of increasing pressure of imprisoned air, kept at constant temperature.

If the air-tube of the apparatus is so modified that the air may be heated electrically the ring method should be equally available for temperature measurements. The results could be compared with a thermo-couple having its fine junction inserted in the tube and read simultaneously.

As a method of pressure measurement, since for a tube 23.8 centimeters long, 3.12 rings vanish per centimeter of mercury, *i.e.*, about 0.1313 ring per centimeter of tube-length per centimeter of mercury pressure, the method is not very sensitive unless a long tube be used. A tube 1 meter long would, for instance, give 13 rings per centimeter of mercury, admitting of the measurement of pressure to 0.08 centimeter per ring. One might estimate to 0.5 millimeter.

The method of pressure measurement has the rare advantage, however, of being absolutely instantaneous, as reproducing, immediately, the state

of the gas. It is, therefore, remarkably well adapted for the study of adiabatic phenomena. Many questions relative to such transformation of gases are thus open to investigation. Since $(\mu-1)=\Delta N/e=n\lambda/2e$ and $p=C(\mu-1)\vartheta$

$$\frac{p}{\vartheta}=C\cdot\Delta N/e=C\lambda n/2e$$

the variations of p/ϑ are directly given by the number, n, of rings vanishing. But the relation of p and ϑ is also given either by the intrinsic equation of the gas or by its adiabatic equation, according to the transformation which has been imposed on the gas, so that p and ϑ are each determinable.

CHAPTER XI.

THE DEGREE OF ADIABATIC EXPANSION IN GASES RAPIDLY COOLED, AS OBSERVED BY DISPLACEMENT INTERFEROMETRY.

86. Introduction. Apparatus.—In the present paper I shall make a first application of the displacement interferometer described in the preceding chapter of this report. The investigation is purely tentative, the endeavor being both to exhibit the interference method for a case in which it is put to a test lying near the limit of its sensitiveness and at the same time to measure the degree of adiabatic expansion attainable in fog-chambers of regularly increasing size. The paper is, therefore, not to be construed as purposing to actually measure the ratio γ of the specific heats of a gas, but rather to determine the degree of adiabatic expansion in any given apparatus in terms of the value of γ found for that apparatus. From this point of view γ will increase from 1 to 1.41 in proportion as the expansion in question is more truly adiabatic.

The adjustment adopted is shown in fig. 59, the angle of incidence I being as small as possible (about 15°), in which case the equation for the position coördinate, N_c, of the movable opaque mirror (micrometer), when the center of ellipses is at the wave-length λ, *viz*,

$$(1) \qquad N_c = e'\left(\mu \cos R - \frac{\lambda}{\cos R}\frac{d\mu}{d\lambda}\right) = e'\left(\mu \cos R + \frac{2b}{\lambda^2 \cos R}\right)$$

takes its simplest form, since the angle of refraction R approaches zero. In the equation e' is the thickness of the grating, μ its index of refraction for the wave-length λ, and b the coefficient of Cauchy's equation. If, as in the present paper, the centers of ellipses after displacement are brought back to the *same spectrum line* (D line for instance) again, immediate reference to change of μ with λ is excluded and the equation for the displacement of the opaque mirror on the micrometer is then apparently

$$(2) \qquad \Delta N_c = e\,(\mu - 1)$$

where e is the thickness of the object placed in one of the interfering beams, μ its index of refraction relative to air for the given wave-length λ.

This simple theory, however, is only approximately true, inasmuch as the ellipses change in size with the amount of compensation introduced by the object. The conditions reëstablished at the D line are thus not quite identical in the presence and the absence of the object. In fact, the grating as in equation (1) is alternately reinforced by a column of dense and rare air through which the beam travels at normal incidence. If ΔN be the difference of the micrometer readings for the two positions, equa-

tion (2), in which the dispersion of air is neglected, is to be modified in the way suggested for equation (1), so that for the D line of the spectrum as fiducial

$$\Delta N/e=\mu_0-\mu-\frac{\lambda}{e}\left(\frac{d\mu_0}{d\lambda}-\frac{d\mu}{d\lambda}\right)=\mu_0-\mu+\frac{2}{e\lambda^2}(b_0-b) \tag{2'}$$

Here e is the length, μ_0 and μ the respective indices of refraction for the high and low densities of the column of air. Equation (2') is, however, apparently too cumbersome for use at the outset, so that equation (2) has been preferably admitted for experimental purposes, the dispersion of air being disregarded. The values of ΔN so found are too large and the consequent values of γ all too small. They will be corrected, however, in § 97, in which the theory is to be developed in full. It will then be found that the data of the interference method agree with the data of the mechanical method as nearly as may be expected.

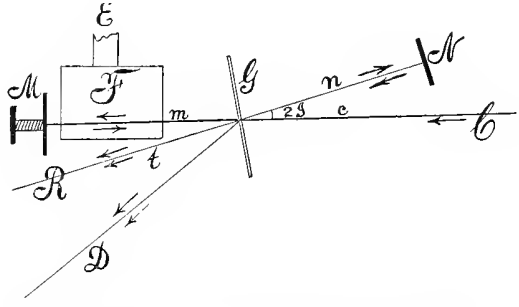

FIG. 59.—Diagram of displacement interferometer, $C\ G\ M\ N\ D$, and the air-chamber F.

If ΔN_c is equivalent to n interference rings of the *mean* wave-length λ,

$$\Delta N_c=n\frac{\lambda}{2} \tag{3}$$

In fig. 59 the pencil of light c enters from a collimator at C and encounters the grating G at a small angle of incidence I. The reflected undeviated beam n is returned by the stationary opaque mirror N, the transmitted beam m by the movable opaque mirror M on the micrometer, after which both enter the telescope R. The arms m and n of the interferometer are of gas-pipe and provided with a circulation of cold water at constant temperature, though in the present chapter this is not needed. The micrometer at M is graduated to 0.0005 cm. on the drum and easily read off by estimation or vernier to 0.00005, *i.e.*, to the mean wave-length of light. The tests below show that the center of ellipses may be placed on a given spectrum line with about the same precision. Hence the displacement method is not much less sensitive than the ring method.

The object F to be examined for change of index of refraction, *i.e.*, the air within a closed chamber, dry or wet, at any temperature, is conveniently

placed in the beam m. If its lateral extent is wide, the angle I must be increased; but it is obviously desirable, apart from the other reasons given above, to have the telescope as near the micrometer M as possible, in order that the micrometer may be manipulated with ease and expedition. Though the telescope at R is needed for adjustment, the position at D is used for observation. Hence if the adjustment is made once for all, a much larger angle is available than for the undeviated beam. Incidental adjustment may be made after the fog-chamber F is inserted, by placing the two diffracted images of the sodium line used in coincidence, together with a simultaneous coincidence of the pairs of sharp shadows (horizontal black line) of dust-specks or a cross-wire at the slit. Finally, in the method used below the pencils m, R, D, etc., may all be made to pass through the plate-glass sides of the fog-chamber (see fig. 63).

To obtain ellipses quite sharp (alternating black and colored bands), a part of the objective of the telescope should be cut off by a small adjustable vertical screen about 1 inch square, or by a wide slit. More than one-fourth of the ¾-inch objective is rarely needed in the horizontal direction. When this is done, undesirable beams of light are excluded and the stationary interferences are also liable to vanish, whereupon in the case of sunlight the Fraunhofer lines (to be used as fiducial lines) become unmistakably sharp and clear. In case of electric arc light, the sodium line from the silicate in the carbons is always strong and a number of them are usually available in the different orders of spectra. The ellipses, too, remain in the field, in spite of rough usage of the apparatus near at hand (air-pump, sudden exhaustion, etc.). The electric arc should be used *directly*, *i.e.*, without lenses or condensation, the arc being adjusted in height, etc., and at a distance of about one foot or less from the slit. The present method depends essentially on the use of *narrow* pencils. The sodium line is apt to be much higher than the spectrum band in the telescope. It is intersected by interference bands even in dark parts of the field of view. With the motion of the rings these move up and down the line.

The use of the coincident sodium lines for reference reduces all the measurements to the wave-length of this line, as the centers of ellipses are invariably brought back to it.

The fog-chamber in the present experiments is much too short for accurate measurements; but it is admitted (as suggested above) to test the details of the method. In definite experiments the component pencils of light should be made to pass (by reflection between mirrors) many times through the fog-chamber, in which case not only would the sensitiveness be increased proportionally but mean increments would be reached for all parts of the air-chamber.

87. Equations.—It is convenient to test the present method of observation by a determination of the ratio γ of the specific heats of constant pressure and of constant volume, as has been suggested. This offers a

serviceable method of arranging results, even if an absolute measurement of γ is not directly aimed at. The degree of adiabatic expansion reached in vessels of different sizes, by sudden exhaustion into a vacuum-chamber by the plug-cock method, is the chief point at issue, both when the exhausted chamber is dry and when it is wet. In proportion as the exhaustion is less adiabatic and more isothermal the value of γ found will decrease from about 1.4 to 1.0.

The normal equation of the transformation impressed on the gas is thus

$$pv^{\gamma} = \frac{p}{\rho^{\gamma}} = \frac{p_0}{\rho_0{}^{\gamma}} \tag{4}$$

for approximately adiabatic expansion, in case of pressure p, specific volume v, and density ρ, for two different states. Similarly the intrinsic equation of a gas and the Lorentz equation (afterwards to be corrected) for the change of index of refraction of air with temperature and pressure (the temperature coefficient being approximately identical with the coefficient of expansion), are

$$p = R\rho\vartheta \tag{5}$$

$$p = C\,(\mu - 1)\,\vartheta \tag{6}$$

Here R is the gas constant and ϑ the absolute temperature. C for refraction thus corresponds to R and $(\mu - 1)$ to ρ. To determine C, since

$$C = \frac{p_0}{\vartheta_0(\mu_0 - 1)}$$

the data in Landolt and Boernstein's tables are available. If Mascart's or Kaiser and Runge's data be taken

$$C = \frac{76}{273} \quad \frac{1}{.000292} = 952.6$$

Mascart's equation differs from equation (6) by the appearance of two corrective members and may be written, if t is temperature in degrees centigrade and the pressure p is expressed in centimeters of mercury,

$$p = C(\mu - 1)\vartheta \frac{1 + .00015\,t}{1 + .0000072\,p}$$

which is nearly equivalent to replacing C in equation (6) by

$$C\,(1 + 10^{-6} \times 150\,t - 10^{-6} \times 7.2\,p)$$

The difference is usually within 0.3 per cent and thus easily allowed for. The full equation will be considered below.

Returning to equations (5) and (6), we obtain by division

$$\rho = \frac{C}{R}(\mu - 1)$$

which in (4) gives

$$\frac{p}{(\mu - 1)^{\gamma}} = \frac{p_0}{(\mu_0 - 1)^{\gamma}} \tag{7}$$

If the air in the chamber F is partially exhausted from p_0 to p, changing the index of refraction of air from μ_0 to μ and ΔN, the displacement of the opaque mirror at the micrometer, is needed to return the center of ellipses to its original position on the sodium line

$$\mu_0 e = \mu e + \mu_0 \Delta N$$

where e is the length, *i.e.*, the thickness of the exhaustion-chamber in the direction of the transmitted beam of light. Hence

$$\mu - 1 = \mu_0 - 1 - \frac{\Delta N}{e}$$

since μ_0 is practically equal to 1 in association with ΔN. This together with (5) and (6) inserted in equation (7) gives

$$\frac{p}{p_0} = \left(1 - \frac{C\vartheta_0}{ep_0}\Delta N\right)^{\gamma} \tag{8}$$

From (8)

$$\gamma = \frac{\lg (p/p_0)}{\lg\left(1 - \frac{C\vartheta_0}{ep_0}\Delta N\right)} \tag{9}$$

where p_0 and ϑ_0 are the initial pressure and temperature in the air-chamber just before exhaustion.

Furthermore, whenever the evanescence of n rings is observed

$$\Delta N = n(\lambda/2)$$

for a mean wave-length λ over which the center of rings passes. Equation (9), which may now be written

$$\Delta N = \frac{e}{C}\left(\frac{p_0}{\vartheta_0} - \frac{p}{\vartheta}\right) \tag{10}$$

shows that ΔN depends simply on the change of density of the gas and not on its temperature and pressure separately. Hence ΔN does not change after exhaustion while the air in the chamber, with rise of temperature and of pressure, gets back to atmospheric temperature. For if the chamber is tight, ρ remains constant. This is true to the extent in which C is constant. Nevertheless in practice, during the short period of apparently stationary minimum temperature and pressure subsequent to exhaustion, it is easy to observe the evanescence of a number of rings in a sense equivalent to an increase of ΔN. This phenomenon will be discussed at length below.

If in equation (8) corrected with reference to Mascart's results the correction factor is placed within the parenthesis and $\delta t = t_0 - t$ and $\delta p = p_0 - p$, the value of γ is very nearly

$$\gamma = \frac{\lg (p/p_0)}{\lg\left(1 - a''\delta\vartheta + \beta\delta p - \frac{C\vartheta_0\Delta N}{ep_0}(1 + a''t - \beta p)\right)} \tag{11}$$

where $a = 0.00015$ and $\beta = 0.0000072$ relative to centimeters of mercury. Thus γ is not quite independent of the individual pressures and tempera-

tures, but it is difficult to state at the outset what will happen. If an expansion in series is to be made from equation (11) to include the correction, δp must be very small and the equation becomes

$$\gamma = \frac{e\delta p}{C\vartheta_0 \Delta N + \alpha''(C\vartheta_0 t \Delta N + ep_0 t_0) - \beta(C\vartheta_0 \Delta N p + ep^2_0)} \tag{12}$$

which shows that γ without the correction is too large.

For the case in which δp and ΔN are small, equation (9), if expanded, thus leads simply to

$$\gamma = \frac{e\delta p}{C\vartheta_0 \Delta N} \tag{13}$$

where δp is the drop of pressure on adiabatic expansion. Here γ depends on the percentage accuracy of δp, e, C, ϑ_0, and ΔN, while p_0 does not enter the equation. The sensitiveness is thus directly increased by elongating the chamber in the direction of the beam of light as suggested above. A similar approximation is obvious when $\gamma = 1$, very nearly. In such a case (13) also applies, or ΔN and δp are here proportional quantities.

In general, if $\gamma a = \log_{10}(p/p_0)$

$$\Delta N = \frac{1 - 10^{a}}{C\vartheta_0 / ep_0}$$

When use is made of the combined air-chamber and vacuum-chamber (the latter having been taken as infinite in size in the above equations) and sudden expansion takes place from one to the other, the initial temperature and pressure p_0 and ϑ_0 in the air-chamber and the initial pressure p of the vacuum-chamber are observed; but the final common pressure, p', when the chambers are in communication, can not as a rule be found by observation. The pressure p' may, however, be computed from the initial pressure p of the vacuum-chamber before exhaustion as follows: Let v be the (small) volume of the air-chamber where γ is observed and which contains a plenum of air and V the (large) volume of the vacuum-chamber. The functions of these chambers may, of course, be reversed, so that low pressure exists in the air-chamber and a plenum in the vacuum-chamber. Since the increase and diminution of volume v' are identical for the two chambers

$$p_0 v^{\gamma} = p'(v + v')^{\gamma}; \; p V^{\gamma} = p'(V - v')^{\gamma}$$

and v' may be eliminated; whence

$$\left(\frac{p'}{p_0}\right)^{1/\gamma} = \left(\frac{p}{p_0}\right)^{1/\gamma} \frac{V}{V+v} + \frac{v}{V+v} = 1 - \frac{C\vartheta_0 \Delta N}{ep_0} \tag{15}$$

and finally

$$\gamma = \frac{\lg(p/p_0)}{\lg\left(1 - \frac{V+v}{V}\,\frac{C\vartheta_0 \Delta N}{ep_0}\right)} \tag{16}$$

so that the initial pressure, p_0, of the air-chamber and p of the vacuum chamber need only be observed, if the relative volumes v/V are known.

If $v/V=0$, the above equation (9) is reproduced. From equation (16) the values of ΔN for $\gamma=1$ and $\gamma=1.41$ may be computed, *viz*,

$$\Delta N_{\gamma=1}=\frac{ep_0}{C\vartheta_0}\left(1-\frac{p}{p_0}\right)\frac{V}{V+v} \tag{17}$$

and

$$\Delta N_{\gamma=1.41}=\frac{ep_0}{C\vartheta_0}\left(1-\frac{p}{p_0}\right)^{.71}\frac{V}{V+v} \tag{18}$$

where $1/\gamma=.71$.

Finally, the fall of temperature appears as

$$\lg\vartheta'=\lg\vartheta_0+(\gamma-1)\lg\left\{\left(\frac{p}{p_0}\right)^{1/\gamma}\frac{V}{V+v}+\frac{v}{V+v}\right\} \tag{19}$$

where ϑ_0 is the initial and ϑ' the final temperature in the air-chamber immediately after exhaustion.

If the rôles of the air-chamber and the vacuum-chamber are exchanged, *i.e.*, if the vacuum-chamber now contains a plenum of air, ΔN becomes negative, so that arithmetically $p>p_0$,

$$\gamma=\frac{\lg\,(p/p_0)}{\lg\left(1+\frac{V+v}{V}\,\frac{C\vartheta_0\Delta N}{ep_0}\right)} \tag{20}$$

which, if $v/V=0$, or the atmospheric pressure, B, becomes the common adiabatic pressure, reduces to

$$\gamma=\frac{\lg\,(B/(B-\delta p))}{\lg\left(1+\frac{C\vartheta_0\Delta N}{e(B-\delta p)}\right)} \tag{21}$$

All the quantities needed in equation (9) are easily measured except ΔN, the micrometer displacement for so small a value of e as has entered into these experiments. The error made in ΔN due to the mere placing of the center of ellipses on the fiducial sodium line is not larger than .00005 cm. But there may be further discrepancy owing to the flexure of glass windows or to their displacement. To compute it, the equation ($v/V=0$)

$$\frac{\partial\gamma/\gamma}{\partial(\Delta N)}=\frac{C\vartheta_0/ep_0}{\left(\lg\left(1-\frac{C\vartheta_0\Delta N}{ep_0}\right)\right)\left(1-\frac{C\vartheta_0\Delta N}{ep_0}\right)} \tag{22}$$

may be used.

Finally, we may add to these equations the value of the actual expansion v' which the volume v of the air-chamber undergoes on sudden change of pressure from p_0 to p', when p is the pressure of the vacuum-chamber of volume V. From equation (15) on reduction

$$\frac{v'}{v}=\frac{p_0^{1/\gamma}-p^{1/\gamma}}{p^{1/\gamma}+\frac{v}{V}p_0^{1/\gamma}} \tag{23}$$

if $V=\infty$

$$v'/v=(p_0/p)^{1/\gamma}-1$$

which is identical with the adiabatic equation.

88. Small brass fog-chamber dry and wet.—The first experiments were tried with a small air-chamber of brass (fig. 60), flanged at both ends and provided with an exhaust-pipe E leading by way of a 1½-inch rubber hose to a large vacuum-chamber. This was kept at a definite low pressure by an air-pump. A cock (not shown) was available for influx of dry air into F. The ends of F are closed with glass plates g g', secured by a ring and bolts which press the plates against the rubber gaskets r r' with complete freedom from leakage. The dimensions of the chamber F were: length, 17 cm., diameter, 3.7 cm. The exhaust-pipe was 2.7 cm. in diameter and somewhat over 50 cm. long. The volumes of the air (v) and vacuum (V) chambers were thus

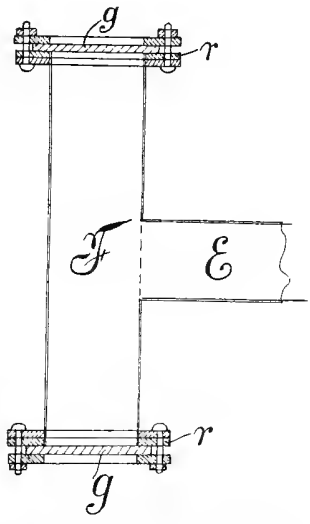

FIG. 60.—Longitudinal section of tubular air-chamber, 17 cm. long.

$$v = 183 + 442 = 625 \text{ cu. cm.}$$
$$V = 12770 + 97 = 12867 \text{ cu. cm.}$$

respectively, whence $v/V = .049$. Unavoidably the pipe comprised a greater volume than the air-chamber. The latter was lined with thick dry blotting-paper to be moistened with water at the end of the experiment.

The measurements were made with this by placing the center of ellipses on the sodium line and noting the micrometer reading, then suddenly exhausting by opening the 1-inch stop-cock into the vacuum-chamber and closing it again by a single sweep of 180°. The ellipses were now brought back to the sodium line by moving the micrometer over the measured distance ΔN from the first position. Table 38 gives an example of the mean results for drops of pressure between 20 and 60 cm. At each of these stages many measurements were made and the mean of the results taken. ΔN, so far as mere measurement is concerned, is correct to 0.00005 cm. in a single reading.

TABLE 38.—Experiments made with the small brass air-chamber attached to the arm m, fig. 59. Method by exhaustion into vacuum-chamber. Barometer, $p_0 = 76.13$ cm.; temperature, $t_0 = 20.7°$, $\theta_0 = 293.7°$; length, $e = 17$ cm.; $C = 952.6$; $v/V = .049$.

p	$10^6 \Delta N$	γ
56.13	1250	0.97
36.13	2500	.96
16.13	3900	.84

Here γ is so nearly 1 that the expansion takes place under virtually sothermal conditions, in view of the small air-chamber and in spite of

the rapidity of exhaustion. That this is not quite the case, however, is shown by the distorted ellipses immediately after exhaustion, indicating that the rays corresponding to different parts of the ellipses have passed through air at different temperatures; but the uniformity is soon again restored. It is also to be borne in mind that γ for the case of equation (2) is inherently too small.

It is not impossible, however, that these low values of γ which imply an excessive ΔN may in a measure be owing to some distortion of the arm m to which the chamber was attached during exhaustion. Strains introduced here are necessarily very serious and they would be largest at the highest exhaustion.

The air-chamber was therefore detached from the arm m and supported on an *independent* standard, screwed to the same table on which the interferometer stood. The results are given in table 39, which again is a mean of many observations.

TABLE 39.—Experiments made with a small brass fog-chamber attached to independent standard on table. Exhaustion into vacuum-chamber. Barometer, $p_0=74.57$; temperature, $t_0=21.2°$, $\theta_0=294.2°$; constants as in table 38.

p	$10^6\Delta N$	γ
54.57	1250	0.97
34.57	2750	.82
14.57	4150	.66

These data for γ are actually worse than the preceding, showing that distortion during exhaustion has been effectively increased. It is disconcerting to find that the individual observations, corresponding to any given drop of pressure, are definite and consistent, *i.e.*, apparently quite trustworthy; but this merely shows the subtle character of the strain error involved when transmitted through the table. If special tests are made they again prove that some adiabatic expansion does occur; for when the cock is left open, the rings continue to move outward, indicating a current from the air-chamber to the vacuum-chamber. This is nearly absent when the cock is rapidly closed. Moreover, by warping the table the effect observed is quite significant, being in part elastic and in part viscous.

Hence the small brass fog-chamber was now detached and *suspended from the wall* on an *independent* bracket and clamp, so as to be entirely free from the interferometer and table. The data are given in table 40.

These values of γ are probably correct, subject to the final correction, for the conditions involved, *i.e.*, for the degree of adiabatic expansion which can be reached in so small a chamber with the given means of exhaustion and so large a drop of pressure. The inadequacy of the small tube for the present purposes is shown (as instanced above) by the distortion of rings immediately after exhaustion, while their figures gradually become symmetrical again as the uniform temperature is regained, and

by the continuous exhaustion if the exhaust cock is left open instead of being swept rapidly from closed to closed over an arc of 180°. If the conditions had been isothermal, $\gamma = 1$, or quite adiabatic, $\gamma = 1.41$, the data

TABLE 40.—Experiments with air-chamber suspended from wall on independent bracket. Dry air. Exhaustion into vacuum-chamber. Barometer, $p_0 = 75.80$; mean absolute temperature, $\theta_0 = 291.8°$; constants as in table 38.

p	$10^6 \Delta N$	γ	$10^6 \Delta N$ for $\gamma = 1$	$10^6 \Delta N$ for $\gamma = 1.41$	γ corrected
55.80	1100	1.08	1170	868	1.12
35.80	2250	1.06	2330	1834	1.11
15.80	3450	1.05	3500	2985	1.13

of ΔN computed in the table should have been found. The error of mere measurement, being not much larger than $\Delta N = 5 \times 10^{-5}$ cm., can not explain any of these discrepancies, though it does account for the irregularities.

TABLE 41.—Small brass fog-chamber remounted. Brass-tube connection. Fog-chamber exhausted. Barometer, $p = 75.26$, $\theta = 290°$ to $290.8°$; $v/V = .014$; $e = 17$ cm.

p_0	$10^6 \Delta N$	γ	Comp. $10^6 \Delta N$ $\gamma = 1$	Comp. $10^6 \Delta N$ $\gamma = 1.41$	γ corrected
65.22	575	1.056	607	426	1.090
55.17	1050	1.138	1214	826	1.172
45.13	1650	1.082	1816	1196	1.112
35.08	2225	1.065	2421	1527	1.091
25.04	2633	1.068	3036	1795	1.116
15.00	3300	1.052	3632	1946	1.070
4.95	4000	1.021	4237	1769	1.034

Some time later experiments were repeated with the same chamber, using, however, a 2-inch brass exhaust-pipe (with the exception of the 1-inch mouth at the chamber), a 2½-inch stop-cock, and a very large vacuum-chamber, $v/V = .014$. The new results are given in table 41.

TABLE 42.—Experiments with fog-chamber suspended from an independent wall-bracket. Wet air. Barometer, $p_0 = 76.00$ cm.; absolute temperature, $\theta_0 = 297.3°$; constants as in table 38.

p	$10^6 \Delta N$	γ	Comp. $10^6 \Delta N$ $\gamma = 1$	Comp. $10^6 \Delta N$ $\gamma = 1.41$
56.00	1050	1.11	1140	852
36.00	2100	1.14	2290	1799
16.00	3400	1.03	3430	2927

The improvements have made little difference in the results for γ. They are still of the same low order as in the preceding case. It is probable, moreover, that the transformation in the large exhaust-pipe unavoidably attached is more nearly adiabatic than in the small fog-chamber.

Additional experiments with dry air did not seem to promise new returns. The air-chamber was therefore converted into a fog-chamber by thoroughly wetting the blotting-paper within. The results obtained with air saturated with moisture are shown in table 42.

These data are virtually the same as for dry air. The computed values of ΔN for $\gamma = 1$ and $\gamma = 1.41$, compared with the observed ΔN, together with the values of γ found, indicate the degree of imperfect adiabatic cooling. The glass faces at the ends of the chamber at first remained quite clear. Later they were apt to become cloudy, making observation exceedingly difficult. The film of moisture may be removed by heating the glass slightly, but this is not a trustworthy procedure, even if time is allowed before the next observation.

89. Larger (wood) fog-chamber. Dry air.—The next experiments were made with an air-chamber, F, fig. 59, of wood with walls about 0.25 inch thick, covered while hot, within and without, with an adhesive coating of resin and beeswax. The ends were perforated with holes about

TABLE 43.—Experiments with small rectangular wood fog-chamber, with wax and resin, suspended from independent wall-bracket, probably too loose. Exhaustion into vacuum-chamber. Dimensions $14 \times 10.7 \times 7.8 = 1155$ c. c. Barometer, $p_0 = 77.08$ cm.; absolute temperature, $\theta_0 = 296.5°$; $C = 952.6$; effective length, $e = 15.32$ cm.; $v/V = .124$. Fog-chamber slightly leaking.

p	$10^6 \Delta N$	γ	Comp. $10^6 \Delta N$ $\gamma = 1$	Comp. $10^6 \Delta N$ $\gamma = 1.41$	t
57.08	650	1.57	970	718	1.51°
37.08	1550	1.37	1930	1515	−26.40
17.08	2500	1.37	2900	2459	−66.81

1½ inches in diameter and closed with glass plates cemented to the wood. The inside as before was lined with thick dry blotting-paper, subsequently to be moistened. The dimensions of the chamber (within) were: length, 14 cm., breadth, 10.7 cm., thickness, 7.8 cm.; and the exhaust-pipe was over 3 cm. in diameter. Thus the volume of the chamber with its pipe as far as the stop-cock was $v = 1155 + 442 = 1597$ c. c., while the corresponding volume of the vacuum-chamber and pipe was $V = 12771 + 96 = 12867$ c. c. Hence $v/V = .124$. With a chamber of this size a reasonable degree of adiabatic expansion may be expected and the results obtained in table 43 show the improvement.

We here encounter the curious result of a value of γ larger than the normal value for air. From the above equations it therefore follows that ΔN is too small or γ too large [equations (10) and (13)]. The values of ΔN computed for $\gamma = 1.41$ or $\gamma = 1$ are given in the table. The large result might therefore occur in consequence of leakage, but in view of the low drop of pressure it is probably to be referred to some residual distortion. If we consider the equation (9) for γ, it will be seen that for a given δp,

γ would decrease from $\propto$ to zero, while ΔN varies from zero to $ep_0/C\theta_0$, the maximum value (about 0.004 in the given work) consistent with a real value of γ, in the absence of all leakage. ΔN must therefore be greater for isothermal than for adiabatic expansion.

TABLE 44.—Experiments with wood-chamber as in table 43. Exhaustion into vacuum-chamber. Barometer, $p_0 = 76.65$; absolute temperature, $\theta_0 = 296.1°$

p	$10^6\Delta N$	γ	Comp. $10^6\Delta N$ $\gamma = 1$	Comp. $10^6\Delta N$ $\gamma = 1.41$	t
56.65	800	1.248	970	720	1.05°
36.65	1750	1.16	1930	1520	−27.05
16.65	2800	1.09	2900	2470	−67.93

It is probable, as suggested, that the excessive γ in question is due to some sort of distortion in the apparatus. Seeing that the efficient length of ray used is relatively small (15.3 cm.), a slight change of the inclination or of the optical properties of the glass plate through which the ray passes during the occurrence of exhaustion might be the cause of it. However, in table 44 the results were repeated with care (5 to 10 observations for ΔN, the means of which were taken), with the apparatus practically free from leakage. The table as before contains the values for ΔN which would obtain when $\gamma = 1$ and $\gamma = 1.41$, as well as the reduction of temperature in degrees centigrade, due to adiabatic cooling, when $\gamma = 1.41$.

TABLE 45.—Experiments with wood fog-chamber as in table 43. Suspension laterally braced. Exhaustion into vacuum-chamber. Barometer, $p_0 = 76.14$; absolute temperature $\theta_0 = 295.5°$.

p	$10^6\Delta N$	γ	Comp. $10^6\Delta N$ $\gamma = 1$	Comp. $10^6\Delta N$ $\gamma = 1.41$	t
66.14	400	1.23	480	350	+11.99°
56.14	810	1.23	970	720	.31
46.14	1260	1.23	1450	1110	−12.86
36.14	1690	1.22	1940	1520	28.03
26.14	2290	1.11	2420	1970	46.18
16.14	2760	1.14	2910	2480	69.46
6.14	3315	1.12	3390	3090	102 96

The adjustment was now further improved by additionally bracing the wall-bracket from which the fog-chamber was suspended. This resulted in a much more definite fiducial reading at the micrometer. The results are given on the same plan as above, in table 45. Readings were taken systematically in series, the drop of pressure δp varying in succession by intervals of 10 cm.

These results are throughout as near the true value as may be anticipated for the case of so short an apparatus.

Another more detailed series of experiments was now made, with the drop of pressure δp increasing in steps of 10 cm. as far as 70 cm., and then decreasing again. These results as a whole are about the same as in the preceding table, except that γ at the beginning is relatively high. The

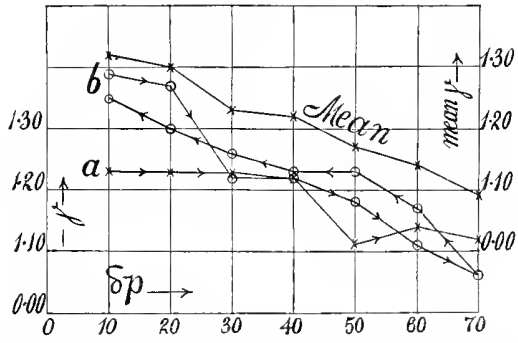

FIG. 61.—Charts showing relation of γ to $\delta p = p_0 - p$ (approximately the drop of pressure) in case of small wood fog-chamber. Curve a corresponds to table 45 and curve b to table 46. Mean result shown above these curves.

two series of table 46 together give a good account of the actual degree of adiabatic expansion reached. The mean results are shown graphically in fig. 61. A few other experiments were incidentally made, showing values of about the same order, and may therefore be withdrawn here.

TABLE 46.—Experiments with wood fog-chamber as in table 43, well braced. Exhaustion into vacuum-chamber. Barometer, $p_0 = 75.75$; absolute temperature, $\theta_0 = 291.7°$ to 292.3°.

p	$10^6 \Delta N$	γ	Comp. $10^6 \Delta N$ $\gamma = 1$	Comp. $10^6 \Delta N$ $\gamma = 1.41$	t
I. Pressure drop δp increasing.					
65.75	360	1.39	490	360	+8.27
55.75	750	1.37	980	730	−3.26
45.75	1280	1.20	1470	1120	16.25
35.75	1710	1.22	1960	1540	31.27
25.75	2230	1.18	2450	2000	49.31
15.75	2820	1.11	2940	2510	72.57
5.75	3400	1.06	3430	3140	108.07
II. Pressure drop δp decreasing.					
5.75	3400	1.06	3430	3140	−108.02
15.75	2750	1.17	2940	2510	72.43
25.75	2170	1.23	2450	1990	49.01
35.75	1700	1.23	1960	1540	30.85
45.75	1230	1.26	1470	1120	15.71
55.75	780	1.30	980	730	2.61
65.75	370	1.35	490	360	+ 9.24

90. The same. Wet air.—The endeavor was now made to obtain the corresponding data for the same (wood) fog-chamber respectively dry and wet in succession. Tables 47 and 48 contain the results given on the same plan as in the preceding tables. Neither of these series, either the dry or the wet set, is satisfactory. In the latter case, in particular, the clouding over of the window, which occurs in the lapse of time, is a constant

TABLE 47.—Experiments with wood fog-chamber as in table 43, well braced. Exhaustion into vacuum-chamber. Barometer, $p_0 = 76.90$; absolute temperature, $\theta_0 = 293.2°$. Dry air.

p	$10^6 \Delta N$	γ	t	p	$10^6 \Delta N$	γ	t
66.86	450	1.10	+12.97°	26.68	2090	1.30	−20.15°
56.81	800	1.26	5.57	16.64	2700	1.20	20.27
46.77	1150	1.36	− 6.07	6.59	3200	1.28	33.51
36.72	1750	1.18	10.25				

TABLE 48.—Experiments with wood fog-chamber as in table 43, well braced. Exhaustion into vacuum-chamber. Barometer, $p_0 = 76.90$; absolute temperature, $\theta_0 = 293.3°$. Wet air.

p	$10^6 \Delta N$	γ	p	$10^6 \Delta N$	γ
66.86	350	1.43	26.68	2330	1.09
56.81	830	1.21	16.64	2840	1.08
46.77	1280	1.19	6.59	3450	.97
36.72	1680	1.24			

annoyance. On the other hand, it is curious to note the essential transparency of the fog produced. The observer at the telescope scarcely notices any difference in the sharpness of the ellipses so long as the windows remain clear. If the wet data are compared with the mean results of tables 45 and 46 above, they show about the same order of behavior, though the wet values for γ are as a rule below those for dry air, as they should be. In

TABLE 49.—Experiments with wet air as in table 48. Barometer, $p_0 = 74.64$; absolute temperature, $\theta_0 = 291.5°$.

p	$10^6 \Delta N$	γ	t
54.55	1000	.98	− 3.90°
34.46	1850	1.10	32.66
14.38	2720	1.21	75 53

general, however, no very marked difference in character has been detected, and it was a disappointment to note that the presence of fog-particles contributed almost nothing to the experiment. The further trials of the wet chamber became more unsatisfactory, owing both to the lack of transparency of the glass and the gradual development of leakage in the chamber. The values in table 49 are of the same order as the preceding and lead to no new conclusions.

In some of the experiments radium was placed on top of the chamber to increase the density of the fog at low exhaustions, but no definite effect was detected.

91. Copper fog-chamber. Exhaustion. Dry air.—A larger vessel of thin copper well braced within, with large glass windows, was now constructed with a special view to an increase of the size of the efflux-pipe and stop-cock. The dimensions of this chamber were $20.4 \times 15.6 \times 18.7 = 5937$ c. c. In the first experiments the inch exhaust-cock with the wide

TABLE 50.—Adiabatic expansion in copper air-chamber, $20.4 \times 15.6 \times 18.7$ cm., well-braced. Exhaustion into vacuum-chamber. $v/V = .496$; barometer, $p_0 = 76.55$; absolute temperature, $\theta_0 = 291°$; $e = 20.89$.

p	Obs. $10^6 \Delta N$	γ	$10^6 \Delta N$ comp. $\gamma = 1$	$10^6 \Delta N$ comp. $\gamma = 1.41$	t $\gamma = 1.41$	t obs. γ
66.51	400	1.29	500	370	+10.3°	+11.99°
56.46	775	1.36	1010	750	1.9	3.22
46.42	1200	1.34	1510	1150	− 7.4	− 4.32
36.37	1650	1.33	2020	1580	17.9	12.61
26.33	2280	1.19	2520	2050	29.9	8.56

rubber tubing was directly attached, increasing the volume by 442 c. c. Hence the total volume was $v = 6379$, while that of the vacuum-chamber (as above) amounted to $V = 12867$ c. c.; hence $v/V = .50$ to be used in the reduction of initial pressure p_0 and temperature θ_0 of the air-chamber and the initial pressure p and temperature θ_0 of the vacuum-chamber to the values when momentarily in communication. A very careful series of

TABLE 51.—Adiabatic expansion in copper air-chamber as in table 50. Exhaustion into vacuum-chamber. Barometer, $p_0 = 74.60$; absolute temperature, $\theta_0 = 294.5°$.

p	Obs. $10^6 \Delta N$	γ	$10^6 \Delta N$ comp. $\gamma = 1$	$10^6 \Delta N$ comp. $\gamma = 1.41$	t $\gamma = 1.41$	t γ obs.
64.56	380	1.34	498	362	+13.5°	+14.5°
54.51	800	1.29	996	742	4.7	8.6
44.47	1316	1.18	1490	1140	− 5.0	7.4
34.42	1738	1.23	1990	1570	16.0	− 2.9
24.38	2125	1.32	2490	2040	28.8	20.6

experiments was now made with dry air, the vacuum increasing in steps of pressure of 10 cm. each as far as $\delta p = 50$ cm. Exhaustion, as above, took place from the air-chamber to the vacuum-chamber. The results are summarized in table 50, experiments being made both for increasing and decreasing exhaustion.

A comparison of the observed ΔN which should be correct to 5×10^{-5} cm. and the computed ΔN both for $\gamma = 1$ and $\gamma = 1.41$, shows the degree

to which the observations may be trusted. The difficulties are naturally most serious at the low and the high values of δp. Neglecting these, the values of γ are as a whole higher than in the mean case of tables 45 and 46, for the small wood fog-chamber. The table, moreover, contains the fall of temperature both for the case of $\gamma = 1.41$ and the actual fall, as computed for the mean values of γ observed. The experiments were now repeated, using an uncompensated interferometer with smaller ellipses. The results are given in table 51, the method being the same as in the preceding case.

These data are lower in general value and correspond to tables 45 and 46. The three causes of discrepancy are (as before) the relatively long interval of communication of the chambers, the distortion of the air-chamber and its effect on interference, and the same in its effect on the volume and density of the gas contained. The mean result of these two tables may be compiled for reference.

δp =	10	20	30	40	50 cm.
γ (mean) =	1.31	1.32	1.26	1.28	1.25

Curiously enough the mean curves so obtained are similar (see fig. 62), showing that the larger chamber is more favorable to adiabatic expansion, as would be anticipated.

If in table 51 instead of equation (16) the corresponding equation (12) correcting the temperature and pressure coefficients is taken, the values of γ are scarcely changed.

$\alpha'' = .00015$; $\beta = .0000072$; $\delta t = t_0 - t$; $\delta p = p_0 - p$

δp =	10	20	30	40	50
γ =	1.32	1.28	1.17	1.21	1.30
δt =	7°	13°	14°	24°	42°
$(\alpha''t - \beta p) \times 10^6$ =	1710	898	+798	−683	−3270
$(\alpha''\delta t - \beta\delta p) \times 10^6$ =	978	1790	1884	3370	5950

In the present experiments, therefore, this correction may be neglected.

In view of the evanescence of two or more rings after adiabatic expansion or compression, always in the same sense as the expansion or compression, *i.e.*, corresponding to an increase of ΔN, it is worth while to compute the possible effect of the Mascart correction on a gas kept at constant volume or density, while p and θ change subject to the intrinsic equation of a gas. If the latter passes from t and p through t_0 and p_0 and ΔN is the corresponding displacement of the micrometer, we may write very nearly

$$-\delta N = \frac{e p_0}{C \vartheta_0}(\alpha''(t_0 - t) + \beta(p_0 - p))$$

Hence in table 51, where $ep_0/C\theta_0 = .00555$, the following values would hold, $\delta p = p_0 - p$,

δp =	10	20	30	40	50 cm.
$\delta N \times 10^6$ =	5.4	9.9	10.4	18.7	33.0

quantities too small to be measured, and even in the latter extreme case equivalent to the evanescence of only a single ring in the sense *opposite* to the motion of those observed. Thus the observed phenomenon is not due to the present correction. It might be due to slight leakage through the 2½-inch stop-cock, from the initially colder to the initially hotter vessels, as these regain atmospheric temperature. In such a case, however, it would not stop with a few rings while the pressure difference remained.

92. The same. Compression. One-inch stop-cock.—An inversion of the method was now made, in which the air-chamber was exhausted, while the former vacuum-chamber contained a plenum of air. The latter may therefore be removed with advantage, and the atmosphere used directly, in which case $v/V=0$ and equation (9) is applicable in the form (21). The results are given in tables 52 and 53. These data for γ are surprisingly small, much below the mean results for the preceding tables. The reason for this will presently appear.

TABLE 52.—Adiabatic compression of air in copper fog-chamber (as in table 50). Dry air. Interference method. $p_0<B$. One-inch stop-cock and pipe. Barometer, $p=76.74$; absolute temperature, $\theta_0=296.5°$.

p_0	Obs. $10^6\Delta N$	γ	Comp. $10^6\Delta\bar{N}$ $\gamma=1$	Comp. $10^6\Delta\bar{N}$ $\gamma=1.41$	t $\gamma=1.41$	t γ obs.
46.61	1868	1.15	2220	1465	69.80°	53.78°
36.56	2553	1.11	2960	1874	94.88	69.36

TABLE 53.—The same. Barometer, $p=75.40$; absolute temperature, $\theta_0=298.3°$.

p_0	Obs. $10^6\Delta N$	γ	Comp. $10^6\Delta\bar{N}$ $\gamma=1$	Comp. $10^6\Delta\bar{N}$ $\gamma=1.41$	t $\gamma=1.41$	t γ obs.
45.27	1781	1.19	2210	1455	72.59°	50.2°
35.22	2481	1.13	2940	1853	99.75	53.0

93. The same. Compression. Two and one-half inch stop-cock.—The endeavor was now made to raise the value of γ by replacing the rubber tube and inch stop-cock previously used with a 2½-inch brass stop-cock and a 2-inch brass tube. It was necessary, however, to make use of the very large vacuum-chamber to which the cock was attached, so that a small ratio of volume enters, as in equation (20) above. The volumes were $v=5937+1374=7311$ c. c., $V=103{,}908+393=104{,}301$ c. c., whence $v/V=.070$. The experiments are given in tables 54 and 55. These data are virtually identical with the preceding set by the same method, in spite of the larger stop-cock used. Supposing that the inevitable leak in the large stop-cock is practically negligible, a sufficient explanation for the low results in the compression method is the inrush of relatively cold air which

at high exhaustion introduces an additional and very serious error, to which the exhaustion method is obviously not subject.

TABLE 54.—Adiabatic compression of dry air in copper fog-chamber (as in table 50). Interference method. $p_0 < B$. Two and one-half inch stop-cock; 2-inch pipe. $v/V = .07$. Barometer, $p = 76.44$; absolute temperature, $\theta_0 = 297°$.

p_0	Obs. $10^6\Delta N$	γ	Comp. $10^6\Delta N$ $\gamma = 1$	Comp. $10^6\Delta N$ $\gamma = 1.41$	t $\gamma = 1.41$	t γ obs.
46.31	1786	1.13	2070	1366	67.88°	40.8°
36.26	2400	1.11	2760	1747	91.89	45.6

TABLE 55.—The same. Barometer, $p = 75.43$; absolute temperature, $\theta_0 = 294.7°$.

p_0	Obs. $10^6\Delta N$	γ	Comp. $10^6\Delta N$ $\gamma = 1$	Comp. $10^6\Delta N$ $\gamma = 1.41$	t $\gamma = 1.41$	t γ obs.
65.39	595	1.16	694	486	33.4°	27.2°
45.30	1783	1.14	2081	1374	66.1	39.8
35.25	2407	1.11	2775	1755	90.6	43.6
25.21	3050	1.09	3469	2064	126.5	48.5

94. Clement and Desormes's apparatus.—It now seemed desirable to compare the above results for the copper air-chamber with the value of γ directly determinable by the classic method of Clement and Desormes. For this purpose the vacuum-chamber was completely removed, so that the partially exhausted air-chamber instantaneously communicated with the air at barometric pressure. To determine the adiabatic temperature an accessory mercury column, h, was considered sufficient, as no great accuracy was aimed at. Thus if p_0 and θ_0 be the initial pressure and temperature of the air-chamber and p and θ_0 those of the atmosphere, while θ is the adiabatic temperature,

$$\frac{\vartheta_0}{\vartheta} = 1 - h/p$$

or no temperature measurement is necessary. Thus if B be the height of the barometer

$$\gamma = \frac{\lg (p_0/p)}{\lg(p_0/(B-h))} \tag{24}$$

quite generally, if p_0 and p are the pressures in the air-chamber and the vacuum-chamber, if at hand. The results are given in tables 56 and 57.

It was not possible to quite overcome the slight leakage of the large 2½-inch plug stop-cock. Hence the final h is too small. In general these results are of the same order of value, though somewhat larger than the corresponding results (air-chamber exhausted) by the interference method.

It is difficult to suggest any reason for this, since any leakage in consequence of the long waiting for h necessary, in the present method, should decrease γ.

TABLE 56.—Clement and Desormes's method for γ. Copper fog-chamber. Exhaustion into air-chamber. Barometer, $p=76.12$; absolute temperature, $\theta=293.8°$.

p_0	h	γ
66.12	2.16	1.257
56.12	4.28	1.234
46.12	6.07	1.199
36.12	7.79	1.169
26.12	9.33	1.139

TABLE 57.—The same. Barometer, $p=75.89$; absolute temperature, $\theta=295°$.

p_0	h	γ
55.89	4.28	1.234
45.89	6.08	1.199
35.89	7.63	1.165
25.89	9.18	1.136

Hence the experiments were repeated with the large vacuum-chamber attached, so that both the reciprocal cases of an exhausted air-chamber

TABLE 58.—Clement and Desormes's method. Copper fog-chamber. Air-chamber exhausted. $v/V=.070$. Barometer, $p=75.08$; absolute temperature, $\theta=290.8°$.

p_0	p' approximate	h	γ
65.04	74.28	3.03	1.315
54.99	73.58	5.59	1.253
44.95	72.93	8.05	1.215
34.90	72.33	10.10	1.172
24.86	71.53	11.95	1.135

TABLE 59.—Clement and Desormes's method. $v/V=.070$. Vacuum-chamber exhausted. Barometer, $p_0=\left\{\begin{matrix}75.08\\75.22*\end{matrix}\right\}$; absolute temperature, $\theta=\left\{\begin{matrix}290.8°\\296.0*\end{matrix}\right\}$

p	p' approximate	h	γ
64.95	65.59	7.19	1.367
55.05	53.36	14.32	1.359
45.03	47.08	22.20	1.344

* First observation, $\delta p=10$.

$p_0<B=p$ and a full chamber $p<B=p_0$ might be compared. The data are given in tables 58 and 59, where p' is the approximate adiabatic expansion as read off on the gauge of the *large* vacuum-chamber.

To compute these results, equation (24), if p' is the adiabatic pressure in question,

$$\gamma = \frac{\lg\,(p'/p_0)}{\lg\,((B-h)/p_0)}$$

may be modified to read

$$\gamma = \frac{\lg\,(p/p_0)}{\lg\left\{\frac{B-h}{p_0}\,\frac{V+v}{V} - \frac{v}{V}\right\}} \tag{25}$$

where p_0 and p are the initial pressures of air and vacuum chambers and v/V the volume ratio of their contents, respectively. If equation (24) be differentiated with respect to h,

$$\frac{\partial\gamma}{\partial h} = \gamma\,\frac{1}{(B-h)\,(\lg\frac{B-h}{p_0})}$$

Hence γ increases with h, if $B-h>p_0$ or when the air-chamber is exhausted, and *vice versa*. In the former case h is followed to a maximum and in the case of leakage is too small; hence γ is too small. If the vacuum-chamber is exhausted, h continually decreases and is liable to be observed too large; hence γ is again too small.

The results of table 58 are slightly larger than the similar case of tables 56 and 57, and they show a definite tendency to reach $\gamma=1.41$ when δp_0 the exhaustion of the fog-chamber vanishes. Possibly the leakage of the large stop-cock was under better control and the diminution of γ with the exhaustion δp is probably a trustworthy exhibit of the actual state of things.

TABLE 60.—Clement and Desormes's method. Copper fog-chamber. Vacuum-chamber exhausted, $v/V=.070$. Barometer, $p_0=75.58$; absolute temperature, $\theta=295°$ (about).

p	p' approximate	h corrected	γ
64.58	64.98	8.2	1.316
55.03	56.18	14.7	1.371
45.08	47.08	21.6	1.406

Since h reaches a definite maximum γ can not be too large. The results of table 59 have not the same certainty, since h must continually decrease, and the expansion after adiabatic exhaustion is indistinguishable finally from the small permanent leak into which it eventually passes. Hence h is too small and the results for γ are thus probably too large in proportion as δp increases.

The data of this method (vacuum-chamber exhausted) tend to approach the order of values of the corresponding interference data, though the latter are again small since equation (2) enters. In all cases, therefore, a full air-chamber shows large nearly normal values of γ, whereas the ex-

hausted air-chamber shows the reverse or small values of γ. True, this is in the same sense as the discrepancy of the leak in the large stop-cock, but it is not probably due to it. The actual value of the error in question per centimeter of h is shown in each table and its magnitude proves that the discrepancy can not be due to the leak.

Nevertheless it was thought advisable to actually evaluate the leak of the stop-cock in case of the latter method. The results so found are given in table 60, which may be regarded as free from the effects of leakage.

These results curiously enough show an increase of γ with the drop of pressure, the value for $\delta p = 40$ cm. being actually excessive. It is extremely difficult to account for this erratic behavior. The experiments were throughout made with great care. In the latter table in particular γ is reduced to the lowest value possible. Under these circumstances the mean values of γ for each method may be taken for reference. They are compared with the corresponding data for the interference method in fig. 62.

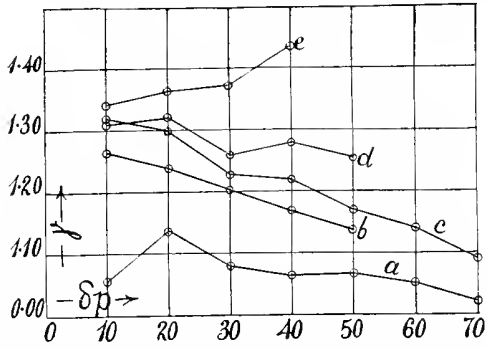

FIG. 62.—Charts showing relation of γ to $\delta p = p_0 - p$, for different fog-chambers and methods. Mean results.

95. Large wood fog-chamber.—The experiments were concluded with the aid of a large wood fog-chamber coated while hot with the mixture of wax and resin. The dimensions in centimeters were $15.6 \times 11.5 \times 45$, being those usually used in my experiments with coronas. This chamber was quite dry at the outset and throughout free from leakage. The volumes, including the 2-inch pipe for exhaustion and the 2½-inch stop-cock (the vacuum-chamber being the same as before), were

$$v = 8073 + 1374 \text{ c.c.} \qquad V = 104300 \text{ c.c.}$$

so that $v/V = .091$. Allowance was made for the very slight leakage of air from the fog-chamber to the vacuum-chamber through the stop-cock (as above), for each observation. In the chief experiments the plenum of air was in the fog-chamber. Table 61 shows the results obtained with dry air by Clement and Desormes's method. They are reproduced in fig. 64.

These results appear to be more trustworthy. The value of γ decreases but slightly up to the highest exhaustion, $\delta p = 40$ cm., which it was safe to apply.

The same chamber was now used for the measurement of γ by the interference method. The adjustments differed slightly from the above, as shown in fig. 63, where C is the light from the collimator incident on the grating G at an angle I, M and N the opaque mirrors, the latter on the micrometer. Both the component beams m and n and the reflected and diffracted R and D pass through the fog-chamber FF, the front and rear

TABLE 61.—Experiments with Clement and Desormes's method. Large wood fog-chamber, $v/V = .091$. Vacuum-chamber exhausted. Barometer, $p_0 = 76.22$; absolute temperature, $\theta_0 = 296°$ (about).

p	h	γ
66.09	6.89	1.374
56.22	13.63	1.403
46.69	21.14	1.361
36.02	29.60	1.361

sides of which are thick plate-glass. E is the 2-inch exhaust-pipe leading through the 2½-inch stop-cock to the vacuum-chamber. Other cocks (not shown in the figure) are at hand for influx of air, etc., together with a large hole for cleaning. The thermometer dipped into the fog-chamber. In the adjustment chosen not only the diffracted beam D (angle of diffraction, $\theta > I$), but another on the inner side of R ($\theta < I$), was available for measure-

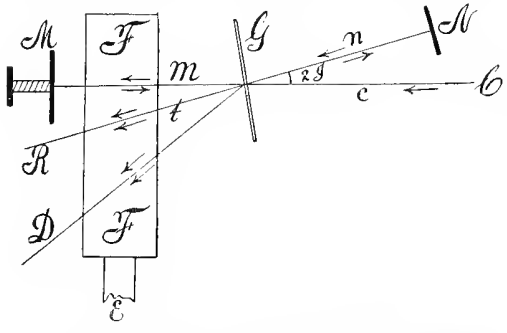

FIG. 63.—Diagram of displacement interferometer, $C\,G\,M\,N$, and large wood fog-chamber, FF, with 2-inch exhaust at E.

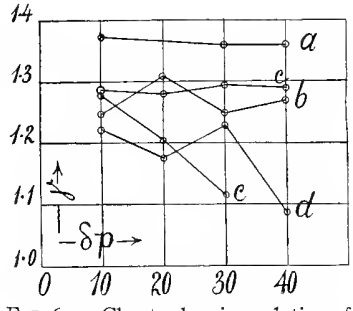

FIG. 64.—Charts showing relation of γ and $\delta p = p_0 - p$ in case of large wood fog-chamber.

ment. In the latter case θ was nearly zero, but though this is more luminous there seemed to be no advantage of one over the other. In view of the thick glass sides of the fog-chamber, it is preferable to put compensator plates in the component beam n to counterbalance those of the beam m. Otherwise the ellipses are too small and move too slowly. The method throughout worked admirably. Even when the inside is wet and a thick phosphorus fog is produced, measurement is still possible *through the fog*, a very unexpected result. In the course of time the glass becomes cloudy and must be rubbed clean. In such a case the observations are much

more difficult, unless the glass plates are very slightly heated by a moving Bunsen burner to evaporate the film of moisture. This procedure would not, however, be favorable to the occurrence of the nearest approach to adiabatic expansion which the chamber affords. From the different beams of spectrum light which pass through the fog-chamber, a number of sodium lines are available as fiducial lines, to which the center of ellipses is to be brought back. But the coincident ones for which the interference is adjusted are necessarily the most convenient. The construction of the interferometer did not permit the beam m to pass near the middle of the apparatus as would have been desirable. The results for γ are given in tables 62 and 63 and in fig. 63. They are as usual below the data of table 61 in case of Clement and Desormes's method for the same chamber. The reason for this has frequently been stated and is due to the assumption of the approximate equation (2) for experimental purposes.

TABLE 62.—Wood fog-chamber. Interference method. $v/V=.091$. Vacuum-chamber exhausted. Barometer, $p_0=75.92$; absolute temperature, $\theta=299.0°$ to $298.6°$; $e=15.6$.

p	$10^6\Delta N$	γ	γ corrected
65.52	425	1.247	1.2919
55.87	813	1.280	1.3292
45.94	1338	1.164	1.2139

TABLE 63.—The same. Barometer, $p_0=75.52$; absolute temperature, $\theta=293.4°$ to $293.1°$. Vacuum-chamber exhausted.

p	$10^6\Delta N$	γ	γ corrected
55.92	775	1.344	1.3950
45.92	1200	1.339	1.3953
35.52	1733	1.270	1.3289

An inverse series of experiments was now made by compressing the air in the exhausted air-chamber, but it was not completed, owing to an accident to the chamber. The data so far as available are shown in table 64 and figure 63. The tendency here is to fall below the data for the exhaustion method, consistently with the earlier experiments.

TABLE 64.—Wood fog-chamber. Interference method. Fog-chamber exhausted. Barometer, $p=75.62$; absolute temperature, $\theta=287.4°$ to $290.6°$.

p_0	$10^6\Delta N$	γ	γ corrected
65.68	400	1.278	1.3195
55.43	833	1.205	1.2415
45.41	1300	1.157	1.1888

Finally, water was introduced into the fog-chamber so as to provide saturated air and the value of γ was redetermined under these conditions. In the first measurements, as stated, no difficulties were encountered, even in the case of a very dense phosphorus fog. Later the glass became permanently cloudy and could only be cleared by slight heating. The data are given in table 65 and figure 63. As a whole these results lie somewhat below the data for the dry chamber, but they are not sufficiently regular to admit of very definite statement.

TABLE 65.—Wood fog-chamber. Interference method. Air saturated with water-vapor. Vacuum-chamber exhausted. Barometer, $p_0 = 76.17$; absolute temperature, $\theta = 291.5°$.

p	$10^6 \Delta N$	γ	γ corrected
65.92	438	1.221	1.2653
56.09	900	1.175	1.2204
45.92	1325	1.229	1.2803
36.09	1950	1.087	1.1406

At $\delta p = 30$ certain tests were made by precipitating a very dense fog with phosphorus with results as follows:

Without phosphorus: $10^6 \times \Delta N = 1350, 1350, 1300$.
With phosphorus; dense fog: $10^6 \times \Delta N = 1300, 1250$.

Thus no effect of the very dense fog could be detected.

The phenomenon of rings vanishing jerkily in the same sense as an increase of ΔN was apparent in all the experiments, immediately after exhaustion. Three or four such rings were counted. The observation is referable as before to some sort of strain in the solid parts of the apparatus, and probably not due to any thermo-dynamic transformation of the gas. The behavior of these rings suggests the properties of a solid under strain and not those of a gas.

In general it is curious to note that whenever any part of the interferometer is strained a succession of rings gradually vanishes, *after* the strain has been imparted. They vanish too soon to be referable to solid viscosity in the ordinary sense. They rather show that full strain does not follow the stress instantaneously.

The same chamber was now used in order to find γ by Clement and Desormes's method, using all the precautions to guard against leaks, etc. The data are given in table 66. Owing to precipitation of fog, these results are as usual distinctly below the results for dry air and the same chamber (table 61). In both tables the value of γ is constant for drops of pressure between $\delta p = 20$ and 40 cm., a very unexpected result, as one would fancy that the data for γ would be more trustworthy (apart from measurement) as δp is smaller and there is less adiabatic cooling. The constancy of these values makes it possible to state a mean value of γ for each individual case apart from δp.

It is clear, moreover, that the difference of values for γ in wet and dry air suggests a practical method of determining the amount of water precipitated per cubic centimeter, seeing that $\gamma_{dry} - \gamma_{wet}$ is sufficiently large for such a purpose. The equation, however, is yet to be deduced.

TABLE 66.—Wood fog-chamber and saturated air as in table 65. Clement and Desormes's method. Vacuum-chamber exhausted. Barometer, $p_0 = 76.81$; absolute temperature, $\theta_0 = 297°$; $v/V = .09$

p	h	γ
66.45	7.5	1.29
56.61	14.93	1.28
46.81	22.4	1.29
36.81	30.6	1.29

96. Air-chamber of vanishing thickness.—To test the adequacy of the interference method it is necessary, in conclusion, to construct a cell of plate-glass, in which the thickness of the layer of air in the direction of the component beam of light shall be negligible. ΔN in this case would therefore reveal the discrepancy due to the chamber itself, and γ, from the small volume of air contained, should be nearly 1. The cell constructed was $e = 2$ cm. thick (within), in the direction of the interfering ray m, fig. 63. It could not be made thinner, seeing that an exhaust-pipe had to be introduced. Its volume was $2 \times 12 \times 9.5$ cm^3. Thus $v = 228 + 245 = 473$ and $V = 12867$, so that $v/V = .03676$. The glass walls were of the same plate-glass used in the preceding wood fog-chamber, being 0.870 and 0.854 cm. thick, respectively.

The results are given in table 67. The drop of pressure was eventually as high as 70 cm. Below $\delta p = 40$ cm., no effect could be determined, as the ellipses scarcely moved.

TABLE 67.—Flat fog-chamber, $e = 2$ cm. in direction of beam of light. Dimensions, $2 \times 12 \times 9.5 = 228$ c.c. Dry air. Exhaustion method. $v/V = .03676$. Glass plates .870 and .854 cm. thick. Barometer, $p_0 = 76.58$; absolute temperature, $\theta = 293.5°$.

δp	$\Delta N \times 10^6$	γ	δp	$\Delta N \times 10^6$	γ
10	0	....	50	400	0.75
20	0	....	60	450	.81
30	0	....	70	550	.78
40	0	....	..	...	....

The value of ΔN for a column of air only 2 cm. long is near the limit of measurement, and the results for γ, to be interpreted, are necessarily crude. ΔN is again distinctly excessive, even in this limiting case, and the data for γ (which can not be less than 1) are deficient in the same manner as above. Something has therefore entered consistently into all these interference experiments in virtue of which ΔN is too large and γ too small

throughout. The value of this discrepancy, the real nature of which is inherent in the use of equation (2), may be considered as given in table 67. It will be seen that it is sufficiently large to increase the mean data for γ found by the interference method to the values obtained by the Clement and Desormes method for identical methods of expansion and air-chambers. As in the case of tubes, the expansion in this thin chamber is practically isothermal.

TABLE 68.—Interpolated data for the dispersion of air. Practical table, $\mu-1=B/\lambda^x$ $B=.0002101$, $x=.0341$.

Line.	B.	C.	D.	E.	F.
$10^6\lambda$.....	68.70	65.63	58.93	52.70	48.61
Observed $10^6(\mu-1)$...	291.4	291.8	292.7	293.9	295.0
Computed $10^6(\mu-1)$...	291.4	291.8	292.9	293.9	294.8
Difference.....	.0	.0	− .2	.0	+ .2

97. Conclusion.—As a whole the results of this long and laborious series of experiments, made with a view to determine the actual value of γ in such particular apparatus as was described, have been unsatisfactory, in spite of the care which was taken with the individual measurements. This is not, however, to be ascribed to the interference method applied; for, in so far as the method is concerned, its sensitiveness could be increased at pleasure by passing the component beams between mirrors and one of them many times through the fog-chamber. The difficulty is rather due to the shortcomings of the fog-chamber itself, which even in the final case was not sufficiently voluminous, nor sufficiently rigidly mounted, and possibly not provided with an exhaust-cock of sufficiently rapid or sufficiently constant action.

Furthermore, the adiabatic expansion is throughout better, *i.e.*, γ is larger, as the chamber is more bulky. In the small brass tube or the shallow cell, for instance, the expansion as actually produced and determined by the value of γ is nearly isothermal. In all cases the method by compression gave very low results, owing clearly to the unavoidable influx of relatively cold air during compression.

The mean results for γ useful for practical purposes are sufficiently given in figs. 62 and 64, when corrected with reference to equation (2).

As the micrometer can be set to 5×10^{-5} cm. on restoring the center of ellipses back to the fiducial sodium line selected, the displacement method is not much less sensitive than the ring method (sensitiveness limited by half a wave-length, or about half the given datum) and the former has the advantage of never losing count. This feature of the experiments was eminently satisfactory.

A curious result is the evanescence of several (2 to 5) rings subsequent to the adiabatic expansion. They vanish in the sense of an increase of the micrometer displacement ΔN. This phenomenon is apparently refer-

able to a non-instantaneous appearance of strain for the given stress in solid parts of the air-chamber. It ceases too soon to be called viscous in the ordinary sense, and it probably has an immediate bearing on Kelvin's "fatigue" of elasticity.

For the coronal fog-chamber (the largest one used above), it is then possible to write for dry air, $\gamma = 1.37$, and for wet air, $\gamma = 1.29$, in case of all the experiments usually made with coronas (drops of pressure exceeding 10 cm.). The data are the mean results obtained with Clement and Desormes's method.

This large difference in the values of γ for dry and for wet air, *cæt. par.*, suggests a method for the measurement of the quantity of fog precipitation per cubic centimeter of nucleated air, when suddenly cooled. An equation for this purpose will be considered elsewhere.

In conclusion, it is necessary to endeavor to account for the excessive values of ΔN and the correspondingly low values of γ given by the interference method as compared with the method of Clement and Desormes. Equation (2), assumed for experimental purposes, it will be remembered, contains no correction for the dispersion of air. It remains, therefore, to resume equation (2′), in which the constant b between the C and E lines has the mean value of $b_0 = 10^{-14} \times 1.64$ for a plenum of air. Equation (2′) may be written

$$\mu_0\left(1+\frac{2b_0}{\mu_0\lambda^2}\right)=\mu\left(1+\frac{2b}{\mu\lambda^2}\right)+\frac{\Delta N}{e} \tag{24}$$

where b_0 and b correspond to an air-column of length e at high (p_0) and low (p) pressure, respectively, and ΔN is the displacement of the micrometer. The simplified Cauchy equation $\mu = a + b/\lambda^2$, however, is inconvenient for the expansion of equation (6) above

$$\mu - 1 = p/C\vartheta \tag{6}$$

at a fixed wave-length λ, since the constants a and b both essentially enter. It is quite sufficient, moreover, to use an equation of interpolation of the form

$$\mu - 1 = B/\lambda^x \tag{25}$$

and to compute x for known values of μ between the B and F lines of the spectrum. When this is done

$$B = .0002101 \qquad x = .0341$$

are mean values applying near the D line, as the table shows.

Equation (1) now takes the form

$$\frac{\Delta N}{e}=\mu_0-\mu-\left(\frac{d\mu_0}{d\lambda}-\frac{d\mu}{d\lambda}\right)\lambda=\mu_0-\mu+\frac{x(B_0-B)}{\lambda^x} \tag{26}$$

or from (6) and (25)

$$\mu_0 - 1 = \mu - 1 + \frac{\Delta N}{e} - \frac{x}{C}\left(\frac{p_0}{\vartheta_0}-\frac{p}{\vartheta}\right) \tag{27}$$

But for adiabatic expansion

$$\frac{p_0}{\vartheta_0}-\frac{p}{\vartheta}=\frac{p_0}{\vartheta_0}\left(1-\left(\frac{p}{p_0}\right)^{1/\gamma}\right) \tag{7'}$$

which in (26) gives

$$\mu_0-1=\mu-1+\frac{\Delta N}{e}-\frac{x}{C}\left(1-\left(\frac{p}{p_0}\right)^{1/\gamma}\right)\frac{p_0}{\vartheta_0} \tag{28}$$

Furthermore, in view of adiabatic expansion, equation (7) above

$$\frac{p}{(\mu-1)^\gamma}=\frac{p_0}{(\mu_0-1)^\gamma} \tag{7}$$

and after inserting equations (6) and (7), equation (28), when solved for γ, becomes

$$\gamma=\frac{\lg(p/p_0)}{\lg\left(1-\dfrac{C\vartheta_0}{e(1+x)p_0}\Delta N\right)} \tag{29}$$

or solved with respect to ΔN, it is

$$\Delta N=(1+x)\,\frac{ep_0}{C\vartheta_0}\left(1+\left(\frac{p}{p_0}\right)^{1/\gamma}\right) \tag{30}$$

The last equation follows at once from (26), (7'), and (25). If p and p_0 refer to the pressures of fog and vacuum chambers, the coefficient $(V+v)/V$ must be inserted before ΔN as in the corresponding equations above. The results obtained in this way are computed for the small tube fog-chamber (tables 40 and 41 above) and for the large coronal fog-chamber (tables 62, 63, 64, 65) and marked corrected.

The mean value of γ obtained by the interference method on exhausting the coronal fog-chamber is now

$$\gamma=1.33 \text{ (dry air)} \qquad \gamma=1.23 \text{ (wet air)}.$$

These values are still below the data obtained by the Clement and Desormes method, but the reason for this may possibly be due to the different conditions involved. The latter refer to the mean volume of air, whereas in the interference method the pencil passes through a definite layer of air, in the present experiments unfortunately too near the bottom or walls of the chamber. The interferometer did not at the time admit of the introduction of bulky chambers, large in their vertical dimensions, though such alterations have since been made with success.